

## CHAPTER 8 LITHOGEOCHEMISTRY

### 8.1 Introduction

Most of the lithogeochemical data utilized in this study, including that generated during the previous CAMIRO-funded project (94E-04) and that compiled from databases donated by the company sponsors, are for ultramafic and mafic rocks. Owing to their intimate association with the magmatic Ni-Cu-(PGE) sulfide mineralization in the TNB, an understanding of the compositional variations of these rocks is critical to understanding the mechanisms of ore genesis and ore localization. However, geochemical data have also been generated for a variety of sedimentary and felsic intrusive rocks in the TNB in order to provide additional constraints on the magmatic models discussed in this chapter and the interpretations of the stratigraphy and tectonics discussed in **Chapters 5 and 6**.

All data discussed in this chapter are included in the geochemical database that accompanies the report (*TNB\_WR\_database.csv*). All analytical methods are described in **Appendix 1**. Additional data are included in **Tables A2.1, A4.1, A4.2, A9.1, and A9.2** in **Appendices 2, 4, and 9**, respectively.

### 8.2 Aims

The aims of the lithogeochemical studies were to:

- 1) Generate a coherent geochemical database for rocks in the TNB, focussing on the ultramafic bodies, sulfide ores, and Oswagan Group sedimentary rocks.
- 2) Develop geochemical methods to discriminate between mineralized and non-mineralized ultramafic bodies.
- 3) Produce chemostratigraphic columns for different regions within the TNB to supplement the existing lithostratigraphy, from which chemical signatures for the recognition of assimilants could be established.
- 4) Define stratigraphic/geochemical/petrogenetic relationships between various types of ultramafic sills and mafic-ultramafic volcanic rocks.
- 5) Refine and supplement geologic and tectonic models developed from the mapping and regional geological studies.

### 8.3 Sampling

Although samples from many different mafic and ultramafic bodies were analyzed for major, minor, and trace elements as part of the previous CAMIRO project or by the company sponsors during their exploration programs, the majority of the data that existed prior to the current project were either:

- 1) Available for only the larger ultramafic bodies within the belt (e.g., those at Oswagan Lake, Pipe, North Manasan, or along the William Lake trend),
- 2) Focussed on the sulfide-rich portions of mineralized bodies, or
- 3) Limited to only major and minor elements.

In order to examine both regional and local variations of the mafic and ultramafic rocks and to examine compositional changes in the metasedimentary rocks along the belt, the geochemical work in this project involved regional sampling of well-characterized outcrops and detailed sampling of mafic, ultramafic, and metasedimentary rocks in recent drill cores. The spatial distribution of sample locations is illustrated in **Figures A2.1 to A2.4** and the numbers of samples from different lithologies are summarized in **Table 8.1**.

**Table 8.1** Summary of samples in project database

<b>Lithology</b>	<b>Lithological Code in Database</b>	<b>Number of Samples</b>
Metasediments (undivided)	10	231
Chert	10A	9
Pelites	10B, 10C, 10D	712
Wacke/Arkose	10E, 10G	51
Quartzite/Arenite	10F, 10H	36
Conglomerate	10I	4
Calc-silicate/Marble/Skarn	10J, 17, 18	53
Silicate-Facies Iron-formation	10K	1
Carbonate-Facies Iron-formation	10L	14
Sulfide-Facies Iron-formation <sup>1</sup>	10M, 1F	104
Oxide-Facies Iron-formation	10O	27
<b>Total Metasedimentary Rocks</b>		<b>1142</b>
Gneiss	13A, 13B, 13C	144
Mylonite	16, 16A	8
Granulite	20	1
Migmatite	22, 22A	4
<b>Total Basement Rocks</b>		<b>157</b>
Granite	4, 4A	60
Granitic Pegmatite	4D	33
Granodiorite	5A	14
Tonalite	5B	4
Monzodiorite	5C	4
<b>Total Felsic and Intermediate Rocks</b>		<b>115</b>
Basalt	9A	297
Komatiite & Komatiitic Basalt	9B	340
Gabbro	6B	166
Mafic Amphibolite	14	151
<b>Total Mafic Rocks</b>		<b>954</b>
Pyroxenite	6E	267
Peridotite	6F	1089
Dunite	6G	737
<b>Total Ultramafic Rocks</b>		<b>2093</b>

**Notes:** <sup>1</sup> Many of the sulfide-facies iron-formations are classified as mineralized metasedimentary rocks (1F). Other sulfides not included in compilation. Table includes data from all sources.

## 8.4 Ultramafic Rocks

### 8.4.1 Mineralization Status

In order to facilitate discussion and interpretation, we have attempted to make a distinction between *economically mineralized*, *subeconomically mineralized*, and *non-mineralized* ultramafic intrusions. It is important, however, to recognize that such classifications are very subjective, because there is a complete continuum between economically- and subeconomically-mineralized intrusions, because the economic status of mineralized intrusions depends on many factors, including metal prices, grades, tonnages, development costs, and mining costs, and because intrusions classified as being non-mineralized or subeconomically-mineralized may contain undiscovered economic mineralization.

**Economically (strongly) mineralized** intrusions contain Ni-Cu-(PGE) sulfides in large enough abundances over sufficient intervals to be exploited economically (e.g., Thompson, Birchtree, Moak Lake, Pipe, Soab, Bucko, Bowden). Most intrusions classified as economically mineralized contain semi-massive to massive Ni-Cu-(PGE) sulfides with >1% whole-rock Ni + Cu and have been mined or subjected to advanced exploration.

**Sub-economically (weakly) mineralized** intrusions either contain low abundances of sulfides or contain sulfide-rich zones that are too thin to be exploited economically (e.g., Ospwagan Lake, William Lake). Most intrusions classified as subeconomically mineralized contain disseminated to semi-massive sulfides with 0.3-1% whole-rock Ni+Cu and have been subjected to advanced exploration. In some cases the degree of mineralization varies within an individual ultramafic body, with some parts containing significant volumes of sulfides and other parts appearing to be barren (e.g., W-56 body at William Lake). Most bodies of this type were classified as subeconomically mineralized.

**Non-mineralized** intrusions are barren or contain only trace amounts of sulfides. Most intrusions classified as non-mineralized contain disseminated mineralization with <0.3% whole-rock Ni+Cu and have not been subjected to advanced exploration.

Samples from bodies not actively studied during the project (e.g., from company databases or the literature, where the mineralization status of the body is unknown) form a fourth, “**Undetermined**” category.

The mineralization statuses of the different sample locations are shown in **Table A2.1**.

### 8.4.2 Petrography

The ultramafic bodies in the TNB have experienced deformation and metamorphism under upper amphibolite facies and serpentine ± carbonate alteration that resulted from the infiltration of volatile-rich fluids from metasedimentary country rocks (**Section 7.2**). Although almost all igneous textures and minerals have been destroyed along the deformed margins of the bodies, primary igneous textures and relict magmatic minerals are commonly preserved in the cores of the bodies. However, as even the most-deformed rocks can often be identified on the basis of metamorphic mineralogy and whole-rock geochemical composition, all of the rocks have been classified in terms of the textures and mineralogy of the igneous protoliths.

On the basis of relict igneous textures and/or whole-rock geochemistry, the ultramafic rocks collected in this study can be classified into three main lithologies: **metadunites**, **metaperidotites** (including harzburgites and rare wehrlites), and **metapyroxenites** (both orthopyroxenites and clinopyroxenites). Many of the ultramafic bodies appear to have preserved a primary igneous zoning, where olivine modal abundances vary systematically through individual drill core intersections (**Figs. 5.6 and 5.7**).

#### 8.4.2.1 Metadunites

Most of the metadunites in the TNB are serpentinized olivine adcumulate rocks with >90% fine to medium-grained serpentine pseudomorphs after olivine in a fine-grained matrix of amphibole  $\pm$  chlorite  $\pm$  serpentine  $\pm$  chromite. Despite pervasive alteration to mesh-textured serpentine, altered olivine grains commonly preserve elements of their original texture, including grain outlines and irregular fracture patterns. Olivine grains are generally equant to elongate, with either curvilinear grain boundaries that meet in triple point junctions and define a close-packed mosaic texture (**Fig. 8.1a**) or with ovoid, occasionally idiomorphic shapes (**Fig. 8.1b**). Olivine grain sizes vary between 0.2 mm and 10 mm, but are generally  $\sim$ 1 mm. Some samples exhibit a weak orientation or flattening of olivine grains. Magnetite rims defining the rims of altered olivine grains indicate that the dunites initially contained <10% intergranular material.

In addition to the fine-grained magnetite generated during serpentinization of olivine, the most-altered dunites commonly contain stockworks of magnetite and/or carbonate veins. These veins indicate that several elements may have been *locally* mobile during alteration, including Fe, Mn, Ca, Sr, and possibly Mg. Although it is difficult to quantify (owing to the large amount of secondary magnetite formed during serpentinization of olivine), most of the dunites appear to have originally contained minor amounts of fine-grained euhedral intercumulus chromite (**Fig. 8.1e and f**).

Unserpentinized dunite cores occur in the central parts of many ultramafic bodies, including the non-mineralized Brostrom Lake, Hambone East, and Mystery Lake North bodies, the weakly-mineralized W-56 ultramafic body at William Lake (particularly DDH WL97-179, which intersected over 300m of unaltered dunite), the weakly-mineralized Mid Lake and North Manasan bodies, and the strongly-mineralized Pipe 1 body (**Figures A2.1 and A2.2**). In all of these bodies, the dunites are composed of >95% olivine with almost complete boundary contact between the grains and relatively little intergranular material (**Figs. 8.1a to d**), suggesting that they might be less altered not only because they are in the cores of the bodies and therefore further from the infiltrating-reacting fluids, but also because they were less permeable than the other rocks. The unaltered dunites commonly contain fine-grained disseminated chromite (1-2%, 60 - 100  $\mu$ m), which may occur both as subhedral to anhedral inclusions within the olivine grains (**Fig. 8.1e**) and as euhedral intercumulus grains (**Fig. 8.1f**). The presence of chromite both within and interstitial to olivine indicates that olivine and chromite were both on the liquidus during the crystallization of the dunites (Leshner & Stone, 1996; Barnes & Brand, 1999).

In addition to coarse chromite inclusions, many of the relict olivines within the dunites contain finely disseminated chromite micro-inclusions or inclusion trails (**Figs. 8.1e and g**). We considered the possibility that these inclusions might represent magnetite trapped in metamorphogenic olivine formed during dehydration of serpentine. However, the olivines

( $\text{Fo}_{88-90}$ ) are not depleted in FeO or MnO relative to the compositions of the whole rocks ( $\text{Mg}/(\text{Fe}+\text{Mg}) \sim 88-90$ ), as would be expected for metamorphogenic olivines formed by dehydration of serpentine, and, with the exception of the samples collected from the Hambone East body, the inclusions themselves are relatively rich in Cr and poor in Al and  $\text{Fe}^{3+}$  (**Section 8.4.3.2**) This suggests that they have not interacted with either serpentinizing fluids or any trapped melt phases. On this basis, the chromite micro-inclusions are interpreted to represent primary igneous inclusions, the unaltered olivines in these samples are inferred to be of magmatic origin, and their compositions are interpreted to reflect the compositions of the parental magmas.

In addition to chromite, most of the dunites collected from the mineralized bodies contain 1-2% fine-grained intergranular blebs of disseminated sulfides (predominantly Pn-Po-Ccp: **Fig. 8.1h**).

#### 8.4.2.2 Metaperidotites

Most of the metaperidotites in the TNB are composed of 40-90% fine- to medium-grained, variably serpentinized subhedral olivine grains in a matrix of fine-grained chlorite  $\pm$  calcic amphibole  $\pm$  serpentine with trace amounts of fine-grained chromite (**Fig. 8.2a**). The replacement of the interstitial material by chlorite  $\pm$  amphibole  $\pm$  serpentine suggests that many of the peridotites were originally composed of olivine and pyroxene (O'Hanley, 1996) and the presence of calcic amphibole in these intergrowths suggests that the pyroxene was originally Ca-rich clinopyroxene (i.e., that the rocks were originally wehrlites) rather than Ca-poor orthopyroxene (i.e., that the rocks were originally harzburgites). Although komatiitic olivines crystallized in rapidly-cooled extrusive environments may contain significant amounts of Ca (see review by Lesher, 1989), the olivines in the ultramafic intrusions in the TNB appear to have crystallized in slowly-cooled intrusive environments and have low Ca contents. Because few unaltered peridotites were found within the ultramafic bodies sampled in this study, most were distinguished from metadunites by the presence of greater amounts of interstitial chlorite and amphibole and/or by lower whole-rock MgO contents and higher incompatible major element contents (e.g.,  $\text{TiO}_2$ ,  $\text{Al}_2\text{O}_3$ , CaO).

Although orthopyroxene-bearing olivine cumulate rocks have been reported in the ultramafic bodies of the TNB by several previous workers, predominantly at the Thompson mine (Peredery, 1982; Paktunç, 1984), few harzburgites were identified either petrographically or geochemically in the ultramafic bodies that were studied during this project. Those that were found were generally poikilitic olivine mesocumulates, in which the orthopyroxene forms oikocrystic grains enclosing cumulus olivine. The paucity of orthopyroxene in most of the samples collected in this study is consistent with the sampling being concentrated on non-mineralized and subeconomically mineralized intrusions (felsification of magma via assimilation of wall-rocks potentially inducing sulfide saturation and orthopyroxene crystallization), as well as with the generally lower metamorphic grade of the ultramafic bodies that were studied. Whereas the ultramafic bodies at Thompson mine appear to have experienced upper amphibolite to granulite-facies metamorphism, during which the assemblage olivine  $\pm$  talc  $\pm$  anthophyllite or chlorite would have been unstable and reacted to form either orthopyroxene or orthopyroxene  $\pm$  olivine  $\pm$  spinel, respectively (Paktunç, 1984), the majority of the ultramafic bodies sampled during this project appear to have experienced only mid- to upper amphibolite-facies metamorphism, during which olivine  $\pm$  talc, olivine  $\pm$  anthophyllite, or chlorite were stable phases.

Partially-serpentinized peridotites, in which the cores of olivine grains are partially preserved, were found in a only few ultramafic bodies (e.g., North Manasan and Spur South: **Fig. 8.2b**). These rocks are characterized by <90% fine to medium-grained, partially serpentinized olivines within a matrix of >10% fine-grained chlorite  $\pm$  amphibole  $\pm$  serpentine. The relict olivines are ovoid, between 0.1 and 3 mm in diameter, and contain opaque micro-inclusions similar to those present in the dunites (see above). However, the olivines in the metaperidotites are less magnesian ( $\text{Fo}_{86}$ ) than those in the metadunites ( $\text{Fo}_{88-90}$ ), suggesting that they formed from less magnesian (more fractionated) magmas.

#### 8.4.2.3 Metapyroxenites

Olivine metapyroxenites occur along the margins of the ultramafic bodies and as layers within the bodies. They are composed primarily of fine to medium-grained olivine and/or pyroxene altered to either mesh-textured serpentine or porphyroblastic calcic amphibole in a matrix of acicular chlorite  $\pm$  amphibole  $\pm$  serpentine. Biotite is present in the matrix near ultramafic–metasedimentary rock contacts and contains very fine-grained, high-relief inclusions surrounded by pleochroic haloes, probably zircon, suggesting assimilation of sedimentary rock during emplacement and/or mobilization of Zr into the pyroxenites during metamorphism. In most samples, the olivine is completely serpentinized. However, relict olivine fragments are preserved in olivine pyroxenites along the margins of the Spur South ultramafic body (DDH 89227: **Fig. 8.2c**). The low magnesium contents ( $\text{Fo}_{81-84}$ ) of the olivines suggest that they crystallized from significantly less magnesian magmas than the olivines in the mesocumulate and adcumulate portions of the ultramafic bodies and/or that the olivines in the pyroxenites re-equilibrated more extensively with their groundmass during metamorphism.

Although pure orthopyroxenite and clinopyroxenite layers are preserved in a few of the ultramafic bodies (e.g., Oswagan Lake, Thompson Mine, Spur South, Grass River, and South Central TNB: **Fig. 8.2d**), such layers are relatively rare in the TNB. In most cases, the pyroxenites have been altered to an assemblage of either tremolite or hornblende  $\pm$  plagioclase (clinopyroxenites) or tremolite  $\pm$  anthophyllite  $\pm$  orthopyroxene (orthopyroxenites) and can only be easily recognized from their whole-rock chemical compositions.

### 8.4.3 Olivine Compositions

In order to supplement the whole-rock elemental data in the interpretation of the petrogenesis and sulfide-saturation history of the ultramafic bodies, the compositions of relict olivines in the William Lake W-56, Brostrom Lake, Hambone Lake, Spur South, Pipe 1, Mid Lake, North Manasan, and Mystery Lake ultramafic bodies were determined by wavelength-dispersive X-ray emission spectrometry using the CAMECA SX-50 electron probe microanalyzer at the Ontario Geoscience Laboratories. Analytical methods are described in **Appendix 1**. Individual analyses are presented in **Table A4.1** and **A4.2** in **Appendix 4**.

#### 8.4.3.1 Textural Characteristics

The majority of the samples containing relict olivine are located in the cores of ultramafic bodies and comprise fine- to medium-grained dunites with minimal amounts of intercumulus material and only minor amounts of accessory chromite. Peridotites only rarely contain relict olivine grains. However, unaltered olivines were found in a single sample of poikilitic

peridotite from the lower part of the North Manasan ultramafic body (DDH 86299), where they are surrounded by a fine-grained groundmass of chlorite and/or calcic amphibole that is inferred to represent altered clinopyroxene oikocrysts. Several of the samples from the Brostrom Lake, Hambone, North Manasan, Mid Lake, and Pipe 1 ultramafic bodies contain minor amounts (0.5-2%) of disseminated intercumulus sulfides. Although olivine grains adjacent to sulfide grains were generally avoided during analysis, owing to their susceptibility to Fe-Ni exchange during post-magmatic cooling or metamorphism (see Binns and Groves, 1976), the compositions of olivines adjacent to sulfides do not appear to differ significantly from those away from sulfides.

Although the margins of the olivines have been partially serpentinized in several samples, the olivine grains in many of the analyzed samples exhibit well-developed cumulate textures, with equant or slightly elongate and subhedral to euhedral outlines, as described above. The larger grains in some samples appear to exhibit considerable strain and to have recrystallized along their edges to form smaller, equant neoblastic grains (**Fig. 8.1c**). However, analyses of both strained and annealed grains in the Mid Lake ultramafic body have nearly identical compositions, suggesting that recrystallization did not substantially affect the chemistry of the grains.

#### 8.4.3.2 Oxide Inclusions

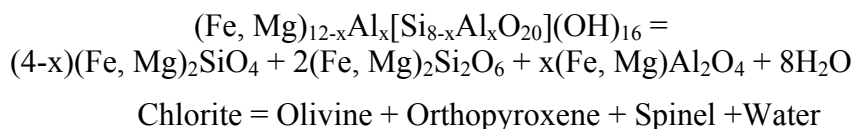
As described above, unaltered olivine grains commonly contain abundant opaque micro-inclusions (<2-20  $\mu\text{m}$ ) that are either disseminated throughout the grains and give the olivines a brown colour in plane-polarized light or form curvilinear inclusion trails. Qualitative analysis by energy-dispersive X-ray emission spectrometry on a scanning electron microscope indicates that these grains belong to the spinel mineral group and have compositions that range from chromian magnetite (“ferritchromite”)  $[\text{Fe}^{2+}(\text{Fe}, \text{Cr})^{3+}_2\text{O}_4]$  through chromite  $[\text{Fe}^{2+}\text{Cr}^{3+}_2\text{O}_4]$  to chromian hercynite  $[\text{Fe}^{2+}(\text{Al}, \text{Cr})^{3+}_2\text{O}_4]$ .

Because the Cr, Al,  $\text{Fe}^{3+}$ , and Ti contents of the enclosing olivines should be low and these elements should diffuse only slowly through the olivine matrix, the compositions of the oxide inclusions may be used to estimate the conditions under which they formed and, by association, the origin of the enclosing olivine. Although electron probe microanalysis of the inclusions was hampered by their small size (commonly less than either the width of the electron beam or its sampling depth), many were sufficiently large to enable accurate determination of their major and minor element compositions (**Table A4.2**). The analyses confirm that most of the inclusions are chromite or Cr-magnetite with  $\text{Mg}/(\text{Fe}+\text{Mg}) = 0.05\text{-}0.4$ ,  $\text{Cr}/(\text{Cr}+\text{Al}+\text{Fe}^{3+}) = 0.5\text{-}0.7$ , and  $\text{Fe}^{3+}/(\text{Cr}+\text{Al}+\text{Fe}^{3+}) = 0.05\text{-}0.4$  (**Fig. 8.3**). However, many of the inclusions in equigranular olivines in the Hambone East ultramafic body (**Fig. 8.1d**) and a single inclusion in an olivine in the Pipe 1 ultramafic body are significantly enriched in  $\text{Al}_2\text{O}_3$  ( $\text{Al}/(\text{Cr}+\text{Al}+\text{Fe}^{3+}) > 0.4$ ) and lie on a trend toward the compositions of metamorphic spinels in porphyroblastic metapicrites of the Bah Lake assemblage in the Pipe, Oswagan Lake, and William Lake areas. A second set of anomalous inclusions, in olivines in the North Manasan ultramafic body and occasional inclusions in olivines in the Mystery Lake North ultramafic body, are enriched in  $\text{Fe}^{3+}$  and lie on a trend toward the magnetite field (**Fig. 8.3**).

With the exception of the Al- and  $\text{Fe}^{3+}$ -rich chromite inclusions in olivines in the Hambone, Pipe 1, and North Manasan bodies, the inclusions in the relict olivines in the TNB ultramafic bodies have compositions that closely resemble the cores of cumulus chromites in the same

ultramafic bodies as well as chromite inclusions in olivine phenocrysts in modern lava lakes (e.g., Scowen et al., 1991) and the cores of cumulus chromites in greenschist-facies komatiitic peridotites in Western Australia (e.g., Barnes, 1998, 2000). The chromites in these studies are interpreted to have re-equilibrated (in the case of the lava lake, through the olivine) with trapped interstitial melt, leading to pronounced enrichment in  $\text{Fe}^{2+}$  (relative to Mg) and Ti and mild enrichment of  $\text{Fe}^{3+}$  relative to Cr and Al. Although the cores of the cumulus chromites in amphibolite-facies komatiites in Western Australia have similar Cr, Al,  $\text{Fe}^{3+}$ , and Ti contents as those in greenschist-facies rocks (**Fig. 8.3**), Barnes (2000) showed that the rims of chromites in amphibolite-facies rocks are significantly enriched in  $\text{Fe}^{3+}$ , depleted in Cr, and may be either significantly enriched or depleted in Ti<sup>1</sup>. Whereas the compositions of the rims around the metamorphosed chromites described by Barnes (2000) resemble those of the  $\text{Fe}^{3+}$ -rich inclusions in the North Manasan and Mystery Lake bodies, they are distinctly different from those observed in the majority of the inclusions in TNB olivines. If the inclusions in the TNB olivines had formed or experienced conditions outside the olivine grains during metamorphism, then, owing to their small size, they would be expected to exhibit a similar compositional changes as those in the rims of the metamorphosed chromites and not preserve compositions similar to those in the cores of larger grains. Consequently, the low- $\text{Fe}^{3+}$ , low-Al, high-Cr inclusions in most of the olivines in the TNB ultramafic bodies are inferred to have been present in the host olivines prior to metamorphism, indicating that the olivines themselves are probably magmatic rather than metamorphic in origin and, as such, may preserve much of their original compositions.

Whereas the compositions of the  $\text{Fe}^{3+}$ -rich oxide inclusions may be accounted for by equilibration of the inclusions with fluids outside the olivine, the compositions of the Al-rich inclusions require that they equilibrated with an Al-rich phase during metamorphism. Paktunç (1984) observed a similar enrichment in Al in the rims of chromian spinels in ultramafic rocks at the Thompson Mine, which can be explained by the breakdown of chlorite under upper amphibolite to granulite facies according to the reaction (Evans, 1977; Peltonen, 1990):



Because the spinel component would most likely be added epitaxially to any pre-existing chromite during this reaction, it would have been necessary for the original oxide phases in the Hambone East and Pipe 1 ultramafic bodies either to have been able to freely exchange Al,  $\text{Fe}^{3+}$ , and Cr with the intercumulus phases of the rock and/or to have increased in size, in order to produce the decrease in Cr and  $\text{Fe}^{3+}$ . Because neither of these is feasible while the oxide is included in the olivine grain, the presence of Al-rich chromite inclusions in the Hambone East ultramafic body suggests that those oxides formed outside the olivines and that the enclosing olivines are probably metamorphogenic, consistent with the equigranular textures of the metadunites. In contrast, although the presence of Al-rich intercumulus oxides in the Pipe 1 ultramafic body indicates that some of the olivines are metamorphogenic,

---

<sup>1</sup> The enrichment in Ti probably reflects the preservation of the effects of post-cumulus magmatic processes, rather than subsequent metamorphic alteration (Barnes, 2000).



because the majority of the inclusions in olivine have similar compositions to those in other bodies, most of the relict olivine observed in this body is inferred to have predated metamorphism and so may preserve original compositions.

#### 8.4.3.3 Major and Minor Elements

In order to increase the size of the analytical database for olivines in TNB ultramafic bodies, the data obtained in this project for primarily non-mineralized or weakly-mineralized ultramafic bodies were combined with data obtained previously by L. Hulbert (GSC) for mostly for mineralized ultramafic bodies. Although it was possible to use the compositions of oxide inclusions to screen the olivines analyzed during the current project to remove those of metamorphic origin, similar information was not available for the data obtained by Hulbert. For this reason, and owing to the large number of data available from each study, the data from each study are plotted on separate diagrams (**Figs. 8.6 to 8.9**).

Although the compositions of relict olivines in the ultramafic bodies exhibit a wide range of forsterite contents ( $\text{Fo}_{81.5} - \text{Fo}_{93.5}$ ; **Fig. 8.4**) and appear to display a trimodal population with peaks at  $\sim\text{Fo}_{91}$ ,  $\sim\text{Fo}_{89.5}$ , and  $\sim\text{Fo}_{83}$ , the compositions of olivines within individual samples/thin sections and individual ultramafic bodies generally show a more limited range of compositions (e.g.,  $\text{Fo}_{90.5-92}$  in the W-56 ultramafic body at William Lake,  $\text{Fo}_{92-93}$  at Brostrom Lake,  $\text{Fo}_{81.5-84}$  at Spur South, and  $\text{Fo}_{88-90}$  at Pipe 1). Thus, the trimodality of the dataset may be the product of biased sampling toward particular bodies and/or thin sections in which olivines were either more abundant or better preserved. The distribution of forsterite compositions between and within the samples indicates that, although the bodies must have formed from variably-evolved magmas, the olivines within each sample either crystallized from a similar magma or re-equilibrated on the scale of individual samples during either post-magmatic igneous processes or metamorphic reheating. Although olivines that form in dynamic lava channels or magma conduits may be unzoned if the composition of the magma remains constant and/or if they cool slowly enough to homogenize, the absence of zonation in any of the olivines in any of the ultramafic bodies in the TNB suggest that they must have been homogenized to some extent. Importantly, where data are available over a range of depths within individual ultramafic bodies, the relict olivines exhibit a greater range in composition, indicating variations in magma compositions during formation (e.g.,  $\text{Fo}_{88-91}$  at Mid Lake,  $\text{Fo}_{82-92}$  at Mystery Lake,  $\text{Fo}_{86-91}$  in the ultramafic body intersected by DH 74381 in Thompson Mine).

The compositions of the most forsterite-rich of the analyzed olivines (e.g.,  $\text{Fo}_{93}$ : Brostrom Lake) coincides with the calculated compositions of olivines that would have been in equilibrium with the most primitive of the Bah Lake assemblage komatiitic rocks at Ospwagan Lake (19-23 wt% MgO: Theyer & Freund, 1998). Because homogenization of a zoned olivine formed by fractional crystallization of komatiitic magma can increase the Fo content of the rim and decrease the Fo content of the core by up to 1-2 mole% (**Fig. 8.5**), the measured Fo contents of the TNB olivines will represent the olivine composition in equilibrium with the “average” magma that passed through the sills, rather than the most primitive magma in the system, and will therefore underestimate the magnesium content of the parental magma. Based on the compositions of the most magnesian olivines in the ultramafic bodies, an MgO content of between 20 and 22 wt% is therefore considered the best estimate of the initial composition of the parental magma. This is consistent with the presence of Cr-poor olivine cumulate rocks in several areas (see **Section 8.1.4.1**).

The Mn and Ni contents of the analyzed olivines are shown as a function of forsterite content in **Figures 8.6** and **8.7**. The compositions of most olivines in the non-mineralized and subeconomically mineralized Mystery Lake and North Manasan ultramafic bodies, the upper parts of two ultramafic bodies intersected by DH74376 at Thompson Mine, and the ultramafic body intersected by DH74391 at Thompson Mine appear to be consistent with those expected for the fractional crystallization of olivine from a sulfide-undersaturated magma with an initial major element composition similar to that of the most mafic Bah Lake assemblage volcanic rocks (with or without the assimilation of upper continental crustal rocks). However, the olivines in the Brostrom Lake, Pipe 1, Mid Lake ultramafic bodies, one of the samples collected from the Mystery Lake ultramafic body, and most of the samples collected from Soab, Birchtree, the lower ultramafic body intersected by DH74376, and the ultramafic body intersected by DH74381 at Thompson Mine are variably depleted in Ni and those in the W-56 ultramafic body at William Lake are significantly enriched in Ni relative to those expected for sulfide-undersaturated fractional crystallization of olivine. Because the Ni-depleted olivines all occur within sulfide-bearing cumulate rocks, the Ni depletion is inferred to reflect equilibration of the olivines with sulfide during emplacement (those situations where *some* but *not all* of the olivines are depleted) or crystallization from a magma that had previously equilibrated with sulfides (those situations where *all* of the olivines are depleted in Ni). The anomalously high Ni contents of the olivines from William Lake, however, occur in sulfide-poor cumulate rocks and cannot be adequately explained by either fractional crystallization or normal sulfide segregation processes. Possible explanations for the Ni enrichment in these samples are discussed in detail in **Section 8.4.3.5**.

#### **8.4.3.4 Sulfide Saturation History of Northern TNB Ultramafic Bodies**

In almost all cases, Ni partitions more strongly into olivine than into the coexisting silicate liquid, but less strongly into olivine than into coexisting sulfides (see discussion by Naldrett, 1989; Lesher & Stone, 1996). The Ni contents of the olivines therefore depend on a) the olivine/liquid, sulfide/liquid, and/or sulfide/olivine partition coefficients, all of which may vary as a function of magma composition,  $fO_2$ , and  $fS_2$  (except in very MgO-rich magmas, olivine Ni contents decrease with decreasing Mg; Beattie et al., 1991, 1993;  $D_{Ni}^{Sul/Ol}$  is greater under metamorphic conditions than under magmatic conditions: Binns & Groves, 1976; see review by Lesher & Stone, 1996), and b) the relative masses of sulfide, olivine, and/or silicate liquid (Duke & Naldrett, 1978; Duke, 1979; Lesher & Burnham, 1999, 2001).

The Ni depletion observed in the olivines in the Brostrom Lake, Pipe 1, Mid Lake, Soab, Birchtree, and Thompson ultramafic bodies may be attributed to any combination of three processes:

- 1) Fractional crystallization of olivine + sulfide from a sulfide-saturated magma, which produced olivine cumulate rocks that contain subeconomic sulfide mineralization and progressive chalcophile element depletion in the magma with increasing differentiation (**Fig. 8.8**).
- 2) Batch equilibration of a magma with a sulfide liquid, leading to the production of massive sulfide mineralization, a Ni-depleted magma, and crystallization of Ni-depleted olivines during subsequent fractionation (**Fig. 8.9**).

- 3) Metamorphic equilibration of olivine with intercumulus sulfide, leading to depletion of Ni in the co-existing olivine, depending on whether the olivine was previously depleted in Ni or not.

### ***Fractional Crystallization***

**Figure 8.8** illustrates the calculated compositions of olivines formed during fractional crystallization of olivine + sulfide from a sulfide-saturated magma, in which sulfide-saturation is achieved without the addition of S from an external source. For such processes to operate, the magmas would have had to have either been close to sulfide-saturation at the time of emplacement (and reached saturation within the magma chamber) or to have lost negligible olivine or sulfide prior to emplacement.

Although several of the dunites containing disseminated sulfides in the Pipe 1 and Brostrom Lake bodies lie on compositional trends similar to those expected for fractional crystallization of olivine + sulfide in cotectic proportions (~60:1 by mass: Duke & Naldrett, 1978; Duke, 1986; **Fig. 8.8**), the most Fo-rich olivines at Brostrom Lake and almost all of the olivines analyzed at Mid Lake are not only too Ni-depleted at their corresponding Fo contents to have formed by such a process, but the samples generally contain olivine and sulfide in proportions that are much greater than the expected cotectic proportions. The low sulfide contents of these samples indicate that the magmas from which the cumulates formed reached sulfide saturation *during* crystallization. Initial fractionation of olivine from the sulfide-undersaturated magma would have produced a mixture of olivine and interstitial liquid. After the magma reached sulfide-saturation, however, a cotectic mixture of olivine + sulfide would have fractionated from the magma, producing a cumulate with an olivine:sulfide ratios greater than the cotectic value. In theory, such a process would be recorded by zonation of Ni within the olivine grains, producing Ni-undepleted cores and Ni-depleted rims. However, such zonation may have been erased by subsequent homogenization of the olivine grains during post-magmatic cooling and/or metamorphism, leading to less pronounced depletion throughout the grains. Similarly, although the compositions of many of the olivines in the Ni-depleted ultramafic body intersected by DH74381 at Thompson and by DH 83087 and 84541 at Birchtree (**Figure 8.8**) lie close to the fractionation trends expected for cotectic crystallization of olivine + sulfide, those in the lower body intersected by DH74376 scatter along a trend that is sub-parallel to the sulfide-undersaturated fractional crystallization trend and cannot be easily accounted for by derivation from a single sulfide-undersaturated magma.

### ***Batch Equilibration***

**Figure 8.9** illustrates the trends expected for olivines produced via batch equilibration of an initially sulfide-undersaturated magma with sulfide liquid at a range of different silicate liquid to sulfide liquid ratios (R factors: Campbell & Naldrett, 1979). Before the magma interacts with the sulfide liquid, it should fractionate normally and should follow a FC or AFC trend (see **Fig. 8.7**). When the magma interacts with the sulfide liquid, the Ni content will be substantially reduced, but the major element composition should remain unaffected, leading to a sharp decrease in the Ni content of olivine without a noticeable change in Mg:Fe ratio (grey line in **Fig. 8.9**). The degree of Ni depletion in the silicate liquid and equilibrium olivines increases with decreasing R (Campbell & Naldrett, 1979; Lesher & Burnham, 1999, 2001). If the magma is separated from the sulfide liquid, it should continue to fractionate

olivine + sulfide in cotectic proportions and evolve along similar trends to those observed in **Figure 8.8** (thin solid lines in **Fig. 8.9**).

**Figure 8.9** demonstrates that the compositions of the Ni-depleted olivines in the Thompson, Brostrom Lake, and parts of the Pipe 1 ultramafic bodies may be successfully reproduced by the interaction of the magma with a sulfide liquid at R values of ~50 at Mid Lake, ~125 in DH74381 at Thompson and in one part of the Pipe 1 ultramafic body, ~400 in a different part of the Pipe 1 ultramafic body and at Brostrom Lake, and ~1000 in DH 74376 at Thompson, prior to the crystallization of the olivine, but that none of the samples have compositions that record the actual batch equilibration process, presumably owing to re-equilibration of the olivines after emplacement. Although significant amounts of intra- and extraparental massive sulfides (**Chapter 9**) have been recognized in and around the Pipe 1 ultramafic body, neither the Brostrom Lake nor Mid Lake ultramafic bodies appear to contain any associated massive sulfide mineralization, indicating that either the mineralization associated with these bodies remains to be discovered or, more likely, that the magmas were depleted in Ni by equilibration with sulfides *prior* to emplacement. Because of the small number of samples analyzed in this study and the absence of individual bodies containing olivines that are both undepleted and depleted in Ni (which would signify local sulfide-saturation), it is not possible to discriminate between these scenarios.

### ***Metamorphic Reequilibration***

The partition coefficient between sulfide and olivine ( $D_{Ni}^{Sul/Ol}$ ) is up to a factor of two smaller than that between sulfide and mafic or ultramafic silicate liquids ( $D_{Ni}^{Sul/Liq}$ ), but it increases by a factor of two between magmatic and metamorphic temperatures (Binns and Groves, 1976; see reviews by Naldrett, 1989; Lesher & Stone, 1996). Although the *rate* of diffusion of Ni in olivine is up to 9 orders of magnitude lower at peak metamorphic temperatures (~700°C) than at maximum magmatic temperatures (~1400°C), the *distance* of diffusion (mm/Ma) is only 4 orders of magnitude smaller over the same temperature range and the time scale of most metamorphic processes is up to 6 orders of magnitude longer than most magmatic processes, so the diffusion rate should not necessarily be a limiting factor. With all else equal, an olivine that equilibrates with sulfide during metamorphism will be more depleted in Ni than an olivine that equilibrates with sulfide during a magmatic process.

Because the same mass balance constraints that apply during magmatic processes (Campbell & Naldrett, 1979; Lesher & Burnham, 1999, 2001) also apply during metamorphic processes, the change in the compositions of olivines in sulfide-bearing rocks during metamorphism may be modelled from the initial compositions of the two phases and their relative proportions in the rock. Mass conservation requires that the mass of Ni distributed between the final olivine ( $Ol_{Ni}^f$ ) and the final sulfide ( $Sul_{Ni}^f$ ) must equal the masses of Ni distributed between the initial (magmatic) olivine ( $Ol_{Ni}^o$ ) and initial (magmatic) sulfide ( $Sul_{Ni}^o$ ):

$$A^f Ol_{Ni}^f + B^f Sul_{Ni}^f = A^o Ol_{Ni}^o + B^o Sul_{Ni}^o$$

where A is the mass fraction of olivine and B is the mass fraction of sulfide.

Substituting  $\text{Sul}_{\text{Ni}}^f = D_{\text{Ni}}^{\text{Sul/Ol}} \text{Ol}_{\text{Ni}}^f$  and  $\text{Ol}_{\text{Ni}}^f = \frac{\text{Sul}_{\text{Ni}}^f}{D_{\text{Ni}}^{\text{Sul/Ol}}}$ , and rearranging, one obtains:

$$\text{Ol}_{\text{Ni}}^f = \frac{A^0 \text{Ol}_{\text{Ni}}^0 + B^0 \text{Sul}_{\text{Ni}}^0}{A^f + B^f D_{\text{Ni}}^{\text{Sul/Ol}}} \text{ and } \text{Sul}_{\text{Ni}}^f = \frac{(A^0 \text{Ol}_{\text{Ni}}^0 + B^0 \text{Sul}_{\text{Ni}}^0) D_{\text{Ni}}^{\text{Sul/Ol}}}{A^f + B^f D_{\text{Ni}}^{\text{Sul/Ol}}}$$

Assuming  $A^0 = A^f$  and  $B^0 = B^f$ , substituting  $R_{\text{Ol/Sul}} = A/B$ , and rearranging, one obtains:

$$\text{Ol}_{\text{Ni}}^f = \frac{(\text{Ol}_{\text{Ni}}^0 R_{\text{Ol/Sul}} + \text{Sul}_{\text{Ni}}^0)}{R_{\text{Ol/Sul}} + D_{\text{Ni}}^{\text{Sul/Ol}}} \text{ and } \text{Sul}_{\text{Ni}}^f = \frac{(\text{Ol}_{\text{Ni}}^0 R_{\text{Ol/Sul}} + \text{Sul}_{\text{Ni}}^0) D_{\text{Ni}}^{\text{Sul/Ol}}}{R_{\text{Ol/Sul}} + D_{\text{Ni}}^{\text{Sul/Ol}}}$$

These mass balance expressions are equivalent to those derived by Lesher & Burnham (1999, 2001). Because there is only so much Ni available, an olivine that equilibrates with a large amount of sulfide will be more strongly depleted in Ni than one that equilibrates with a small amount of sulfide. There are other phases present (e.g., magnetite, chromite, pyroxene, amphibole, chlorite, serpentine) for which additional terms can be added (see Lesher & Burnham, 1999, 2001). However, their abundances are small in meso- and adcumulate rocks and they do not contain significant amounts of Ni, so they can be safely omitted.

The initial (magmatic) Ni contents of the olivine and sulfide will depend on the initial abundance of Ni in the magma, the values of  $D_{\text{Ni}}^{\text{Sul/Sil}}$  and  $D_{\text{Ni}}^{\text{Ol/Sil}}$  under the prevailing conditions of  $T$ ,  $f\text{O}_2$ , and  $f\text{S}_2$ , and the relative masses of olivine, sulfide, and silicate magma (see Lesher & Burnham, 1999, 2001). If the olivine and sulfide segregate from a relatively large mass of silicate magma (high  $R_{\text{Sil/Ol}}$  and  $R_{\text{Sil/Sul}}$ ), they will not be significantly depleted in Ni, but if they segregate from a relatively small mass of magma (low  $R_{\text{Sil/Ol}}$  and  $R_{\text{Sil/Sul}}$ ), both may be significantly depleted in Ni (see Lesher & Burnham, 1999, 2001). In either case, if the olivine and sulfide in meso- and adcumulate rocks are subsequently metamorphosed in the absence of significant amounts of silicate magma, Ni will be redistributed in favour of the sulfide phase. This means that an olivine that crystallizes under conditions of high  $R_{\text{Sil/Sul}}$  and high  $R_{\text{Sil/Ol}}$ , but is subsequently metamorphosed under conditions of low  $R_{\text{Ol/Sul}}$ , may end up with a Ni content that might be misinterpreted to reflect a lower  $R_{\text{Sil/Sul}}$  and  $R_{\text{Sil/Ol}}$ . The final (metamorphic) Ni content of the olivine will therefore not only depend on a) the initial (magmatic) abundance of Ni in the olivine, b) the value of  $D_{\text{Ni}}^{\text{Sul/Ol}}$  under the prevailing conditions of  $T$ ,  $f\text{O}_2$ , and  $f\text{S}_2$ , and c) the relative masses of olivine and sulfide at the magmatic stage, but will also depend on d) the value of  $D_{\text{Ni}}^{\text{Sul/Ol}}$  (metamorphic). If  $D_{\text{Ni}}^{\text{Sul/Ol}}$  (metamorphic) is twice that of  $D_{\text{Ni}}^{\text{Sul/Ol}}$  (magmatic) (as proposed by Binns & Groves, 1976 and discussed by Lesher & Stone, 1989), then our calculations suggest that the Ni contents of the olivines in a metamorphosed adcumulate rock containing cotectic proportions of olivine and sulfide (~60:1) would be ~40% lower than their the initial (magmatic) contents.

Although there are situations in which the metamorphic olivine may end up with a Ni content higher than that of the igneous olivine (e.g., if an olivine that formed under low  $R$  accumulated with a sulfide that had formed under high  $R$ , in which case the Ni content of the olivine would increase during metamorphism), this scenario is not likely to occur in most

magmatic sulfide deposits. In most cases, equilibration with sulfide will result in depletion of Ni in the olivine.

#### 8.4.3.5 William Lake Olivines

Although most of the olivines in the TNB can be modeled by some combination of fractional crystallization or batch equilibration of olivine and sulfide, with or without wall-rock assimilation, the Ni contents of the olivines in the W-56 ultramafic body at William Lake are much higher than predicted by such models (**Fig. 8.7**). We have considered several possible models for generating these high Ni contents: a) beginning with a more Ni-rich magma, b) evolving the magma via an equilibrium crystallization (EC) and/or assimilation fractional crystallization (AFC) process, c) adding Ni by assimilation of Ni-Cu-(PGE) sulfides, and d) increasing  $D_{\text{Ni}}^{\text{Ol/Sil}}$  by increasing  $f\text{O}_2$ .

#### *Ni Content of the Parental Magma*

Because the Ni in normal, asthenospheric mantle is housed both by sulfides, which are consumed at relatively low degrees of partial melting (e.g., Naldrett & Barnes, 1986; Keays, 1995) and olivine, which is progressively (but never completely) consumed at moderate to high degrees of partial melting, the Ni contents of magmas produced by progressive degrees of partial melting increase systematically with Mg content. The high Mg and PGE contents of the magmas that are inferred to have produced the William Lake dunites (**Sections 8.4.4 and 9.5.2**) indicate that they were derived by high degrees of partial melting of the mantle and therefore should have had high initial Ni contents. However, because the Ni content of olivine depends on both the composition of the magma and  $D_{\text{Ni}}^{\text{Ol/Sil}}$ , which decreases with increasing T and Mg content (Beattie et al., 1991, 1993), the Ni contents of olivines that crystallize from high-Mg komatiitic magmas initially increase with decreasing Mg content and subsequently decrease with decreasing Mg content, yielding a maximum Ni content of ~3500 ppm at ~ $\text{Fo}_{92}$  (**Fig. 8.7a**). The maximum Ni contents of the olivines in the models is much less than those observed in the olivines in DDH WL97-179 (3500 – 4500 ppm), suggesting that the anomalously high Ni contents of the olivines in the William Lake body cannot be accounted for by fractionation of a more Ni-rich magma that was simply produced by higher degrees of melting of a normal mantle source.

Although remelting of a strongly-depleted mantle source may produce ferropicrites that are enriched in Ni (e.g., Pechenga, Russia; Boston Creek, Ontario: Stone et al., 1995), such magmas have distinctive whole-rock major and minor element compositions that are unlike any of the mafic and ultramafic rocks observed in the TNB (e.g., very high LREE, Fe, and Ti relative to komatiitic rocks of the same Mg and Al contents) and crystallize olivines that are considerably less magnesian than those observed at William Lake (< $\text{Fo}_{84}$  vs.  $\text{Fo}_{91-92}$ ). This suggests that the anomalously high Ni contents of the olivines in the William Lake body also cannot be accounted for by remelting of a depleted mantle source.

#### *Equilibrium vs. Fractional Crystallization*

Leshner & Stone (1996) showed that the Ni contents of olivines crystallized from a low-Mg komatiite magma derived by equilibrium crystallization of a high-Mg komatiitic magma will be higher than the Ni contents of olivines crystallized from a low-Mg komatiite derived by moderate-degree partial melting of the mantle and/or fractional crystallization of olivine from a high-Mg komatiite. However, the Ni contents of all of these olivines are still lower than

those in the William Lake body. This suggests that the anomalously high Ni contents of the olivines in the William Lake body cannot be accounted for by EC processes.

#### ***Assimilation-Fractional Crystallization processes***

Arndt (1991) and Leshner & Stone (1996) have shown that the Ni contents of olivines crystallized from a low-Mg komatiite magma that was derived by high-degree partial melting of the mantle, contaminated by upper crust (or sedimentary rocks derived from upper crust), and fractionally crystallized olivine will be higher than the those of olivines crystallized from a low-Mg komatiite that was derived by moderate-degree partial melting of the mantle and/or fractional crystallization of olivine from a high-Mg komatiite without any contamination (AFC trends: **Fig. 8.7**). However, the Ni contents of such olivines are still substantially lower than those in the William Lake body, so it does not appear that the olivine compositions can be accounted for by AFC processes involving average upper continental crustal rocks or Ospwagan Lake sedimentary rocks.

#### ***Assimilation of Magmatic Sulfides***

Although assimilation-fractional crystallization (AFC) processes involving average upper continental crustal rocks cannot account for the Ni enrichment in the William Lake olivines, sufficient enrichment might be possible if the contaminant initially contained significant amounts of Ni. The only Ni-rich components in the area are either previously-formed olivine and/or magmatic sulfides. Because any pre-existing olivine is likely to have been in equilibrium with a silicate melt that should not have differed significantly from those with which it interacted, assimilation or interaction of olivine cannot significantly enrich the melt in Ni. However, if a sulfide-undersaturated magma were to interact with a sulfide-bearing cumulate formed from an earlier pulse of magma that had reached sulfide-saturation, it might be able to melt and dissolve the sulfides, thereby significantly enriching the magma in highly chalcophile elements. The olivine in the early-formed cumulate would be refractory during interaction with the magma, but the lower melting point of the sulfide phase (~992-1190°C, depending on Ni and Cu contents: see Ebel and Naldrett, 1996) would enable it to melt and dissolve in the new pulse of magma. Provided that the magma was not already saturated in sulfide and that the amount of sulfide dissolved was small, this would not necessarily have induced sulfide saturation. This scenario is consistent with the small amount of fine disseminated mineralization in the W-56 ultramafic body, which indicates that the magma reached sulfide saturation only at a very late stage in its crystallization history. Mass balance calculations using realistic estimates of the compositions of the magma (e.g., 19.6 wt% MgO, 770 ppm Ni, and 625 ppm S) and sulfide-bearing assimilant (~0.5% sulfide formed under moderate-R conditions, containing 8.5 wt% Ni and 38.8 wt% S) would be able to produce a sulfide-undersaturated magma that contains 1100 ppm Ni and 2550 ppm S and could have been in equilibrium with olivines with compositions similar to those in the W-56 intrusion (**Fig. 8.10**). Assimilation of a more Ni-rich (higher R factor) sulfide or a lower initial S content in the magma would decrease the amount of sulfide required and the final sulfide content of the magma.

#### ***Increasing Oxygen Fugacity***

$D_{\text{Ni}}^{\text{ol/sil}}$  probably also varies as a function of oxygen fugacity ( $f\text{O}_2$ ). Calculations using the olivine-silicate liquid exchange coefficients for Mg, Fe, and Ni compiled by Beattie et al. (1991, 1993) and the compositions of typical komatiitic magmas indicate that whereas

$D_{\text{Ni}}^{\text{ol/sil}}$  should increase with increasing  $f\text{O}_2$  (as the number of octahedral sites in the magma is decreased),  $D_{\text{Fe}}^{\text{ol/sil}}$  should also decrease with increasing  $f\text{O}_2$  (as the amount of FeO in the magma is decreased). With all else equal, the Ni and Fo contents of olivine should therefore increase with increasing  $f\text{O}_2$  and decrease with decreasing  $f\text{O}_2$ . The strong negative correlation between Ni and Fo in the W-56 ultramafic body (**Fig. 8.7a**) is of the correct sense to have been produced by variations in  $f\text{O}_2$ . Although we do not have sufficient data to determine whether the range of  $f\text{O}_2$  necessary to account for the compositional variations is within that expected for normal mafic or ultramafic magmas, it seems unlikely that the range in this case was any more than that inferred in other deposits of this type (Leshner & Campbell, 1993), which do not show this effect. In addition, oxidation of the magma would also reduce the solubility of S, potentially leading to sulfide saturation and rapid depletion of Ni in the magma. Nevertheless, oxidation of the magma remains a possibility.

An important consequence of both of the latter models, assimilation of sulfide and oxidation of the magma, is that they would bring the magma closer to sulfide saturation, which would eventually result in the segregation of sulfides and, as a consequence of the higher Ni contents of the olivines, higher Ni tenors in associated sulfides. Although the whole-rock data for samples collected from several places along the William Lake ultramafic body do not show any evidence of Ni-depletion that might be consistent with an ore-forming process, there is still potential for small, high-grade deposits in the area.

#### 8.4.3.6 Interim Summary

- 1) Oxide inclusions can be used to constrain the origin of olivines in highly metamorphosed rocks. Oxides included in primary (igneous) olivines should be enriched in  $\text{Cr}^{3+}$ , whereas oxides included in secondary (metamorphic) olivines should be enriched in  $\text{Al}^{3+}$  or  $\text{Fe}^{3+}$ . Olivines containing primary oxide inclusions are more likely to preserve magmatic major and/or minor element compositions.
- 2) Olivines of inferred primary (igneous) origin exhibit a range of forsterite contents ( $\text{Fo}_{93.5} - 81.5$ ) that vary both within and between the ultramafic bodies.
- 3) The majority of the primary (igneous) olivines have compositions between  $\text{Fo}_{88}$  and  $\text{Fo}_{90.5}$ , which would have been in equilibrium with magmas with between 16 and 18 wt% MgO, but these compositions may represent the average, homogenized compositions of originally zoned grains (with more magnesian cores and less magnesian rims) rather than equilibrium compositions.
- 4) The most magnesian olivines ( $\text{Fo}_{93}$ ) found during this study have compositions that are similar to those expected to be in equilibrium with the most magnesian volcanic rocks found within the Bah Lake assemblage and suggest the initial magma composition may have been between 20 and 22 wt% MgO.
- 5) Variations in the Mn and Ni contents of olivines in different mineralized and non-mineralized ultramafic bodies record:
  - a) Fractional crystallization of a sulfide-undersaturated magma with or without the assimilation of pelitic or gneissic wall rocks (e.g., the ultramafic body intersected by DH74391 at Thompson Mine and the base of the upper ultramafic body intersected by DH74276 at Thompson Mine).



- b) Fractional crystallization a sulfide-undersaturated magma accompanied by the assimilation of a Fe and/or Mn-rich, sulfide-poor component, that may represent a silicate-facies iron-formation (e.g., Mystery Lake, the lower ultramafic body intersected by DH74376 at Thompson Mine, or parts of the North Manasan ultramafic body).
  - c) Fractional crystallization of a sulfide-saturated magma either with or without the assimilation of an Mn-rich component (the mineralized ultramafic body intersected by DH 74381 at Thompson Mine or parts of ultramafic bodies from Birchtree).
  - d) Batch equilibration of a sulfide-undersaturated magma with sulfide liquid at different R factors followed by fractional crystallization of a sulfide-saturated magma (e.g., the mineralized ultramafic body intersected by DH 74381 at Thompson Mine (low R-factor), Brostrom Lake (intermediate R-factor), and the lower ultramafic body intersected by DH 74376 at Thompson Mine (high R-factor)).
- 6) Although Ni depletion in olivine appears to correlate with mineralized locations, Ni depleted olivines also occur in several reportedly non-mineralized bodies in the exposed part of the belt (e.g., Brostrom Lake) and several mineralized bodies (in particular Thompson and Pipe Pit) either exhibit negligible Ni-depletion (signifying a lack of mineralization) or a heterogeneous distribution of depletion within the body (indicating that the mineralization process is only recoded in the olivine compositions in parts of the bodies).

## 8.4.4 Whole-Rock Compositions

### 8.4.4.1 Major and Minor Elements

The whole-rock major and selected minor element compositions of the analyzed rocks are presented as MgO variation diagrams in **Figures 8.12 to 8.14**. Also plotted are the calculated compositions of magmas and cumulate rocks produced by fractional crystallization of a likely parental magma with and without the assimilation of sedimentary rocks (shown separately without any sample data in **Figure 8.11**).

The presence of sulfides in the samples increases the abundances of S, Fe, Co, Ni, and Cu in the rocks and at the same time decreases the abundances of all other elements owing to dilution of the silicate phases, hampering comparisons of the silicate components of mineralized and non-mineralized samples. Normative methods can be used to recalculate the samples sulfide-free. However, such calculations involve assumptions regarding the Fe contents of the sulfide/oxide/silicate phases and the Ni and Co contents of the sulfide phases, they commonly ignore the presence of oxides in the sulfide phase, and they are inaccurate when only minor amounts of sulfides are present. For this reason a second series of diagrams are presented that plot only samples with low sulfide contents for each element for the northern region of the TNB and for Fe, Ni, and Co (elements housed in both sulfide and silicate phases) for the central and southern regions. Because the amount of sulfide in the samples from the central and southern regions is generally low, the effect of dilution is small for most of these samples.

### ***Fractional Crystallization-Assimilation models***

As discussed by Leshner and Stone (1996), elemental variations during crystallization can be modeled using fairly simple equations (Shaw, 1970), but in order to accommodate variations in partition coefficients with changing lava composition (see above), the crystallization of mafic-ultramafic magmas is normally modeled using non-predictive iterative incremental techniques (Duke and Naldrett, 1978; Duke, 1979; Arndt and Jenner, 1986; Barnes et al., 1995; Leshner and Arndt, 1995) or using predictive thermodynamic methods (e.g., Nielsen, 1988; Ghiorso & Sack, 1995).

There are several physical models by which crystallization may occur, including: 1) *equilibrium crystallization* (EC), in which the crystallizing solids remain in equilibrium with the evolving liquid, which results in less fractionation than FC, 2) *pure fractional (Rayleigh) crystallization* (FC), in which crystallized solids are completely removed from the magma, which normally results in the strongest depletions in compatible elements and strongest enrichments in incompatible elements, 3) *partial fractional crystallization* (PFC), in which some of the liquid is trapped and removed with crystallizing solids, reducing the degree of fractionation of both compatible and incompatible elements, 4) *fractional crystallization-replenishment* (FCR) in which the evolving magma is replenished with less evolved magma, which also retards fractionation, and 5) *assimilation-fractional crystallization* (AFC), in which the magma is contaminated, typically by upper continental crustal rocks, which normally accelerates fractionation. For example, Duke and Naldrett (1978) and Arndt and Jenner (1986) used an FC model, Budahn (1986) and Barnes et al. (1995) used an EC model, and Leshner and Arndt (1995) used an AFCR model. The differences between the models are most significant for highly compatible elements (i.e., high D), such as Ni in olivine and PGE in sulfide.

In nature, the type of crystallization probably varied within the volcanic-subvolcanic system and within individual units and changed with time. For example, komatiites lavas probably convected vigorously (Turner et al., 1986), but spinifex-textured zones appear to have crystallized rapidly (Donaldson, 1982) and accumulated both olivine (Leshner et al., 1981; Bickle, 1982; Arndt, 1986) and trapped liquid, and the cumulate zones appear to have accumulated olivine (Barnes et al., 1983; Leshner et al., 1984; Stolz and Nesbitt, 1981) and trapped liquid. Thus, crystallization of spinifex-textured rocks is probably best modeled by PFC during the initial stages and by EC during the final stages. Crystallization of orthocumulate, mesocumulate, and adcumulate rocks in volcanic and subvolcanic settings is probably best modeled by FCR during the initial stages, with FC:R decreasing with increasing degree of accumulation, by PFC during the intermediate stages, and by EC during the final stages. Crystallization of crescumulate rocks (including "harrisites") is probably best modeled by PFCR. It is also quite likely that the most rapidly cooled zones crystallized under disequilibrium conditions, in which case the efficiency of the fractionation process will also depend on the relative rates of diffusion and crystallization, which will vary for each element. Although the geochemical differences between the different physical models can be quite significant (see Leshner and Stone, 1996), they are bracketed in many cases by FC and AFC. Therefore, in order to reduce the number of models, we have concentrated on modeling FC and AFC.

**MELTS Models**

In order to compare the trends in the major element data with those expected from various types of fractionation processes, several models were generated using MELTS (Ghiorso & Sack, 1995)<sup>2</sup>:

- 1) Pure FC of an ultramafic magma without country-rock assimilation (labelled “FC Trend”).
- 2) FC of an ultramafic magma contaminated with up to 30% pelitic sedimentary rock (labelled “AFC Pelite”).
- 3) FC of an ultramafic magma contaminated with up to 30% silicate facies iron-formation (labelled “AFC Iron-formation”).

In the initial models, the parental magma composition (Magma 1) was assumed to be similar to the most magnesian basalts or komatiitic rocks of the Bah Lake assemblage (sampled at Upper Ospwagan Lake and Mystery Lake by P. Theyer and D. Peck and described in Theyer et al., 1999). However, it was found that a different, more silicic initial composition (Magma 2) was required to model many of the ultramafic bodies in the northern and central regions of the TNB (see below). The compositions of the two potential parental magmas and other components used in the modeling are listed in **Table 8.2**.

Although each of the three models calculated using Magma 1 as the initial melt composition predicts that olivine ± chromite will be the main phases to crystallize from an ultramafic magma during both “pure” fractional crystallization (Model 1) and fractional crystallization combined with assimilation of either pelitic or iron-rich sedimentary rocks (Models 2 and 3), the melt trajectories and the phase assemblages that fractionate from the more evolved magmas differ significantly between the three fractionation models owing to the felsification of the magma by the sedimentary rocks, leading to differences in the trends on TiO<sub>2</sub>-MgO, Al<sub>2</sub>O<sub>3</sub>-MgO, and SiO<sub>2</sub>-MgO plots.

**Model 1** (FC): Pure fractional crystallization of the inferred parental magma produces olivine-rich cumulate rocks (e.g., dunites and/or peridotites), leading to a progressive enrichment in Ti, Al, Ca, and Fe in the magma. At approximately 8-10 wt% MgO, the magma becomes saturated in clinopyroxene and produces a small volume of clinopyroxenite cumulate before plagioclase appears on the liquidus and the magma starts to crystallize a melanogabbroic (clinopyroxene + plagioclase) cumulate assemblage.

---

<sup>2</sup> Although the MELTS model is thermodynamically predictive and is therefore able to determine both the phase assemblage present at each point along the fractionation path and the major element compositions of the liquidus phases, it is only able to model the behaviour of the major elements and a few minor elements (e.g., Ni and Cr), so is cannot be used directly to aid in the interpretation of the trace element compositions of mafic and ultramafic rocks.

**Table 8.2** Whole-rock compositions of components used in MELTS models

	<b>Magma 1</b>	<b>Magma 2</b>	<b>Pelitic Sedimentary Rock</b>	<b>Silicate-Facies Iron-formation</b>
SiO <sub>2</sub>	47.00	49.35	66.14	59.00
TiO <sub>2</sub>	0.56	0.38	0.63	0.28
Al <sub>2</sub> O <sub>3</sub>	8.49	8.73	18.64	7.41
Fe <sub>2</sub> O <sub>3</sub>	0.00	0.00	0.00	0.00
FeO <sup>t</sup>	11.37	10.95	5.01	18.16
MnO	0.17	0.16	0.04	0.90
MgO	22.32	22.44	1.88	6.15
CaO	8.52	6.47	1.19	4.20
Na <sub>2</sub> O	0.91	0.83	1.69	1.42
K <sub>2</sub> O	0.06	0.06	4.51	1.15
P <sub>2</sub> O <sub>5</sub>	0.06	0.06	0.07	0.26
S	1480	1480	350	18599
Ni	980	950	40	450
Cr	2158	2200	108	77

**Note:** Parental magma composition 1 estimated from the pyroxenitic portions of TNB ultramafic bodies and the least fractionated volcanic rocks of the Bah Lake assemblage. Calculations carried out at 0.1 kbar,  $f_{O_2}$  = FMQ and for temperatures between the liquidus (~1500°C) and 1100°C. 30% assimilated at an initial temperature of 20°C added in 20 equal increments between T = 1500 and 1300°C. Major element oxides in wt%. S, Ni, and Cr in ppm.

**Model 2** (AFC Pelite): The initial phases to crystallize from a magma that assimilates a pelitic component are similar to those formed during FC (i.e., olivine ± chromite). However, because the average Ospwagan Group pelitic rock has lower Fe and higher Si contents than the evolving ultramafic magma, the assimilation of pelitic material produces both magma and olivine compositions that are depleted in Fe relative to those produced by pure fractional crystallization and crystallizes orthopyroxene (hypersthene) as a cumulus phase prior to clinopyroxene and clinopyroxene + plagioclase saturation (**Fig. 8.11**). Thus, the most obvious expression of contamination by a pelitic component will be the formation of orthopyroxenites or harzburgites (in which Opx is an intercumulus phase) instead of dunites or wehrlites (in which Cpx is an intercumulus phase).

**Model 3** (AFC Iron-formation): The addition of Fe- and Mn-rich material (e.g., the Pipe Formation silicate-facies or sulfide-facies iron-formations) should result in higher Si and Fe or Mn contents in the magma and the production of more Si- and Fe- or Mn-rich cumulus phases than would be produced by pure fractional crystallization (**Fig. 8.11**). This is confirmed by the MELTS models, which also indicate that the assimilation of such sedimentary rocks results in the crystallization of orthopyroxene. However, because the MELTS program is not currently able to model the compositions of silicate magmas in equilibrium with an immiscible sulfide phase, it cannot properly model melting and *partial* assimilation of a sulfide-rich contaminant, in which chalcophile components in the magma are selectively partitioned into the sulfide phase. Although most komatiitic magmas are strongly undersaturated in sulfide (Keays, 1982, 1995; Leshner & Groves, 1986; Leshner &

Stone, 1996; Leshner et al., 2001) and have the heat capacity to dissolve up to 50% of their mass before crystallizing completely (see discussion by Leshner & Arndt, 1995; Williams et al., 1998), the maximum amount of S that can dissolve in mafic-ultramafic magmas is quite small (~0.3%: Shima & Naldrett, 1975). The sulfur content at sulfide saturation (SCSS) varies with  $fO_2/fS_2$  and decreases with decreasing Fe content and decreasing temperature (Haughton et al., 1974; Shima & Naldrett, 1975; Wallace & Carmichael, 1992; Li & Naldrett, 1993; O'Neill & Mavrogenes, 2002). The amount of S than would be dissolved also depends on the initial S content, which would be lower in more magnesian, higher degree partial melts and higher in less magnesian, lower degree partial melts. Bulk mixing calculations indicate that a high-Mg komatiite would require the addition of only ~2% sulfide facies iron-formation containing 50% FeS to achieve sulfide saturation, whereas a low-Mg komatiitic magma would require only ~1% of such a component to have the same effect. After reaching sulfide saturation, a magma would be able to dissolve additional silicate components (see discussion by Leshner & Campbell, 1993; Leshner & Burnham, 2001), but no more sulfide. This would limit the amount of Fe that could be dissolved and would reduce the Co, Ni, Cu, and PGE contents of the magma, depending on the relative abundances of magma and residual sulfide. Nevertheless, the assimilation of Fe-rich sulfidic sedimentary rocks should produce fractionation trends and cumulate compositions that differ from those formed by the assimilation of Fe-poor sedimentary rocks.

### ***Major Element Compositions of TNB Mafic and Ultramafic Rocks***

Although the compositions of most of the mafic volcanic rocks plot along the trends expected for fractionation of olivine  $\pm$  chromite, clinopyroxene, or clinopyroxene + plagioclase, as predicted by the MELTS models for normal fractional crystallization processes, the whole-rock major element compositions of the TNB ultramafic bodies and some of the amphibolites associated with them exhibit considerable scatter on many of the plots in **Figures 8.11 to 8.14** and many do not plot along the model curves. Whereas most of the scatter in the Ca, Na, and K contents of the ultramafic rocks may be accounted for by the mobilization of these elements during serpentinization (see **Section 7.2** and discussion by Leshner & Stone, 1996) and their relatively low abundances, the scatter in other elements (e.g., SiO<sub>2</sub>, Al<sub>2</sub>O<sub>3</sub>, MnO, and FeO<sup>4</sup>) and departures from the models suggest that processes other than FC and alteration were involved.

One of the most obvious features of the major element plots is the difference between the major element trends shown by the most magnesian basalts of the Bah Lake assemblage and the Winnipegosis komatiites and those of the ultramafic bodies, with the former exhibiting significantly higher TiO<sub>2</sub> and CaO and lower MnO and SiO<sub>2</sub> at similar MgO contents. Because the two trends overlap at moderate MgO contents, the differences in the trends probably indicate differences in the initial compositions of the magmas from which the two groups of rocks formed. These differences are evident in the trace element abundances and ratios of the two groups (see below). In order to investigate the effects of starting with a more silica-rich initial composition, a fourth MELTS run was performed for FC of a magma with an initial composition similar to that of an olivine pyroxenite at Thompson Mine (Magma 2 in **Table 8.2**, based on sample 74378-0-1475.15 collected by L. Hulbert).

Whereas the cumulate rocks produced by FC of Magma 1 are dominated by olivine, oxides (Mg-chromite, chromite *sensu stricto*, and magnetite with increasing degrees of differentiation), and clinopyroxene, and only contain orthopyroxene when the magma is

contaminated by the assimilation of upper continental crustal rocks (Models 2 and 3, above), the cumulate rocks produced by FC of Magma 2 are dominated by olivine, oxides, and orthopyroxene, even without the addition of crustal material, and the magma only begins to fractionate clinopyroxene and feldspar at a late stage of differentiation ( $\text{MgO}_{\text{liquid}} < 6.8 \text{ wt\%}$ ). The differentiation of Magma 2 also appears to be characterized by the crystallization of less MnO-rich olivines, leading to a significant increase in MnO in the liquid during differentiation.

When the compositions of the most olivine-rich cumulates of the ultramafic bodies are compared to those expected for the fractionation of an initial magma similar to Magma 2, they not only plot along the mixing lines expected for the mixtures of olivine and trapped liquid of the correct concentration (and show much better agreement than with the olivine-magma mixing trends expected if the initial magma were similar to Magma 1), but also show the MnO depletion expected in cumulate rocks that form from a magma of this initial composition. Some samples also plot toward significantly higher  $\text{SiO}_2$  and lower  $\text{TiO}_2$ , CaO, and  $\text{Al}_2\text{O}_3$  contents, consistent with the accumulation of orthopyroxene. Most of these anomalous samples are from the northern region of the TNB (e.g., lower mineralized ultramafic body intersected by DH74376 at Thompson Mine and the Thompson Airport, North Manasan, Oswagan Lake, Pipe 1 and 2, and Grass River ultramafic bodies). However, several samples from the central region (e.g., W-56 and W-22 ultramafic bodies at William Lake and one of the ultramafic bodies in the Davidson Lake area) and rare samples from the southern TNB also show anomalous compositions. Although both the clinopyroxene and orthopyroxene that are expected to fractionate from the ultramafic magma have higher  $\text{SiO}_2$  and lower  $\text{TiO}_2$  and  $\text{Al}_2\text{O}_3$  contents than the liquid, and could therefore equally well explain the observed compositions, the low CaO contents of the anomalous samples may indicate the presence of cumulus orthopyroxene, consistent with significant assimilation of a crustal component either prior to or during emplacement.

### ***Pearce Element Ratio Diagrams***

Because in many cases the anomalous samples described above originated from the less cumulate-rich (or more evolved) parts of the ultramafic bodies, in which there was very poor textural or mineral preservation, the inferred presence of orthopyroxene could not be verified petrographically. In order to confirm the mineral assemblages involved in the crystallization of the ultramafic and mafic rocks, Pearce Element Ratio (PER) diagrams were constructed using the  $\text{SiO}_2$ ,  $\text{FeO}^{\text{t}}$ , and MgO contents of the samples from the different regions of the TNB (**Fig. 8.15**). Because  $\text{TiO}_2$  data were available for all samples, because Ti should be both immobile and behave as a conserved (incompatible) element through most of the fractionation crystallization history of the ultramafic magma, and because it exhibits a very low variance (see **Section 7.2.2**), it was used as the denominator in the ratios. In each figure only samples with low S contents were considered, to avoid samples with elevated Fe owing to the presence of magmatic sulfides.

On plots of molar  $(\text{Fe}+\text{Mn}+\text{Mg})/\text{Ti}$  vs. molar  $\text{Si}/\text{Ti}$  (**Fig. 8.15**), the majority of the ultramafic rocks plot close to an olivine control line with molar  $(\text{Fe}+\text{Mn}+\text{Mg})/\text{Si} \approx 2$ , with some scatter toward slightly lower  $(\text{Fe}+\text{Mn}+\text{Mg})/\text{Si}$  ratios. Although the displacement of samples from the olivine control line appears to increase in the more altered rocks, indicating that it may result from the addition of silica during serpentinization, even relatively fresh rocks occasionally plot off the olivine array, consistent with the presence of small amounts of pyroxene in some

of the samples. Most of the samples with high  $\text{SiO}_2$  and low  $\text{TiO}_2$ ,  $\text{Al}_2\text{O}_3$ , and  $\text{CaO}$  that were identified in the bivariate plots as potentially containing orthopyroxene plot along a line with molar  $(\text{Fe}+\text{Mn}+\text{Mg})/\text{Si} \approx 1$ , consistent with the accumulation of either orthopyroxene or olivine + clinopyroxene in a constant 1:1 ratio. Because olivine and clinopyroxene are not predicted (or observed) to be cotectic phases during either pure fractional crystallization or fractional crystallization with sedimentary rock assimilation and because the samples that plot along the trend with lower gradient generally have lower Ca contents, the PER plots are interpreted to confirm the presence of orthopyroxene in these samples and the probable assimilation of sedimentary rock during the production of these bodies.

In addition to the confirmation of the phase assemblages that fractionated to form the cumulate rocks of the ultramafic bodies, PER diagrams may be used to estimate the compositions of the cumulus olivine using a plot of molar  $\text{Mg}/\text{Ti}$  vs. molar  $(\text{Fe}+\text{Mn})/\text{Ti}$  (**Fig. 8.16**). In this plot, samples derived from a similar parental magma composition plot along lines with constant molar  $(\text{Fe}+\text{Mn})/\text{Mg}$ .

On the basis of this PER plot, olivine cumulate rocks from different ultramafic bodies in the TNB may be separated according to the estimated compositions of their olivines:

- 1)  $\text{Fo}_{86-88}$ : Winniepegosis komatiites
- 2)  $\text{Fo}_{88}$ : Grass River and Spur South
- 3)  $\text{Fo}_{88-90}$ : Hambone East, Pipe 2, Birchtree, North Manasan, and Mystery Lake North and East
- 4)  $\text{Fo}_{88-92}$ : Bucko Lake, Ospwagan Lake, and Thompson
- 5)  $\text{Fo}_{90-92}$ : other William Lake bodies, Mid Lake, and Nichols Lake
- 6)  $\text{Fo}_{92}$ : Brostrom Lake and William Lake W-56
- 7)  $\text{Fo}_{90-94}$ : William Lake W-22

Although some of the differences between the trends on the  $\text{Mg}/\text{Ti}$  vs.  $(\text{Fe}+\text{Mn})/\text{Ti}$  plots may be accounted for by the restricted range of depths sampled within some of the ultramafic bodies (e.g., only the top, more evolved part of the Spur South body was intersected by the drill hole that was studied, hence the samples only represent the more evolved part of the system), where relict olivines have been preserved, the ranges in average olivine compositions deduced from the whole-rock trends generally coincides with the measured compositions of the olivines, indicating that the different trends do represent original differences in the compositions of the magmas from which the sills formed.

### ***Minor Element Compositions***

#### **Chromium**

The ultramafic rocks in the TNB may be divided into three groups on the basis of their Cr contents (**Figs. 8.12 to 8.14**):

- 1) Cr-rich cumulates, which exhibit a positive correlation between Cr and  $\text{MgO}$  that extrapolates toward the compositions of the mafic and ultramafic rocks of the Bah Lake assemblage. Similar rocks in other areas have been interpreted to represent fractionation and accumulation of olivine + magnesiochromite in roughly cotectic proportions (~50:1:

Leshner & Stone, 1996; Barnes & Brand, 1999) from a chromite-saturated komatiitic basalt magma.

- 2) Intermediate-Cr cumulates, with moderate Cr contents (3000 – 6000 ppm) that plot below the correlation shown by the Cr-rich cumulate rocks. Whereas Barnes & Brand (1999) interpreted similar rocks as olivine-rich cumulates derived from chromite-undersaturated magma in which chromite had been physically added, Leshner & Stone (1996) interpreted them as cumulates derived from a magma that reached chromite saturation *during* accumulation (i.e., as rocks that contained an early-crystallized component of olivine and a later-crystallized component of olivine + chromite).
- 3) Cr-poor cumulates, which plot along a trend between ~2500-3000 ppm Cr at 20 - 22 wt% MgO and ~1500 - 2000 ppm Cr at 50% MgO. Similar rocks in other areas have been interpreted to represent fractionation and accumulation of olivine from a chromite-undersaturated komatiitic magma (Leshner & Stone, 1996; Barnes & Brand, 1999).

Although there are considerable overlaps in the Cr contents of different ultramafic bodies in the TNB, Cr-rich cumulates derived from komatiitic basaltic magmas are more abundant in non-mineralized or weakly mineralized bodies, whereas Cr-poor cumulates derived from komatiitic magmas are more abundant in mineralized bodies.

Variations in the olivine:chromite ratios of ultramafic cumulates may occur in response to changes in one or more of the different parameters that control the solubility of chromite in ultramafic magmas. Although the primary control on chromite solubility in most ultramafic magmas is interpreted to be the temperature and MgO content of the melt (with most magmas reaching chromite saturation at ~1400°C and ~20 wt% MgO: Leshner & Stone, 1996), experimental studies (e.g., Murck & Campbell, 1986) have shown that redox conditions can also markedly influence chromite solubility such that high-Mg komatiites may become saturated in chromite earlier under oxidised conditions and low-Mg komatiites may remain undersaturated in chromite under reduced conditions (see discussion by Leshner & Stone, 1996).

Because most of the mineralized channelized flow units in many Western Australian Ni-Cu-(PGE) deposits are composed of Cr-poor olivine cumulates and most of the non-mineralized laterally-adjacent sheet flows are composed of Cr-rich olivine cumulates, Woolrich & Giorgetta (1978), Leshner & Groves (1984), Leshner & Stone (1996), and Barnes & Brand (1999) suggested that the variation in Cr with Mg (together with variations in the Ni:Cr ratio) may be used to discriminate between mineralized and non-mineralized komatiites. Woolrich & Giorgetta (1978) interpreted the differences to reflect variations in the oxidation states of different magmas that formed the two lithologies, but Leshner & Groves (1984), Leshner & Stone (1996), and Barnes & Brand (1999) interpreted these lithologies as lateral facies that simply differed in terms of MgO content and therefore chromite saturation state. Within the context of the ultramafic bodies in the TNB, the greater abundance of low-Cr cumulate rocks in mineralized ultramafic bodies and association of high-Cr cumulate rocks with non-mineralized bodies suggests that a similar relationship may exist in the TNB and that the magmas from which the non-mineralized bodies formed were either initially closer to chromite-saturation or reached it earlier during differentiation.

The abundance of Cr in cumulate rocks in the *central* TNB correlates negatively with the average Fo contents of the cumulate olivines calculated from the PER plots, implying a



relationship between low magnesium contents, chromite-saturation, and the absence of mineralization (or the association of mineralization with more magnesian, chromite undersaturated magmas). However, the similarity between the measured and/or estimated compositions of the olivines from both mineralized (e.g., Pipe, Thompson, Birchtree, and Ospwagan Lake) and non-mineralized ultramafic bodies (e.g., Spur South, Mystery Lake North and East, and Hambone East) in the *northern* TNB indicates that the presence or absence of mineralization in that region is not related to the MgO content of the magma and that the link between the behaviour of chromite and the mineralization status of the bodies may represent changes in the oxidation state of the magma. The consequences of contamination on the Si and Fe contents, oxidation state, and chromite and sulfide solubility in komatiitic magmas are summarized in **Table 8.3**.

**Table 8.3** General consequences of contamination on the Si and Fe contents, oxidation state, and chromite and sulfide saturation states of komatiitic magmas

Assimilant	Si Content	Fe Content	Oxidation State	Chromite Solubility	Sulfide Solubility
Continental crust	increase	decrease	(increase)	(decrease)	(decrease)
Pelite	increase	decrease	(increase)	(decrease)	(decrease)
Graphitic pelite	increase	decrease	decrease	increase	increase
Magnetite-chert IF	increase	increase	increase	decrease	<b>decrease</b>
Silicate-chert IF	increase	increase	no change	no change	(decrease)
Pyrite-chert IF	increase	increase	increase	decrease	<b>decrease</b>
Carbonate	decrease	decrease	(increase)	(decrease)	(decrease)

The precise effects are actually more complex, as sulfide solubility depends on a large number of interrelated factors, including T, P,  $a_{\text{FeO}}$ ,  $f_{\text{O}_2}/f_{\text{S}_2}$ , the amount of contamination, and the rate of exsolution of volatiles.

Although the solubilities of chromite and sulfide both decrease with increasing  $f_{\text{O}_2}$ , suggesting that the presence of chromite may be a favourable indicator for mineralization in sulfide-poor PGE-(Cu)-(Ni) reefs (Page, 1971), reducing sulfide solubility via oxidation is not a particularly efficient way of making a sulfide-rich Ni-Cu-(PGE) deposit because the amount of S that can dissolve in magmas, even high-T mafic-ultramafic magmas, is quite small ( $\leq 0.3\%$ ; Shima & Naldrett, 1975) and one would have to oxidize all of the  $\text{Fe}^{2+}$  in the magma to  $\text{Fe}^{3+}$  to quantitatively extract the S. Before that could occur, much of the S would likely be lost as  $\text{SO}_2$ . A much better way to generate a magmatic sulfide deposit is to melt sulfide (Leshner & Groves, 1986; Leshner, 1989; Naldrett, 1989). For example, if the magma is undersaturated in sulfide, which is probably the case for most komatiitic magmas, melting and assimilation of small amounts of a sulfide-chert IF will increase the Si content (decreasing sulfide solubility slightly), either oxidize or reduce the magma slightly (depending on the graphite/pyrite content of the IF and leading to either an increase (graphitic) or decrease (pyritic) in sulfide and chromite solubility), and increase the FeS content of the magma significantly (until it reaches sulfide saturation). Further addition sulfide-chert IF to the sulfide-saturated komatiitic magma will further increase the Si content (further decreasing sulfide solubility), further oxidize or reduce the magma (changing sulfide

and chromite solubility), but will not result in any further increase in the FeS content of the magma<sup>3</sup>, leaving the remainder to form a sulfide xenomelt.

Melting and assimilation of barren carbonate (e.g., parts of the Thompson Fm.) would likely oxidize some of the Fe<sup>2+</sup> in the magma and therefore *decrease* the solubility of both chromite and sulfide. Melting and assimilation of pelite or semi-pelite (e.g., parts of the Manasan Fm. or Setting Fm.) would increase the Si content and decrease the Fe content of the magma and therefore also *decrease* the solubility of both chromite and sulfide. Although these processes may decrease the solubility of *some* of the endogenous S, the amount will be quite small unless the amount of contamination is catastrophic, which would result in the crystallization of abundant *high-Cr* cumulates<sup>4</sup>. In order to account for the association of mineralization with *low-Cr* cumulates in the northern TNB, it would necessary for the ultramafic magmas to have interacted with a *reduced* sulfide source. One such source may be a graphitic sulfide-facies IF of the lower unit of the Pipe Formation (which typically contain >3% total carbon). Although the reducing conditions generated by the presence of graphite may increase the solubility of sulfide slightly, the amount of additional S that would become available to dissolve additional S as FeS would be limited by the amount of Fe<sup>3+</sup> available to be reduced to Fe<sup>2+</sup>, which is normally less than 10% of total Fe, so the amount of sulfide in the IF should be far in excess of that needed to reach sulfide saturation and generate ores. It should be noted that in the absence of sulfide, the melting and assimilation of a graphitic pelite (e.g., parts of the Setting Fm.) would likely reduce some of the Fe<sup>3+</sup> in the magma and *increase* the solubility of chromite and sulfide, leading to low Cr cumulates, but no ore.

### Nickel and Cobalt

Because the presence of even small quantities of sulfide can significantly affect the total Ni and Co contents of an olivine cumulate rock and therefore obscure *magmatic* trends, samples with low S contents (S <0.3 wt%) will be discussed before considering the entire database of both mineralized and non-mineralized samples, in order to examine the normal petrogenetic processes that acted on the TNB magmas before discussing the mineralizing processes.

With the exception of the ortho- and clinopyroxenite rocks at Ospwagan Lake and Thompson Mine, which have lower than normal Ni and Co contents in their silicate components owing to the accumulation of Ni-poor Opx and Cpx rather than Ni-rich Ol, the majority of the sulfide-poor mafic and ultramafic samples collected from the northern region of the TNB plot within the range expected for mixtures between variably-fractionated sulfide-undersaturated ultramafic magmas (with an initial composition similar to the most magnesian picrites and komatiitic basalts of the Bah Lake assemblage) and calculated equilibrium

---

<sup>3</sup> As noted above, the capacity of silicate magmas to dissolve S, even high-T komatiitic magmas with significant Fe contents, is quite limited, so the effect of melting additional sulfide-chert IF will be to dissolve the silica (which should be miscible) but not the sulfide (which should be immiscible). The addition of Si to the magma may reduce the solubility of some of the endogenous S, but the amount will be small compared to the amount of exogenous S.

<sup>4</sup> A good example of the inefficiency of contamination to generate magmatic sulfide deposits is the Paríngas Basalt at Kambalda, which has been interpreted to have been generated by up to 30% contamination of high-Mg komatiite by continental crust but has remained undersaturated in sulfide (Leshner & Arndt, 1995; Leshner et al., 2001). The only arguable example of crustal contamination *by itself* generating a significant magmatic sulfide deposit is Sudbury.

olivine compositions (**Fig. 8.13**). Such a variation indicates that most of the cumulate and mafic rocks formed from magmas that were not significantly depleted in Ni. Exceptions are the whole-rock compositions of many (but not all) of the chromite-poor olivine adcumulate rocks collected from the Mid Lake and Mystery Lake ultramafic bodies, together with both the whole-rock and mineral compositions of dunites in the Brostrom Lake ultramafic body. These samples plot significantly below the trend expected for sulfide-undersaturated olivine cumulates. Although this suggests that the magmas from which these rocks formed might have been depleted in chalcophile metals, most of these samples have very low sulfur contents, indicating that the magmas from which they formed were sulfide-undersaturated at the time of emplacement. There are several possible explanations for this: the rocks may have formed from magmas that were initially depleted in Ni (see discussion in **Section 8.4.3.4**), some of the sulfides may have been dissolved (i.e., that these rocks are complementary in terms of process to the Ni-enriched rocks in the W-56 William Lake body: **Section 8.4.3.5**), and/or Ni and S may have been mobile during metamorphism. At this time, there are insufficient data available to determine which process has been most important, although the presence of minor Ni-undepleted samples in the same bodies suggest that the second or third situations are more likely.

When plotted as a function of MgO content (**Fig. 8.13**), the Ni contents of the non-mineralized ultramafic bodies located outside the William Lake area define an array along a tie-line between the inferred parental magma composition and the compositions of olivine calculated to be in equilibrium with it. This is also consistent with the accumulation of olivine from a sulfide-undersaturated ultramafic magma. However, the weakly mineralized bodies located in the William Lake area are characterized by anomalously high Ni contents at similar MgO compared to the other bodies, which mirror the high Ni contents determined in their constituent olivines (**Section 8.4.3.5**). The exclusion of samples containing more than trace amounts of sulfide from **Figure 8.13** indicates that the contrast between the two groups of bodies cannot be accounted for by variations in the abundance of disseminated sulfides between the two groups of cumulates and supports the interpretation that the magma from which these bodies formed was either anomalously Ni-rich or that the Ni was more efficiently removed from the magma by the olivines that make up the William Lake ultramafic bodies.

## Sulfur

Although the sulfide contents of the mineralized ultramafic bodies are generally greater than those of the non-mineralized ultramafic bodies, both groups show significant variations in S content at similar MgO, consistent with the presence of olivine and sulfide in variable proportions. Calculations of the compositions of cumulate rocks containing olivine and sulfide in approximately cotectic proportions (~60:1: Duke, 1986) indicate that the most magnesian rocks (olivine + sulfide adcumulates) should contain 5000-6000 ppm S and that samples containing variable proportions of trapped silicate liquid should define an array extending toward the melt composition. Although many of the most magnesian rocks containing disseminated sulfides in both mineralized and non-mineralized bodies have S contents in the range expected for cotectic accumulation of olivine and sulfide, a large number of the ultramafic bodies contain either more or less S than is predicted by the calculations. Whereas the presence of excess sulfide in the mineralized bodies suggests that sulfide has been physically concentrated relative to olivine, following cotectic crystallization

or following a process that generated sulfide in amounts greater than the cotectic proportion, the low sulfide contents in parts of both the mineralized and non-mineralized ultramafic bodies indicates that the parental magmas must have been initially sulfide-undersaturated and may have only reached sulfide saturation during an intermediate stage of their crystallization history (see discussion by Leshner & Stone, 1996).

### ***Interim Summary***

- 1) Whereas most of the mafic volcanic rocks of the TNB have compositions consistent with fractional crystallization of olivine  $\pm$  chromite, clinopyroxene, or clinopyroxene + plagioclase from a komatiitic magma, most of the olivine cumulate rocks and pyroxenites of the ultramafic bodies have compositions consistent with fractional crystallization of olivine  $\pm$  chromite, orthopyroxene, or clinopyroxene + plagioclase from a more silicic initial magma composition, suggesting that there were at least two distinctly different parental magmas in the TNB.
- 2) Although the parental magmas to both the ultramafic bodies and the mafic and ultramafic volcanic rocks were initially undersaturated with respect to chromite, the degree of undersaturation was greater in the mineralized ultramafic bodies, either as a result of an initially higher MgO content (as a result of variable degrees of differentiation or the amount of initial mantle melting) or emplacement under more reducing conditions.
- 3) Several samples with intermediate MgO contents are enriched in SiO<sub>2</sub> and depleted in TiO<sub>2</sub>, Al<sub>2</sub>O<sub>3</sub>, and CaO, consistent with accumulation of orthopyroxene as a result of felsification of the magma by the assimilation of sedimentary rock.
- 4) Trends between the whole-rock cation ratios of the ultramafic rocks indicate that average olivine compositions range from Fo<sub>88</sub> in the more evolved portions of some of the ultramafic bodies in the northern region of the TNB to between Fo<sub>92</sub> and Fo<sub>94</sub> in ultramafic bodies in the southernmost part of the exposed TNB and the central region of the TNB. Such olivine compositions would be consistent with the crystallization and accumulation of olivine from magmas containing between 23.5 and 13.5 wt% MgO.
- 5) Mineralization appears to be associated with Cr-poor cumulates in both the central and northern regions of the TNB. Whereas this relationship may be accounted for by the association of mineralization with bodies formed from hotter and more magnesian magmas in the central region of the TNB (William Lake area), there appears to be less of a connection between MgO content and mineralization in the northern region of the TNB, where the redox state of the magma following assimilation appears to be a more important factor.
- 6) Most of the cumulates and mafic rocks formed from magmas that were not significantly depleted in Ni, indicating that they had neither lost significant amounts of sulfide nor interacted with a sulfide liquid prior to emplacement.

#### **8.4.4.2 Lithophile Trace Elements**

##### ***Incompatible Lithophile Elements***

Whereas the assimilation of continental crust (or sedimentary rocks derived from it) by an ultramafic magma may lead to only subtle changes in its major element composition and those of the cumulate rocks that form from it, the same contaminant should significantly

affect the trace element chemistry of the magma owing to the more pronounced differences between the trace element signatures of the two components. Whereas many mantle-derived ultramafic magmas (including normal MORB and many plume-derived basalts, picrites, and komatiites) are strongly depleted in highly incompatible lithophile trace elements (HILE: e.g., U, Th, and LREE<sup>5</sup>; **Fig. 8.17**) relative to the inferred composition of the primitive mantle, most upper continental crustal rocks are strongly enriched in such elements, but anomalously depleted in Ta, Nb, and to a lesser extent Ti relative to U, Th, and MREE (**Fig. 8.17**). Because the abundances of incompatible elements are considerably greater in the crustal component than the magma, contamination of komatiitic magma by even small amounts of crustal material will introduce a recognizable crustal signature, which will be characterized by variable enrichment in HILE with negative Ta-Nb-Ti anomalies (**Fig. 8.17**).

Although the changes in trace element compositions that result from assimilation processes are readily displayed on mantle-normalized multielement abundance diagrams similar to **Figure 8.17**, the trends for large amounts of data are better summarized using ratios between key elements. Some of the more important ratios are La/Sm or Ce/Sm (measures of the degree of LREE enrichment) and Th/Nb (a measure of the magnitude of a negative Nb-Ta anomaly). Because the elements in each of these ratios may be expected to behave similarly and therefore not vary significantly during both high degree partial melting of the mantle and fractional crystallization of olivine  $\pm$  chromite, but will be affected differently by the assimilation of upper crustal material, these ratios are very sensitive indicators of crustal contamination. Because there is evidence that La has been mobile in strongly serpentinized and recrystallized rocks (see **Section 7.4.2.1**), we will use the Ce/Sm ratio instead of the La/Sm ratio as a measure of LREE enrichment.

When interpreting variations in Ce/Sm and Th/Nb, it is important to appreciate that because many Archean, Proterozoic, and Phanerozoic mafic and ultramafic volcanic rocks are depleted in HILE and exhibit positive  $\epsilon_{\text{Nd}}$  signatures, they are interpreted to have been derived from source that was depleted in HILE during the low-degree (1-2%, integrated) melting event that produced the HILE-enriched upper continental crust and Nb-Ta-(Ti)-enriched lower continental crust from primitive mantle (Hofmann, 1988; Rudnick et al., 2000). Thus, normal mantle at 1.9 Ga was depleted in HILE in the order  $\text{U} > \text{Th} > \text{Nb} \sim \text{Ta} > \text{LREE} > \text{Zr} \sim \text{Hf} \sim \text{MREE} \sim \text{Ti} \sim \text{HREE}$ , resulting in  $[\text{Ce}/\text{Sm}]_{\text{mn}} \sim 0.6\text{-}0.7$  and  $[\text{Th}/\text{Nb}]_{\text{mn}} \sim 0.4\text{-}0.5$  (**Fig. 8.18**), and the upper continental crust and sedimentary rocks derived from continental crust show complementary enrichments in HILE, resulting in higher Ce/Sm and much higher Th/Nb ratios (**Fig. 8.18**). Magmas derived from sources that have become enriched by inclusion of subducted oceanic crustal components (e.g., E-MORB, OIB; **Fig. 8.18**) or by addition of fluids from subducting slabs (e.g., boninites:  $\text{Cs}/\text{Sm} \sim 1.1$  and  $\text{Th}/\text{Nb} \sim 3$ , not shown), exhibit slightly higher Ce/Sm and Th/Nb compared to depleted mantle.

The mantle-normalized Ce/Sm and Th/Nb ratios of the TNB ultramafic bodies are plotted in **Figure 8.18**. Almost all of the ultramafic bodies in the northern region of the TNB are highly enriched in LREE ( $[\text{Ce}/\text{Sm}]_{\text{mn}} = 1.2 - 10$ ) and depleted in Nb relative to Th ( $[\text{Th}/\text{Nb}]_{\text{mn}} = 2 - 10$ ), consistent with contamination of the parental magmas by Ospwagan Group sedimentary rocks during their emplacement (modelled in the figure as AFC trends for ultramafic magmas

---

<sup>5</sup> Cs, Rb, K, Sr, and Ba are also highly incompatible lithophile elements, but they are normally mobile during deuteric alteration, seafloor alteration, and/or regional metamorphism.

from different mantle sources and a typical Op2 metapelite). In contrast, the majority of the mafic and ultramafic volcanic rocks in the areas around Bah Lake and Ospwagan Lake, and other locations within the northern region of the TNB exhibit trace element ratios that resemble those of the depleted mantle and plot in a distinctly different field.

The contrast between the two groups of rocks is highlighted when the Th/Nb and Ce/Sm ratios are plotted as a function of magnesium content (**Fig. 8.19** and **8.20**). With the exception of a small group of basalts in the Mystery Lake and Setting Lake areas (described in **Section 8.5.2.2**), the basalts and picrites collected from drill cores in the Mystery Lake, Ospwagan Lake, and Pipe areas and from surface exposures in the northern region of the TNB are either depleted or only marginally-enriched in Th and LREE relative to Nb and MREE. In contrast, the associated ultramafic rocks are almost all strongly enriched in highly incompatible trace elements and have negative Nb anomalies, irrespective of their mineralization status.

In each case, the trace element ratios are similar for all MgO contents within the group and there are considerable overlaps in MgO contents between the two groups. Because the initial incompatible element contents of both the volcanic and intrusive mafic and ultramafic rocks may be expected to decrease with increasing MgO contents (see plots of Zr, Nb, and Yb vs. MgO in **Fig. 8.12** to **8.14**), the absence of any recognizable relationship between incompatible trace element enrichment and MgO content in either the mafic or ultramafic rocks is inferred not to have resulted from the greater susceptibility of the ultramafic rocks to alteration (owing to their lower initial trace element contents: **Section 7.2.3**), but to represent a compositional differences that arose from different degrees of crustal assimilation during emplacement.

Although many of the mafic and ultramafic rocks in the central region of the TNB (in the William Lake area and elsewhere) are enriched in incompatible elements relative to either the primitive or depleted mantle reservoirs (**Fig. 8.18**), the degree of enrichment is considerably less than that observed in the northern region of the TNB and does not correlate with observed variations in either the major element chemistry or the mineralization status of the ultramafic bodies. Indeed, some of the most trace element enriched samples are amphibolite layers within the upper parts of the ultramafic bodies (described in **Section 5.4.3**). When plotted as a function of whole-rock MgO content, the samples from the amphibolites, ultramafic bodies, and mafic/ultramafic volcanic rocks in the region exhibit overlapping ranges of  $[\text{Th}/\text{Nb}]_{\text{mn}}$  and  $[\text{Ce}/\text{Sm}]_{\text{mn}}$  ratios (**Figs. 8.19** and **8.20**), as well as an apparent increase in trace element enrichment with increasing MgO content at high MgO contents. The enrichments in highly incompatible lithophile elements are not accompanied by proportionate increases in Th/Nb ratios, which may be attributed to minor errors in the determination of Th at low concentrations. Because both Ce and Sm are present at higher concentrations than Th, there should be less error associated with the analysis of these elements and the increasing Ce/Sm ratios at high MgO contents cannot be accounted for by analytical errors. Whereas the range of Th/Nb contents may reflect changes in magma composition and crustal assimilation during the emplacement of the ultramafic bodies, the variations in Ce/Sm may reflect LREE mobility during alteration and/or metasomatism. Although the Ce/Sm ratios of the ultramafic bodies are inferred to be unaffected by the regional serpentinization of the ultramafic bodies (**Section 7.2.3**), the apparent spread of the data away from the AFC trends in **Figure 8.18** ( $[\text{Th}/\text{Nb}]_{\text{mn}}$  vs.  $[\text{Ce}/\text{Sm}]_{\text{mn}}$ ) suggests that Ce

may have been mobile in many of the samples from the central and northern TNB. In **Figure 8.20**, the MgO-rich samples with low Ce/Sm ratios are all *unserpentinized* dunites in the W-56 ultramafic body intersected in DDH WL97-179, whereas the samples with the highest Ce/Sm ratios occur in *serpentinized* rocks from the same body, consistent with mobility of Ce (and presumably other LREE) during serpentinization.

### ***Magma Source Enrichment vs. Contamination***

Because it appears that even Ce may have been mobile in the ultramafic rocks of the TNB under certain conditions, further investigation of the trace element compositions of the mafic and ultramafic rocks bodies utilized only high field-strength elements<sup>6</sup> (HFSE: Th<sup>4+</sup>, Nb<sup>5+</sup>, Ta<sup>5+</sup>, Zr<sup>4+</sup>, Hf<sup>4+</sup>, and Ti<sup>4+</sup>) in order to identify primary variations in whole-rock compositions. Because HFSE do not form complexes with the low-charge ligands that dominate most metamorphic and many hydrothermal fluids and therefore appear to be less mobile under metamorphic conditions than many of the elements that are commonly employed in petrogenetic models (e.g., LREE and LILE), it is probable that they were less affected by metasomatism and therefore maintain a record of both source magma compositions and magmatic contamination processes (see **Section 7.2.2**).

Of the six HFSE analyzed in most of the samples, Th, Nb, and Ti were utilized for evaluation of the petrogenesis of the mafic and ultramafic rocks of the TNB owing to their contrasting behaviour during different magmatic processes such as melt extraction and/or enrichment of the mantle source or crustal contamination, which leads to the production of distinct geochemical trends (summarized below and in **Fig. 8.21**).

During mantle melting (**Fig. 8.21a**), the compatibility of Th, Nb, and Ti increases in the order Th < Nb << Ti. Because both Nb and Th are highly incompatible in almost all mantle phases, they are both rapidly consumed during partial melting to leave a highly depleted residue. In contrast, because Ti is weakly compatible in the melt residue (especially at low degrees of melting, when ortho- or clinopyroxene are still present), it is less rapidly depleted, resulting in low Th/Ti and Nb/Ti ratios in the residue. Because the trace element composition of an ultramafic magma (which forms by high degree partial melting leaving only olivine and possibly orthopyroxene in the residue) should be strongly dependent on the composition of the mantle source, prior melt extraction will result in low Th/Ti and Nb/Ti ratios in magmas that are formed by later melting events (**Fig. 8.21b**). As noted above, it is this process that accounts for the depletion of HILE relative to MILE in N-MORB-like magmas.

Owing to the varying compatibilities of Th, Nb, and Ti, magmas produced by small to moderate degrees of melting of an undepleted or enriched source will exhibit an enrichment that qualitatively mirrors that of the mantle source, with elevated Th and Nb contents relative to Ti and the HREE. Such magmas will have characteristically high Th/Ti and Nb/Ti ratios that resemble those of an ocean island basalt (OIB) component. Mixing between magmas derived from enriched and depleted source regions leads to hybrid magmas with intermediate to high Th/Ti and Nb/Ti ratios (**Fig. 8.21c**). Although the trace element compositions of such magmas may resemble those of magmas produced either by lower degrees of melting of a depleted source or similar degrees of melting of a less-depleted source (**Fig. 8.22**), the major

---

<sup>6</sup> High field-strength elements have high charges (4+ and 5+) and small ionic radii (<1Å).

element contents of the latter magmas should be less magnesian, enabling the two processes to be distinguished.

Whereas the mantle processes described above would be expected to produce a nearly linear primary mixing line between the depleted and enriched source regions on a plot of Nb/Ti versus Th/Ti (**Fig. 8.22**), contamination of the magma by assimilation of upper continental crust (or sedimentary rocks derived from upper continental crust) should produce significant enrichment in Th relative to both Nb and Ti (**Fig. 8.21d**). Most sedimentary rocks are characterized by mantle-normalized HFSE abundances that decrease in the order  $\text{Th} \gg \text{Nb} \geq \text{Ti}$  and exhibit significant negative Nb and Ti anomalies relative to other elements of similar incompatibility during most magmatic processes. Because the abundance of Th in the contaminant is much higher than that of the magma, Th increases rapidly with progressive incorporation of crustal materials. However, because the abundances of Nb and Ti in the contaminant are more similar to those of the magma, Nb is only enriched after the magma has incorporated moderate amounts of material and Ti generally exhibits negligible change. Low to moderate degrees of assimilation (<5%) are therefore characterized by a trend of increasing Th/Ti ratios without much change in Nb/Ti. Owing to the high angle between the trends resulting from contamination and primary melting/enrichment processes, it is possible to use the variation in Nb/Ti ratio to discriminate between different magma sources even in the presence of large amounts of contamination.

**Figure 8.23** shows plots of mantle-normalized Nb/Ti and Th/Ti for rocks from different areas within the TNB. Because the trace element contents of many of the most olivine-rich cumulate rocks were very low and approached analytical detection limits (~0.04 ppm for Th, ~0.04 ppm for Nb, and ~300 ppm for Ti), the data were filtered prior to plotting to remove the less reliable values. Although this eliminated about a sixth of the samples for which there were trace element data, the resulting trends were considerably clearer after filtering.

Most of the mafic and ultramafic rocks from different areas of the TNB exhibit trends of increasing Th/Ti ratio with only a small change in Nb/Ti ratio (**Fig. 8.23**). When rocks from different areas are compared, most of the samples from each area appear to be characterized by primary magmatic trends that originate from the N-MORB – OIB mixing line and project toward the field of upper continental crustal rocks, consistent with the assimilation of crustal material by discrete batches of magma derived from variably depleted and/or enriched mantle-sources.

Using **Figure 8.23**, it is possible to recognize at least four different groups of magmas:

- 1) Moderately- to highly-contaminated mafic and ultramafic magmas derived from a highly-depleted mantle source and contaminated with sedimentary rocks similar to those of the Ospwagan Group (e.g., the Thompson, Birchtree, Halfway Lake, North Manasan, Pipe 1 and 2, and Spur South ultramafic bodies and rare basalts and picrites from Ospwagan Lake: **Figs. 8.23a to c**).
- 2) Slightly- to moderately-contaminated basalts and komatiitic basalts derived from an undepleted or slightly-enriched mantle-source and contaminated with sedimentary rocks similar to those of the Ospwagan Group (Ospwagan Lake, Pipe Pit, and Grass River Lineament: **Fig. 8.23c**, the area between Moak and Mystery Lake: **Fig. 8.23d**, some of the mafic rocks in the Setting Lake area: **Fig. 8.23e**, and the eastern part of the Winnipegosis Belt in the Rabbit Point and Baker Lake areas: **Fig. 8.23f**).



- 3) Variably-contaminated basalts and gabbros derived from an enriched source and contaminated with sedimentary rocks similar to those of either the Oswagan or Sickie/Grass River Groups (mostly areas north and west of Setting Lake, e.g., Bah Lake, Fish Lake, and Five Mile Lake: **Fig. 8.23e**).
- 4) Highly-enriched basaltic and/or pyroxenitic dikes from Oswagan Lake, Spur South, Taylor River, and Mystery Lake (**Fig. 8.23c**).

The samples from the William Lake and Mystery Lake areas fail to define a single magmatic trend (**Figs. 8.23f** and **8.23g**), which may indicate that magmas with a range of different initial trace element compositions were present in these areas.

Although further work may be required to integrate the HFSE data with other geochemical data for the mafic and ultramafic rocks of the TNB and potential tectonic regimes, as well as to investigate the variations in areas surrounding Setting, Mystery, and William Lakes, the observed variations in source magma compositions have several implications for the petrogenesis of the TNB mafic and ultramafic rocks:

- 1) There was probably both a temporal and spatial variation in either the source of volcanism or the degree of mantle-melting that produced the mafic and ultramafic magmas of the TNB, as indicated by the restriction of magmas from a depleted source region to the northern part of the belt and the occurrence of magmas from three distinctly different source regions in the area surrounding Pipe Pit and Spur South.
- 2) The degree of incompatible element enrichment appears to increase to the south and west, as indicated by elevated Nb/Ti ratios in the least contaminated samples from the Setting Lake and William Lake areas, consistent with either isolated plume activity or source heterogeneity along a rifted margin,
- 3) Mineralization is primarily associated with ultramafic cumulate rocks derived from magmas originally highly depleted in trace elements (Group 1 above).

### ***Interim Summary***

- 1) Almost all of the ultramafic bodies of the northern region of the TNB and many of the ultramafic bodies (and the amphibolite layers that they contain) from the central region of the TNB are strongly enriched in incompatible lithophile elements, irrespective of their mineralization status or cumulus olivine content.
- 2) The majority of the sampled mafic rocks in the northern and central regions of the TNB are either depleted or unenriched in incompatible lithophile trace elements, consistent with derivation from either a depleted or marginally-enriched mantle source.
- 3) A strong contrast between the trace element compositions of the ultramafic bodies and those of the local mafic volcanic rocks indicates that the two lithologies are *not* co-magmatic and that the mafic volcanic rocks *do not* represent magmas that erupted after passing through (and forming) the ultramafic bodies (cf. Bleeker, 1990).
- 4) The ultramafic bodies have experienced significant trace element metasomatism subsequent to emplacement, leading to mobilization of La (see **Chapter 7**) in strongly serpentinized ultramafic rocks and also Ce, Nd, and possibly Sm in the most olivine-rich cumulate rocks.

- 5) Owing to their higher ionic charges, however,  $\text{Th}^{4+}$  and  $\text{Nb}^{5+}$  have been considerably less mobile during metamorphism and may represent original contamination signatures.
- 6) Although mineralization is primarily associated with ultramafic cumulate rocks derived from magmas originally highly depleted in trace elements, many non-mineralized bodies have similar trace element signatures and the lithophile trace elements do not exhibit a unique signature associated with mineralization.

#### 8.4.4.3 Highly Chalcophile Trace Elements (PGE and Au)

The Pd and Ir contents of the olivine cumulate rocks sampled from almost all of the ultramafic bodies within the TNB are enriched relative to those expected for the fractionation and/or accumulation of olivine from a sulfide-undersaturated magma (blue line, **Fig 8.24**). Comparison of the whole-rock Pd, Ir, and MgO data with those expected for the fractionation of olivine + sulfide under a range of silicate magma:sulfide ratios (red and green lines, **Fig. 8.24**) indicates that the PGE contents of the majority of the bodies are consistent with mixtures of olivine and sulfide liquid formed under low-R conditions, but that the olivine:sulfide ratios are significantly lower than those expected for cotectic fractionation (<30:1 compared to the 60:1 ratio inferred for cotectic fractionation: Duke, 1986). The high Pd and Ir contents of these rocks suggest that the magmas from which they formed were sulfide-undersaturated and that they reached sulfide saturation *in situ* (as suggested by the low Ni contents of some of the olivines from non-mineralized bodies: **Section 8.4.3.4**). However, the low olivine:sulfide ratios indicate that the sampled rocks accumulated excess sulfide after reaching sulfide saturation and/or that  $f\text{S}_2$  was higher than normal, decreasing the solubility of sulfide relative to olivine.

Although a few samples (primarily pyroxenites from Thompson Mine and Ospwagan Lake, but also a few peridotites from the North Manasan and Nichols Lake ultramafic bodies) have lower Pd contents than expected, the general absence of cumulate samples depleted in Pd or Ir indicates that if the magmas were sulfide-saturated prior to emplacement, they did not segregate significant amounts of sulfide.

In **Figure 8.24**, the highly chalcophile element compositions of the William Lake ultramafic bodies plot toward significantly higher PGE contents than those from other parts of the TNB. Such compositions indicate that the bodies either formed under higher R conditions or from an abnormally PGE-enriched magma (as described in **Section 8.4.3.5**)

In contrast to the enrichment in highly chalcophile elements observed in the sampled ultramafic bodies in the TNB, most of the sampled mafic volcanic rocks in the TNB have low PGE contents, consistent with fractionation of a sulfide-undersaturated magma (**Fig. 8.24**). The fact that the mafic and ultramafic volcanic rocks show neither significant enrichment nor depletion in highly chalcophile elements indicates that the magmas from which they formed only reached sulfide saturation at a late stage of their differentiation history and had not segregated any sulfide prior to eruption. The absence of chalcophile element depletion is interpreted as further evidence that the volcanic rocks could have been derived from magmas that were processed through ultramafic sills that contained either massive or disseminated sulfide-bearing cumulate rocks, the formation of which would have significantly depleted them in PGE.

#### 8.4.4.4 Nd Isotope Compositions of Mafic and Ultramafic Rocks

In order to further constrain the petrogenetic histories of the different elements of the magmatic system in the TNB, to investigate the processes of contamination and/or metasomatism that may have led to the incompatible element enrichment observed in many of the ultramafic bodies, and to supplement the isotope data previously presented by Ansdell & Bleeker (1997) for rocks collected exclusively from the northern TNB, Nd isotope determinations were carried out on a suite of 12 peridotites and mafic volcanic rocks collected from the northern and central TNB during years 1 and 2 of the project. The results of the analyses are presented in **Table 8.4**.

The data for the mafic and ultramafic rocks from the central TNB may be divided into four groups:

- 1) Dunites and peridotites in the Pipe 1 ultramafic body (DDH 86232) containing variable amounts of sulfide mineralization
- 2) Dunitic rocks in the W-56 ultramafic body (DDH WL97-179)
- 3) Amphibolite-facies metavolcanic rocks in the southern part of the central TNB (DDH WL95-106)
- 4) Greenschist facies metamorphic rocks in the northern extension of the Winnipegosis Belt to the east of William Lake (DDH WL96-134)

Whereas the Sm-Nd isotopic compositions of some samples (most notably some of those from the Pipe ultramafic body and one of the metavolcanic rocks collected to the east of William Lake) exhibit anomalous Nd isotopic compositions that indicate mobility of the radiogenic daughter  $^{143}\text{Nd}$  isotope relative to the radioactive parent  $^{147}\text{Sm}$  isotope, samples from other areas of the TNB exhibit potentially primary variations in  $\epsilon_{\text{Nd}}$  (at 1.9 Ga).

#### *Amphibolite-facies mafic and ultramafic rocks in Central TNB*

The Nd isotope compositions of the four samples of komatiitic basalt and dunite collected from the William Lake area *sensu stricto* appear to exhibit a range of values that would have been significantly less radiogenic than the mantle reservoir at 1.9 Ga, but converge toward the Nd isotope compositions of Pipe Group sedimentary rocks at  $\sim 2.7$  Ga (**Fig. 8.25**), at values that are less than those of the contemporaneous depleted mantle. Because the continental crust is strongly enriched in LREE and has a much lower Sm/Nd ratio than mantle-derived magmas, the decay of radioactive  $^{147}\text{Sm}$  to radiogenic  $^{143}\text{Nd}$  in the crust rapidly increases the abundance of radiogenic  $^{143}\text{Nd}$  relative to stable  $^{144}\text{Nd}$  (and therefore the  $^{143}\text{Nd}/^{144}\text{Nd}$  ratio) over time relative to chondritic mantle. This is commonly expressed as the  $\epsilon_{\text{Nd}}$  value, which is  $10^4$  times the deviation of  $^{143}\text{Nd}/^{144}\text{Nd}$  from the chondritic mantle at a given time. Because of the potentially large isotopic contrast and the much greater abundance of LREE in upper continental crustal rocks compared to mantle-derived magmas, the Nd isotopic compositions of mantle-derived magmas are very sensitive to crustal contamination by older crust (see discussion by Burnham, 2000). For this reason, the  $\sim 2.7$  Ga convergence of the Sm-Nd isotope data for the William Lake mafic and ultramafic rocks is interpreted to result from contamination of the magmas by a crustal component with a late Archean depleted-mantle model age (similar to the Ospwagan sedimentary rocks: **Section 8.6.3.3**) rather than the age of volcanism, just as the  $\sim 3.2$  Ga apparent Sm-Nd age of the 2.7 Ga Kambalda komatiites is interpreted to represent contamination by older continental crust

(Chauvel et al., 1985). On the basis of the Nd isotope compositions of the samples alone, it is not possible to identify which unit(s) of the Oswagan Group sedimentary rocks were responsible for the contamination. However, when the Nd isotope ratios of these samples are plotted as a function of incompatible element enrichment (e.g., Ce/Yb, Ce/Sm, or Th/Nb: **Fig. 8.26**), both sets of samples plot along the mixing arrays expected for the contamination of a mafic or ultramafic mantle-derived magma by a component with trace element and isotopic characteristics similar to the analyzed Pipe Formation sedimentary rocks.

**Table 8.4** Nd isotope compositions of mafic and ultramafic samples analyzed during CAMIRO Project 97E-02

Sample	DDH	Description	Nd (ppm)	Sm (ppm)	$^{147}\text{Sm}/^{144}\text{Nd}$	$^{143}\text{Nd}/^{144}\text{Nd}$	+/-	$\epsilon_{\text{Nd}}$ (1.9)	$T_{\text{DM}}$
<b>Pipe 1 Ultramafic Body</b>									
86232-3805	86232	Mineralized unaltered peridotite	0.93	0.34	0.19387	0.512518	8	-1.7	
86232-3841.5	86232	Mineralized unaltered peridotite	0.66	0.19	0.17050	0.512079	24	-4.5	
86232-3869.9	86232	Non-mineralized unaltered peridotite	0.34	0.12	0.21823	0.512152	20	-14.8	
86232-3918	86232	Non-mineralized serpentinized peridotite	0.47	0.11	0.13528	0.512215	20	6.8	
86232-3986.2	86232	Non-mineralized serpentinized peridotite	0.25	0.07	0.16828	0.511927	13	-7.0	
<b>Dunitic Rocks in the W-56 ultramafic body</b>									
WA37927	WL97-179	Unaltered dunite	0.3	0.11	0.21111	0.512916	26	1.9	
WA37928	WL97-179	Unaltered dunite	0.51	0.17	0.20480	0.512790	13	1.0	
WA37929	WL97-179	Unaltered dunite	0.31	0.1	0.20670	0.512803	10	0.8	
WA37931	WL97-179	Unaltered dunite	0.26	0.09	0.21560	0.512917	11	0.8	
<b>Low-Grade Metabasaltic Rocks East of William Lake</b>									
WB02016	WL96-134	Pyroxenite cumulate	1.64	0.55	0.20153	0.512884	10	3.6	1.95
WB02019	WL96-134	Massive basalt flow	4.07	1.64	0.24315	0.513262	13	0.8	1.14
WB02029	WL96-134	Massive basalt	6.77	2.2	0.19635	0.512793	14	3.1	2.18
<b>Amphibolite-Facies Metabasaltic Rocks at William Lake</b>									
WB02044	WL95-106	Picritic basalt	4.74	1.59	0.20331	0.512772	70	1.0	
WB02050	WL95-106	Ol-phyric komatiitic basalt	2.48	0.87	0.21258	0.512961	33	2.4	
WB02052	WL95-106	Komatiitic basalt	4.28	1.27	0.17979	0.512363	13	-1.2	

Analyses by Dr. K. Ansdell, University of Saskatchewan. Analytical methods described in **Appendix 1**.  $\epsilon_{\text{Nd}}(1.9) = 10^4 \times$  deviation in  $^{143}\text{Nd}/^{144}\text{Nd}$  ratio from the chondritic uniform reservoir (CHUR) at 1.9 Ga.  $^{143}\text{Nd}/^{144}\text{Nd}_{\text{CHUR}}$  at 1.9 Ga calculated from present day using  $^{143}\text{Nd}/^{144}\text{Nd}_{\text{CHUR}} = 0.512638$ ,  $^{147}\text{Sm}/^{144}\text{Nd}_{\text{CHUR}} = 0.1967$ , and  $\lambda(^{147}\text{Sm}) = 6.54 \times 10^{-12} \text{ y}^{-1}$  (Jacobsen & Wasserburg, 1980).  $T_{\text{DM}}$  = depleted mantle model ages calculated using the mantle evolution curve of Ben Othman et al. (1984).

### ***Basalts east of William Lake (Winnipegosis Belt)***

In contrast to the mafic and ultramafic rocks hosted by amphibolite facies metasediments of the central TNB, two of the three unaltered mafic samples collected to the east of William Lake (in the inferred northern extension of the Winnipegosis Belt) exhibit Nd isotopic

compositions that extrapolate to values similar to those estimated for the depleted mantle reservoir at ~1.9 Ga (**Fig. 8.25**), indicating that they may represent mantle-derived magmas of a similar age to those dated at Rabbit Point in the southern region of the TNB (Hulbert et al., 1994).

### ***Further analyses***

In order to investigate more fully the relationships between magma source, contamination, and the age of eruption, an additional 63 samples were submitted for Nd isotopic analysis during the third year of the project. These samples included 28 samples of mafic and ultramafic volcanic rocks from the Lake Winnipegosis, Setting Lake, Bah Lake, Mystery Lake, and Ospwagan Lake areas, as well as 9 samples from the William Lake, North Manasan, and Mystery Lake ultramafic bodies. However, owing to delays in the analyses of these samples as a result of laboratory refurbishments and instrument problems, data for these samples were only obtained during the production of this report. Although these data are included in the main geochemical database, they were not received in time to be interpreted as part of this project.

### **8.4.4.5 Summary**

- 1) A comprehensive database of whole-rock major, minor, and trace element geochemical data for ~3000 mafic and ultramafic rocks was compiled from existing databases and new sampling in all parts of the TNB. The data were levelled and filtered for quality. Owing to the complexity of the belt and large volume of data that have been collected during the study, only parts of the database have been discussed in this report. However, we expect that the database will provide an excellent resource for future research in the TNB and in the exploration for Ni-Cu-(PGE) mineralization within and outside of the TNB.
- 2) Most of the olivine cumulate rocks and pyroxenites in the ultramafic bodies have compositions consistent with fractional crystallization and accumulation of olivine  $\pm$  chromite followed by orthopyroxene then clinopyroxene + plagioclase from a relatively silicic initial magma composition. However, several samples with intermediate MgO contents are more significantly enriched in SiO<sub>2</sub> and depleted in TiO<sub>2</sub>, Al<sub>2</sub>O<sub>3</sub>, and CaO, consistent with the accumulation of orthopyroxene owing to felsification of the magma by the assimilation of sedimentary rock.
- 3) Calculated average olivine compositions for the bodies ranged from Fo<sub>88</sub> to between Fo<sub>92</sub> and Fo<sub>94</sub> and are consistent with the compositions of analyzed relict grains, which range up to Fo<sub>94</sub>. This and the low Cr contents in many of the cumulate rocks indicate that the parental magmas to the bodies were significantly more magnesian than previously thought and may have been komatiites *sensu stricto* with up to 23 wt% MgO.
- 4) The degree of chromite undersaturation was greater in the mineralized ultramafic bodies, either as a result of an initially higher MgO content (resulting from greater amounts of partial melting and/or lower degrees of fractional crystallization) or emplacement under more reducing conditions.
- 5) Most of the cumulate and mafic rocks formed from magmas that were relatively undepleted in Ni and PGE, indicating that they had neither lost significant amounts of sulfide nor interacted with significant amounts of sulfide liquid prior to emplacement.

- 6) Although most LILE (Cs, Rb, K; Ba, Sr, Ca;  $\text{Eu}^{2+}$ ) and LREE (La, probably Ce, and sometimes Nd and Sm) have been mobile in most of the mafic and ultramafic rocks during deuteric and/or metamorphic alteration and cannot be used to evaluate crustal contamination, HREE and most HFSE (Zr, Nb, and Th) appear to have been relatively immobile and are also enriched in many non-mineralized and mineralized ultramafic bodies, suggesting that most of the ultramafic bodies in the TNB, regardless of mineralization status, have been contaminated by upper continental crustal rocks. Although this confirms previous studies that contamination alone is insufficient to cause mineralization and that a S-rich contaminant is normally required to generate an economic Ni-Cu-(PGE) deposit, it also indicates that there is no readily apparent, unique signature for mineralization in the trace element compositions of the silicate portions of the ultramafic bodies.
- 7) The most promising indicators of mineralization appear to lie in the major and minor element whole-rock and mineral compositions of the ultramafic rocks and include lower Cr contents in the whole-rock, Ni depletion in olivines and higher initial silica contents of the magmas (leading to orthopyroxene rather than clinopyroxene as the second silicate phase on the liquidus).
- 8) In addition to, and consequence of, differences in the fractionation paths of the ultramafic bodies and mafic and ultramafic volcanic rocks, the major, minor, trace and chalcophile element compositions of the two groups of rocks differ significantly. These differences were shown to be primary features, indicating that the two groups of rocks are probably not consanguineous.

## 8.4.5 Discriminant analysis

### 8.4.5.1 Introduction

Discriminant analysis is a multivariate statistical technique used to classify samples into pre-defined groups. By selecting a set of standard samples that have already been classified as belonging to one of two or more groups, it is possible to calculate one or more linear functions of the measured variables that will achieve the greatest discrimination between the groups. The functions have the form:

$$F_i = a_i x_1 + b_i x_2 + c_i x_3 + \dots + p_i x_p$$

where  $x_1, x_2, \dots, x_p$  are the discriminant function *variables* (e.g., major or trace element contents, element ratios, or isotopic compositions),  $a_i, b_i, c_i, \dots, p_i$  are the discriminant function *coefficients*, and  $F_i$  is the discriminant function *score*.

### 8.4.5.2 Application to Ultramafic Bodies of the TNB

In the absence of a simple relationship between the mineralization status of the TNB ultramafic bodies and their chemical compositions, discriminant analysis was applied to whole-rock data for several of the better characterized bodies in the belt, as well as some of the bodies of uncertain mineralization status. Within this analysis, the grouping variable was the mineralization status of the bodies (economically-, subeconomically-, or non-mineralized), as described in **Section 8.4.1**. Because the data were divided into three separate groups, the analysis calculated two functions.

### ***Choice of Elements***

The most effective variables to use in a discriminant function are those which 1) are determined with the highest analytical precision, 2) vary independently, 3) exhibit a significant variation between the pre-defined groups, and 4) are available for the maximum number of the samples within the dataset. Although some of the more important elements for the discrimination functions could be predicted from the observations made during the discussion of the major, minor and trace element compositions of the ultramafic bodies (e.g., MgO, Cr, Th, Nb, and LREE) or from the constituents of the ores (e.g., Fe, Ni, Cu, Co, and S), the relationship between other element concentrations and mineralization was less certain. Examination of the compiled geochemical database showed that of the ~2100 ultramafic samples (samples with >20 wt% MgO), most were either not fully characterized in terms of major, minor, and trace elements or contained concentrations of one or more of the potentially important elements that were below the limit of quantification. In the end, 368 samples for which major element (SiO<sub>2</sub>, TiO<sub>2</sub>, Al<sub>2</sub>O<sub>3</sub>, FeO<sup>t</sup>, MnO, MgO, and CaO), minor element (Cr, Ni, Co, Cu, Zn, Sc, and V), trace element (Hf, Nb, Th, Ce, Sm, Dy, Yb), and S data were available were selected for statistical analysis. The samples were from 36 different locations (mostly in the northern region of the TNB, but including many samples from the southern and central regions) and are believed to reasonably representative of the different mineralization groups.

In order for discriminant analysis to work well, it is necessary that the data be normally, or near normally, distributed. Chi-squared tests of the data for normality indicated that the distributions of most of the incompatible elements (e.g., Ti, Al, Ca, Zn, Hf, Nb, Th, and Yb) and some of the compatible elements (e.g., Cr, Ni) were significantly skewed toward lower concentrations, presumably because of the predominance of olivine-rich cumulates in the database. Because the data for many of these elements appeared to more closely approach a log-normal distribution, the logarithms of their concentrations were used during the discriminate analysis instead of the raw data.

As a first stage of the construction of the discriminant functions, the elements that contributed most to the separation of the groups were selected by automatic forward stepwise insertion into the functions using the “Stepwise” option of the Discriminant Analysis routine of the SYSTAT<sup>®</sup> statistical program. At each step, the program entered the variable that showed the greatest statistical difference between the three proposed groups, as determined by its F-value, until all of the remaining elements had F-values less than a predetermined cut-off (in this case the default of  $F = 4$ ). During this process, it was discovered that Mn, Sc, V, Ce, Sm, Dy, Co, and (surprisingly) Cu showed the weakest links to the mineralization processes and were therefore eliminated from the analysis.

### ***Training and Test Data Sets***

During conventional discriminant analysis, samples are randomly allocated to either a *training* dataset (from which the discriminant functions are calculated) or a *testing* dataset (which is used to test the efficiency of the functions). However, in order to maximise the number of samples and locations that could be used in the construction of the discriminant functions for the TNB ultramafic bodies, it was decided to allocate all of the available data to the training dataset and then compare the results for different bodies and locations. Although less statistically rigorous, this allowed greater geographical coverage and more samples to be used in the function.

**Table 8.5** Coefficients for mineralization discriminant functions

	Raw Coefficients		Scaled Coefficients	
	Function 1	Function 2	Function 1	Function 2
Variation Accounted For	71.5%	28.5%		
SiO <sub>2</sub>	0.091	0.188	0.33	0.686
Log (TiO <sub>2</sub> )	2.193	-0.267	0.935	-0.114
Log (Al <sub>2</sub> O <sub>3</sub> )	-3.273	-1.903	-1.474	-0.857
FeO <sup>t</sup>	0.222	0.319	0.505	0.727
MgO	-0.039	0.119	-0.323	0.989
Log (CaO)	-0.468	0.402	-0.410	0.352
Log (Cr)	1.158	1.41	0.207	0.252
Log (Ni)	-1.146	-1.476	-0.290	-0.373
Log (Zn)	-0.872	0.426	-0.297	0.145
Log (Hf)	-0.396	2.234	-0.171	0.962
Log (Nb)	0.821	1.05	0.368	0.471
Log (Th)	-1.725	-0.702	-0.866	-0.352
Log (Yb)	1.812	0.638	0.768	0.270
Log (S)	-0.743	0.238	-0.487	0.156
Constant	-1.171	-15.03	-	-

**Notes:** Coefficients scaled using a pooled estimate of the within-sample variance.

#### 8.4.5.3 Results

The unstandardized (raw) coefficients for the two discriminant function are shown in **Table 8.5**.

**Function 1** accounts for 71.5% of the differences between the groups and, on average, increases from mineralized (mean  $F_1 = -0.987$ ), through weakly-mineralized (mean  $F_1 = -0.203$ ) to non-mineralized samples (mean  $F_1 = 1.089$ ). The coefficients for the 14 elements used in the functions indicate that, on average, the samples collected from mineralized bodies are enriched in Al, Th, S, Ca, Mg, Ni, and Zn and depleted in Ti, Yb, Fe, and Nb relative to those collected from non-mineralized bodies. Although the positive correlation between chalcophile element contents and mineralization state is easily explained by the higher sulfide contents of the samples from mineralized ultramafic bodies, the pattern of enrichment in selected incompatible elements confirms that crustal contamination is a characteristic of mineralized bodies in the region. Because many of the elements whose concentrations should show opposite variations during the fractionation and/or accumulation of olivine  $\pm$  chromite (e.g., MgO and Cr vs. Al<sub>2</sub>O<sub>3</sub> and Ca) correlate with mineralization, the differences in the major and trace element contents between the three groups cannot be accounted for by variations in the amounts of trapped melt and indicate that the compositions of the trapped melts or the olivines are different for the mineralized and non-mineralized bodies, such that mineralization appears to be associated with initially more magnesian, but also more contaminated magmas.



**Function 2** accounts for 28.5% of the differences between the groups and is more difficult to interpret, because it primarily differentiates between weakly-mineralized bodies (mean  $F_2 = -1.001$ ) and either strongly-mineralized (mean  $F_2 = 0.409$ ) or non-mineralized bodies (mean  $F_2 = 0.241$ ). It contains high, positive coefficients for MgO, Hf,  $\text{FeO}^t$ ,  $\text{SiO}_2$ , and Nb, and negative coefficients for  $\text{Al}_2\text{O}_3$ , Th, and Ni. Although this is consistent with lower MgO and Ni contents and less contamination (lower Th/Nb ratios) in the weakly-mineralized bodies relative to the strongly- or non-mineralized bodies, it is not clear which elements reflect the differences between non-mineralized and weakly-mineralized bodies and which relate to the differences between weakly- and strongly-mineralized bodies.

**Table 8.6** Classification matrix for TNB Ultramafic bodies.

	Strongly Mineralized	Weakly Mineralized	Non-Mineralized	Correct
<b>Strongly Mineralized</b>	104	19	14	76%
<b>Weakly Mineralized</b>	16	64	10	71%
<b>Non-Mineralized</b>	19	19	103	73%
<b>Total</b>	139	102	127	74%

**Notes:** Rows contain the number of samples originally allocated to each group, columns contain results of the classification.

The discriminant functions scores calculated for the 368 samples used in the analysis are plotted in **Figure 8.27** and the success of the discrimination functions are summarized in a classification matrix (**Table 8.6**). As seen in the plot and matrix, there are considerable overlaps between the different groups of samples, in particular those from the central TNB, and the functions are only able to successfully classify ~75% of the samples. There may be several reasons for the low success of the functions including: 1) the non-normal distribution of the concentration data for many of the elements (even after transformation), 2) alteration of the samples, 3) misallocation of samples to their respective mineralization groups prior to statistical analysis (e.g., the assignment of samples from a non-mineralized portion of a mineralized to the mineralized group or the assignment of samples from a body containing undiscovered economic mineralization to the non-mineralized or weakly-mineralized group), or 4) decoupling of the silicate magma and sulfide liquids such that the magmas that formed the bulk of the ultramafic bodies are not those petrogenetically related to the ores.

A few of the cases where misclassification occurred are highlighted below:

#### ***Moak Lake (Mineralized)***

The majority of the ultramafic samples from the Moak Lake area were collected from drill cores that intersected the mineralized ultramafic body and were therefore allocated to the “mineralized” group. In **Figure 8.28a**, these samples plot on the boundary between the mineralized and non-mineralized fields. Although the average location of the samples on the plot would place the body in the mineralized field, if only a few samples were selected for

analysis, the body could easily be misclassified as non-mineralized. In order to reduce the possibility of misclassification, several samples should always be analyzed.

#### ***Mystery Lake (Strongly- to Non-mineralized)***

Drilling and mapping indicate that there are several ultramafic bodies with different degrees of mineralization in the Mystery Lake area. Whereas the discriminant analysis successfully differentiates between the mineralized Mystery Lake South ultramafic body (located close to the surface at the southwest end of the lake and intersected at depth by two of the sampled drill cores in the centre of the lake) and a larger non-mineralized part of either the same body or an entirely different body located at shallower depths further north in the centre of the lake, it appears that the thick dunitic body intersected by a drill hole (DDH89234) to the east of the Mystery Lake South body may be weakly mineralized rather than non-mineralized, as initially thought (**Fig. 8.28b**).

#### ***Thompson (Mineralized)***

Although most of the samples collected from the Thompson ultramafic body plot within the field of strongly-mineralized ultramafic bodies, many scatter toward and into the weakly-mineralized field and appear to have been misclassified during the analysis (**Fig. 8.28c**). The majority of these samples originate from three drill cores that either intersected the weakly or non-mineralized portions of one of the ultramafic bodies or failed to intersect mineralization. The results for these samples reinforce the necessity of analyzing several samples from any particular ultramafic body. If only single samples had been selected for analysis from each of these cores, then the discriminant plot would have classified them as being only weakly mineralized and would have failed to identify the strong mineralization in the area. In contrast, if several samples had been selected, then the trend toward the mineralized field should be apparent and the presence of potentially economic mineralization elsewhere in the body should be identified.

#### ***Mid Lake (Weakly Mineralized)***

The samples from Mid Lake that were used in the discriminant analysis include samples from the suite collected for this project and the database compiled by L. Hulbert. In **Figure 8.28d**, almost all of the samples from this ultramafic body plot within or close to the weakly-mineralized field, but were classified as being either weakly mineralized (CAMIRO 97E-02 database) or non-mineralized (GSC database). In this case, it appears that many of the samples were initially misclassified and should have been placed in the weakly mineralized group.

#### ***Pipe 1 and 2 (Mineralized)***

All but one of the 30 ultramafic samples from the strongly mineralized Pipe 1 and Pipe 2 ultramafic bodies plot within the mineralized field of **Figure 8.28e**, irrespective of their location within the ultramafic bodies, confirming that the discrimination functions can successfully identify mineralized intrusions even when the samples themselves are not strongly mineralized.

#### ***Spur South (Non-Mineralized)***

Because the ultramafic body at Spur South is located in the hinge of a fold, only the upper pyroxenitic and peridotitic parts of the body were intersected by drilling. From the absence of

significant amounts of sulfide and the normal Ni contents of the ultramafic samples collected from the body, it was inferred to be non-mineralized. However, when plotted on the discriminant diagram (**Fig. 8.28f**), four of the six samples plot in the weakly mineralized field and one plots in the strongly mineralized field, suggesting that mineralization may be present at depth in the body. On the basis of the discriminant plot, further investigation of this body may be merited.

#### ***Northern Winnipegosis Belt (Non-Mineralized)***

The samples from the northern extension of the Winnipegosis Belt east of the William Lake area (**Figure A2.2**) in the central TNB were collected from two different drill cores (DDH WL96-134 and BK93-64) that intersected barren greenschist-facies komatiitic rocks. Whereas the samples from DDH WL96-134 all plot in the non-mineralized field of the discrimination plot (**Fig. 8.28g**), the variably carbonate altered samples from DDH BK93-64 scatter across the strongly, weakly, and non-mineralized fields. This scatter is inferred to be the result of carbonate alteration, which may have increased the CaO and decreased the SiO<sub>2</sub> contents of the rocks, leading to erroneously low values for Function 1. The misclassification of these samples indicates that the discriminant plot is not well-suited to the classification of highly altered samples and that samples should be screened for anomalously high CO<sub>2</sub> or LOI prior to plotting. Eliminating Si and Ca from the discriminant function might make it more suitable for carbonated rocks, but would reduce the discriminating power for non-carbonated rocks.

#### ***William Lake (Weakly- to Non-Mineralized)***

Although the samples from the William Lake trend generally plot in the fields predicted from the known mineralization in the area, several samples that are inferred to have originated from either weakly- or non-mineralized bodies plot in the field of strongly-mineralized bodies (**Fig. 8.28h**). Examination of the raw data for the anomalous samples does not provide any indication of why the function scores calculated for these samples appear to be different from the rest. The samples from bodies categorized as weakly mineralized are not significantly enriched in any of the elements that are positively loaded in Function 2 or depleted in those that are negatively loaded in this function, each of which would result in higher scores. Similarly, the samples from bodies categorized as non-mineralized are not significantly depleted in any of the elements that are positively loaded in Function 1 or enriched in those that are negatively loaded in this function, each of which would result in higher scores. Additional work is required to investigate whether the differences reflect the presence of better mineralization than that which has been discovered in these bodies to date, but it may be significant that seven of the eight most anomalous samples originate from two ultramafic bodies (W-36 and W-56) in which moderate amounts of mineralization have previously been identified.

#### ***Winnipegosis Belt (Non-Mineralized)***

With the exception of one anomalous sample, the ultramafic bodies associated with the komatiitic basalts of the Winnipegosis Belt all plot in the non-mineralized field of the discrimination plot (**Fig. 8.28i**), consistent with the inferred absence of sulfide mineralization in the area.

#### 8.4.5.4 Conclusions

- 1) The discriminant function analyses indicate that although statistical methods may be used to identify compositional differences between ultramafic bodies with different mineralization states, multiple samples from individual bodies are often required to ensure an accurate assessment of the mineralization potential of an unknown body.
- 2) Mineralized bodies are enriched in Al, Th, S, Ca, Mg, Ni, and Zn and depleted in Ti, Yb, Fe, and Nb relative to non-mineralized bodies, consistent with the contamination and sulfide-saturation of a highly magnesian ultramafic magma.
- 3) All samples should be screened for alteration and data for strongly-altered samples should be discarded prior to use in the discriminant functions.
- 4) Although re-characterization of the mineralization status of a few of the samples in light of the results of the initial analysis may provide more accurate discrimination functions, the form of the calculated functions should not change markedly and the functions may provide reasonably robust indicators of the mineralization state of ultramafic bodies within the belt.

### 8.5 Mafic Rocks

#### 8.5.1 Introduction

This section provides a brief review of the geochemical characteristics of mafic to ultramafic volcanic rocks in the Bah Lake assemblage, differentiated mafic-ultramafic dikes (e.g. Grass River intrusion), and volcanic- or sediment-hosted mafic sills (e.g., Bah Lake intrusion). The field and petrologic characteristics of these rocks are described in **Sections 5.2.7** and **5.2.8**. A comparison of the geochemical characteristics of these rocks and the ultramafic sills is given in **Section 8.4.4** and detailed discussions of geochemical variations within each of the major sample suites are given in previous CAMIRO TNB Project Annual Reports.

Although this project has been very successful in developing a detailed geochemical database for parts of the Bah Lake assemblage and related mafic-ultramafic sills, this database is quite skewed in terms of sample density to the Winnipegosis komatiite belt (WKB) in the southern part of the project study area and the Bah Lake-Ospwagan Lake-Mystery Lake areas in the western part of the exposed, northern portion of the TNB. Very few unequivocal, laterally-continuous mafic volcanic sequences have been reported in the central part of the TNB (e.g., William Lake – Ponton region). This problem likely reflects both the difficulty in recognizing mafic flows in high grade terrains within drill core and the fact that target drilling in the TNB has focussed on thickened parts of the Pipe Formation or petrologically-equivalent sedimentary sequences that contain conductive sulfides and are known to host most of the Ni deposits in the TNB (e.g., Bleeker, 1990). Accordingly, there remains a tremendous disparity between the number of analyses available for TNB ultramafic sills and TNB mafic and ultramafic flows and dikes and mafic intrusions.

#### 8.5.2 Whole rock Compositions

##### 8.5.2.1 Major and Minor Elements

The mafic and ultramafic metavolcanic rocks, sills, and dikes in the WKB and TNB exhibit a wide range in whole-rock geochemical compositions (**Figs. 8.29** and **8.30**). Both belts show a

similar range in compositions, from peridotite to ferrogabbro, and both plot in the field for komatiitic rather than tholeiitic magmas (**Fig. 8.29**). A small suite of Molson dike samples from the adjacent parts of the northwestern Superior Province shows a similar compositional range as the TNB volcanic rocks, dikes, and sills (**Fig. 8.29**). Dikes in both the TNB and the Molson swarm in the Superior Province display a pronounced Fe-enrichment trend at  $\text{Al}_2\text{O}_3$  contents of ~15%, corresponding to the fractionation of plagioclase.

When the major and minor element compositions of the gabbroic dikes and sills in the Setting Lake Formation around Setting Lake are compared to those of the basaltic rocks of the Bah Lake assemblage in the type area around Bah Lake there appear to be three separate groups of intrusions:

- 1) Gabbroic sills with intermediate MgO contents and major and minor element compositions that lie within the range exhibited by the Bah Lake volcanic rocks (5.7-8.5 wt% MgO) and appear to be consanguineous with them.
- 2) Leucogabbros with lower MgO contents than the Bah Lake volcanic rocks, but which lie along the same fractionation trends calculated from the MELTS program (**Section 8.4.4.1**).
- 3) A suite of “early tectonic mafic dikes” with highly variable MgO contents (2.8-11.5 wt% MgO) that are anomalously enriched in  $\text{SiO}_2$  and depleted in  $\text{TiO}_2$ , FeO, MnO, CaO, and  $\text{Na}_2\text{O}$ .

Whereas the anomalous compositions of the early tectonic dikes indicate that they may be unrelated to the Bah Lake volcanic rocks, the similarity between the major and minor element compositions of the gabbroic sills and the overlying volcanic rocks corroborates the suggestion that the gabbros represent subvolcanic sills and that much of the Bah Lake assemblage is autochthonous with respect to the Oswegan Group and the TNB (**Section 5.2.2.5**).

### ***Chromium***

WKB volcanic rocks define a linear array of points on a Cr-MgO plot that suggests derivation from komatiitic basaltic magma that was crystallizing olivine and chromite in cotectic proportions (**Fig. 8.31**; cf. **Fig. 8.12** and discussion in **Section 8.4.4.1**).

TNB volcanic rocks form two populations, one of which defines a linear array of points at low MgO and Cr contents and a second that forms a fairly random array of points at high MgO and Cr contents (**Fig. 8.31**; cf. **Fig. 8.12**). In the case of the TNB volcanic rocks, mafic dikes, and sills, and the Molson dikes, there is a compositional gap between ca. 13% and 18% MgO, the significance of which is not known. At high MgO contents, most of the rocks studied show no significant correlation between Cr and MgO contents that may reflect the fact that these rocks are more evolved cumulates comprising variable proportions of olivine, chromite, and pyroxene.

### ***Nickel***

One of the major objectives during the investigation of the geochemistry of the mafic rocks in the TNB was to determine if they provided any indication of significant Ni sulfide deposition in deeper, ultramafic subchambers, possibly represented by the TNB ultramafic sills. Although the lithophile trace element data indicate that very few of the volcanic rocks

investigated in the current study could be cogenetic with most of the TNB ultramafic bodies (**Section 8.4.4**), many of the WKB flows and several of the TNB volcanic rocks appear to be depleted in Ni relative to the general fractionation trend defined by the majority of the samples (**Fig. 8.32**). Given that these rocks are not associated with any known Ni-Cu-(PGE) sulfide deposits, the cause of this apparent Ni depletion certainly merits additional investigation.

#### **8.5.2.2 Trace Elements**

The Th/Ti and Ce/Sm ratios of the mafic and ultramafic volcanic rocks are plotted as a function of Nb/Ti in **Figures 8.23** and **8.33**, respectively. As discussed in **Sections 7.2.3** and **8.4.4**, these elements are believed to represent the least-mobile trace elements and should be accurate indicators of petrogenetic processes.

Although most of the mafic and ultramafic volcanic rocks, dikes, and sills in the TNB are not significantly enriched in immobile, incompatible trace elements relative to the inferred depleted mantle source, some of the rocks display evidence of either limited source enrichment or limited assimilation of upper continental crustal rocks (see discussion in **Section 8.4.4.2**). Some of the WKB samples and Molson dikes appear to be moderately enriched in LREE, as shown by elevated Ce/Sm ratios and a few of these samples, as well as some flows from the northern part of the TNB, also show elevated Th/Nb values (relative to primitive mantle), such that they plot well off the main cluster for TNB and WKB samples on a Ce/Sm vs. Th/Nb plot (**Fig. 8.34**).

Although there are insufficient data to establish firm groupings on a geographical or stratigraphic basis, on the basis of incompatible trace element abundances, the TNB volcanic rocks, dikes, and sills can be subdivided into four distinct compositional types (**Fig. 8.35**).

##### ***Group 1***

Group 1 comprises a small number of samples that are strongly enriched in Th, weakly enriched in LREE, and strongly depleted in Nb (**Fig. 8.35a**), which is interpreted to represent source enrichment or assimilation of upper continental crustal rocks. Most of the samples in this group occur in one flow sequence in the WKB (drill hole RP-96-20); only one sampled flow at Oswagan Lake displays this “enriched” signature.

##### ***Group 2***

Group 2 comprises samples with relatively flat primitive mantle-normalized element profiles (**Fig. 8.35b**) and are interpreted to be derived from a slightly enriched mantle source.

##### ***Group 3***

Group 3 comprises a small but significant number of volcanic rocks, dikes, and mafic sills, including examples from both the Bah Lake volcanic rocks and the inferred subvolcanic sills within the Setting Formation at Setting Lake that are weakly to strongly depleted in LREE, sometimes coupled with Th and U depletion (**Fig. 8.35c**), consistent with derivation from a depleted mantle source.

##### ***Group 4***

Group 4 comprises samples that are strongly enriched in LREE with high total REE abundances, but no corresponding negative Nb or positive Th anomalies. These include

samples from the Taylor River gabbro dike and flows from Upper Oswagan Lake (**Fig. 8.35d**), some of the volcanic rocks from the Bah Lake area, and some, but not all of the subvolcanic sills in the Setting Formation at Setting and Mystery Lakes (described by H. Zwanzig, 1999). These samples are primarily from the westernmost part of the exposed segment of the TNB and may represent a chemically and genetically distinct magmatic suite, possibly derived from a more fertile mantle source region.

### 8.5.3 Interim Summary

During this study the database for the mafic and ultramafic volcanic rocks of the TNB has been substantially enlarged with the collection of well-characterized samples from several localities along the length of the belt. The new data have demonstrated that:

- 1) The majority of the mafic and ultramafic metavolcanic rocks, dikes, and sills in the TNB represent variably evolved products of the differentiation a komatiitic magma by the fractionation and/or accumulation of olivine  $\pm$  clinopyroxene  $\pm$  plagioclase without assimilation of significant amounts of crustal material.
- 2) There are significant regional and local variations in both the major and trace element compositions of the volcanic rocks that may indicate derivation from different magma sources exhibiting a range of incompatible element enrichment. On the basis of their trace element compositions, the TNB volcanic rocks, dikes, and sills can be subdivided into four distinct compositional types.
- 3) Many of the gabbroic sills in the Setting Formation have compositions similar to those of the overlying mafic volcanic rocks of the Bah Lake assemblage, suggesting that much of the Bah Lake assemblage may be autochthonous with respect to the Oswagan Group and the TNB.
- 4) Whereas both the volcanic rocks of the Bah Lake assemblage and the ultramafic sills that host the Ni-Cu-(PGE) deposits appear to have formed from originally komatiitic magmas, the major and trace element compositions of two groups of rocks are significantly different. Although there are a few crustally-contaminated and chalcophile element-depleted rocks in the Bah Lake assemblage and a few crustally uncontaminated and chalcophile-element unenriched rocks in the ultramafic sills, the majority of the rocks in the Bah Lake assemblage are not only uncontaminated and undepleted in chalcophile elements, but also have higher TiO<sub>2</sub> and lower MnO and SiO<sub>2</sub> at similar MgO contents (**Section 8.4.4.1**).
- 5) Although we cannot exclude the possibility that the lavas in the Bah Lake assemblage passed through the UM sills and left no crystallized products, at this stage there is no evidence that the sills acted as feeders for the mafic-ultramafic lavas, sills, and dikes in the Bah Lake assemblage.

## 8.6 Metasedimentary Rocks

### 8.6.1 Introduction

The original aims of this component of the project were to:

- 1) Produce chemostratigraphic columns for the northern, central, and southern regions of the TNB to supplement existing lithostratigraphy.
- 2) Establish geochemical methods of distinguishing between mineralogically- and texturally-similar lithologies in different stratigraphic units of the Oswagan Group.
- 3) Establish geochemical signatures of the different stratigraphic units to aid in the identification of specific units assimilated by magma during the emplacement of the ultramafic bodies.

Although each of these objectives was addressed during the project, the absence of systematic geochemical variations that are independent of major element composition meant that not all of original questions could be answered using the current database.

The samples analyzed during this study may be divided into two groups:

- 1) Samples collected by J. Macek from type sections in the Northern TNB (in particular the Pipe Pit, Thompson Pit, Setting Lake, Grass River, and Tracy Lake areas).
- 2) Samples collected from three drill cores that intersected recognizable units in the William Lake and Minago River areas of the central region of the TNB.

## 8.6.2 Petrography

The majority of the samples from the type section analyzed during this study have been independently characterized by McGregor (1997, 1998, 2000) as part of a detailed study of the petrography and mineralogy of the metasedimentary rocks of the Oswagan Group and the rocks in close proximity to them (e.g., the Kisseynew gneisses and reworked Archean gneisses). The results of this study will be published as a Manitoba Geological Survey report that is currently in preparation.

The samples collected from the central region of the TNB covered most of the main lithologies of the Oswagan Group stratigraphy from the upper parts of the Manasan Formation to the top of the Thompson formation (DDH MN96-141) and from the middle of the Pipe Formation to the base of the Setting Formation (DDH WL95-110 and WL95-111). The locations, lithologies and petrography of the samples are summarized in **Table 8.7**.

## 8.6.3 Whole Rock Compositions

### 8.6.3.1 Major and Minor Elements

#### *Northern TNB*

Although the whole-rock major and minor element compositions of the Oswagan Group metasedimentary rocks are highly variable, the variations correspond well with observed changes in lithology (**Fig. 8.36**). As would be expected, quartzites and cherts of the Manasan (Om1), Pipe (Op3), and Setting Lake Formations (Os) have higher silica contents than the adjacent pelites, semi-pelites, and silicate-facies iron-formations, and the semi-pelites and pelites are characterized by higher  $\text{Al}_2\text{O}_3$  and  $\text{K}_2\text{O}$  contents that reflect greater abundances of clay and/or feldspar in the protolith. Similarly, silicate-facies iron-formations have higher Fe, Co, and Mn contents and lower Ni contents than quartzites and pelites.

Although it is possible to recognize different lithologies of the Oswagan Group on the basis of their major element compositions, it is difficult to discriminate between similar lithologies



in different formations or stratigraphic units on the basis of elemental abundances alone, indicating that some other method is required. Because there is not as simple a relationship between the primary mineralogy and chemical compositions of clastic or carbonaceous rocks (and their metamorphosed equivalents) as there is for igneous rocks, the normal geochemical methods of classifying sedimentary rocks do not match those based on mineralogy (e.g., the relative proportions of quartz, feldspar, and lithic fragments or the carbonate grain type and amount of mud matrix), but focus on the division of sedimentary rocks according to their chemical maturity and/or an estimate of the provenance of their sources.

### Chemical maturity

On a plot of  $\text{Fe}_2\text{O}_3/\text{K}_2\text{O}$  vs.  $\text{SiO}_2/\text{Al}_2\text{O}_3$  (**Fig. 8.37**), pelites and semipelites of the Manasan Formation plot within the geochemical fields for litharenites or arkoses and at higher  $\text{SiO}_2/\text{Al}_2\text{O}_3$ , but similar  $\text{Fe}_2\text{O}_3/\text{K}_2\text{O}$  ratios to those of the Pipe Formation and Archean basement. Because the majority of the  $\text{Al}_2\text{O}_3$  in the protolith would have been present in either feldspars and clays, the higher  $\text{SiO}_2/\text{Al}_2\text{O}_3$  ratios of the Manasan Formation rocks indicates that they may have originally contained a higher proportion of quartz than those in the Pipe Formation or basement and that the degree of chemical maturity decreased with time in the region. If it is assumed that the whole-rock major element compositions of the metasedimentary rocks were not significantly affected during metamorphism, then the variation in chemical maturity through the sequence indicates a change in either the provenance of the sediments (e.g., a change in the proportion of felsic vs. mafic source rocks through time) or the distances over which the sediments were transported (leading to variations in the amount of breakdown of detrital feldspars vs. ferromagnesian minerals).

### Sediment provenance

One way in which to distinguish between a change in provenance and a change in transport distance is to classify the whole-rock major element compositions of the metasedimentary rocks and gneisses using a discriminant diagram similar to that proposed by Roser & Korsch (1988), in which the sediments are separated into four different compositional groups characteristic of their sources (mafic, intermediate, or felsic igneous or quartzose-sedimentary) according to linear functions of their major element compositions (**Fig. 8.38**).

On this discriminant plot, the variation in the  $\text{SiO}_2/\text{Al}_2\text{O}_3$  and  $\text{Fe}_2\text{O}_3/\text{K}_2\text{O}$  ratios of the Manasan Formation and the lower members of the Pipe Formations (especially Op2) observed in **Figure 8.37** appears to correlate with a change from a primarily quartzose sedimentary provenance to a source dominated by felsic igneous rocks (or with a component from an intermediate or mafic igneous source) that is similar to some of the samples collected from the Archean basement. With increasing stratigraphic height, however, this trend is reversed, such that the pelites of the uppermost Op3 member of the Pipe Formation plot within the quartzose sedimentary field. The observed grouping of the samples from different units of the Ospwagan Group into separate fields on the discrimination diagram and the reversal of the trend from sedimentary to igneous sources is most consistent with the chemical compositions of the Ospwagan Group pelites being determined by changes in the source of the sediments rather than transport distance.

**Table 8.7** Descriptions of metasedimentary samples collected from central region of TNB

Sample Number	Hole Number	Depth	Location	Stratigraphic Unit	Lithology	Description
WB09873	WL95-110	345.10	William Lake Dome	Setting (Os)	Quartzite	medium grained-coarse grained impure quartzite with K-feldspar, trace biotite & trace vein sulfide
WB09872	WL95-110	317.68	William Lake Dome	Setting (Os)	Quartzite	medium grained impure quartzite with biotite + feldspar +/- chlorite +/- tremolite +/- magnetite/ilmenite + disseminated sulfide, well foliated/laminated
WB09871	WL95-110	241.12	William Lake Dome	Pipe (Op3)	Semi-pelite	fine grained-medium grained strongly altered biotite-chlorite schist, moderately foliated, similar to semi-pelites in WL96-111, but possibly uppermost P3
WB09870	WL95-111	462.7	William Lake Dome	Pipe (Op2-Op3)	Semi-pelite/ Calc-silicate	medium grained biotite-muscovite schist, well foliated with trace garnet, calcareous band in upper part of sample
WB09869	WL95-111	335.45	William Lake Dome	Pipe (Op2)	Semi-pelite	medium grained-coarse grained biotite-muscovite schist, well foliated, non-magnetic, trace disseminated sulfide
WB09868	WL95-111	305.65	William Lake Dome	Pipe Upper (Op2)	Quartzite	fine grained pale-grey laminated impure quartzite with trace medium grained garnet & trace disseminated sulfide (pyrite)
WB09867	WL95-111	216.45	William Lake Dome	Pipe Upper (Op2)	Semi-pelite	medium grained dark-grey garnet-biotite schist, moderately foliated, slightly magnetic
WB09866	WL95-111	212.81	William Lake Dome	Pipe Upper (Op2)	Semi-pelite	medium grained-coarse grained light-grey/green garnet-muscovite schist, well foliated, non-magnetic, trace disseminated sulfide
WB09865	MN96-141	239.65	Minago River	Thompson Ot3)	Marble	Very coarse grained pink/dark-green/light-green megacrystic marble
WB09864	MN96-141	213.63	Minago River	Thompson Ot2)	Quartzite	grey/pink impure quartzite with cm scale laminated
WB09863	MN96-141	180.00	Minago River	Thompson Ot2)	Calc-silicate	green thinly laminated calc-silicate with occasional cherty bands
WB09860	MN96-141	132.36	Minago River	Thompson Ot2)	Calc-silicate	green-dark-green laminated/foliated calc-silicate gneiss
WB09862	MN96-141	155.34	Minago River	Thompson (Ot1?)	Calc-silicate	fine grained-medium grained green-dark-green laminated/foliated calc silicate with occasional siliceous segregations
WB09861	MN96-141	149.14	Minago River	Manasan (Om2)	Semi-pelite	white/dark-green/pink biotite-K-feldspar gneiss, well foliated

In order to confirm these results, the minor element compositions of the Oswagan Group metasedimentary rocks were compared using elements that are expected to be relatively immobile during metamorphism and which are enriched in accessory minerals derived from either mafic or felsic igneous rocks (e.g., Cr and Zr: **Fig. 8.39**). On this plot, there is a decrease in the Zr/Cr ratio of the pelitic and semi-pelitic rocks up section from the Manasan Formation to the Op1 member of the Pipe Formation, then a gradual decrease up section through the Op2 and Op3 members of the Pipe Formation and into the Setting Formation (Os). This is also seen in the profile plotted in **Figure 8.36**. The higher Cr contents of the lowermost Pipe Formation may indicate the introduction of a mafic detrital component (as suggested by the trend toward the mafic or intermediate provenance field in **Fig. 8.38**). Whereas the sandstones and pelites of the Pipe formation (in particular the Op2 member) have similar Cr and Zr contents (indicating a similar accessory mineral assemblage), the iron-formations within each of the units of the Pipe Formation are relatively enriched in Cr, suggesting that they contain a greater mafic detrital component. The variation in the Cr contents of the Oswagan Group metasediments indicates that there may have been a significant contribution from a mafic source during their deposition and that mafic or ultramafic rocks were exposed or erupted in the area prior to the eruption of the Bah Lake assemblage picrites and basalts that are currently observed at the top of the stratigraphic sequence.

### ***Central TNB***

Although the number of clastic metasedimentary rocks from the central region for which there are accurate stratigraphic locations is small, the whole-rock compositions of the pelitic and/or arenitic metasedimentary rocks collected from the William Lake area suggest that the major element compositions of most units and the minor element compositions of the upper parts of the Oswagan Group are similar between the central and northern regions of the TNB, but that the minor element compositions of the lower parts of the Oswagan Group may differ significantly between the two regions.

Although the single semi-pelitic sample inferred to originate from the Manasan Formation (Om) plots at low Fe contents in the shale field in the classification of Herron (1988) (**Fig. 8.40**), indicating that it may be chemically less mature than similar rocks from the Pipe Pit, the Thompson Ot2 quartzite plots in the subarkose field close to the compositions of pelites and semi-pelites in the northern region of the TNB and is consistent with the inferred moderately chemically mature compositions determined for the lowermost Oswagan Group sedimentary rocks in the northern region of the TNB. The semi-pelites of the Op2 and Op3 members of the Pipe Formation in the William Lake area all have major element compositions similar to Op1 and Op2 pelites and semi-pelites in the Pipe Pit and plot in the shale field at moderate Fe contents, consistent with the inferred lower chemical maturity of the sedimentary rocks of the Pipe Formation. Similarly, the quartzites in both the northern and central regions of the TNB plot at low  $\text{Fe}_2\text{O}_3/\text{Al}_2\text{O}_3$ , in either the subarkose or arkose field or **Figure 8.40**, consistent with an increase in chemical maturity toward the top of the sequence and similar sources for the sediments in both regions.

On the discriminant diagram of Roser & Korsch (1988) (**Fig. 8.41**), the Om semi-pelite and Ot2 quartzite plot on the far left of the diagram, on the boundary between an inferred felsic igneous and quartzose sedimentary provenance, whereas the Op2 and Op3 pelites and semi-pelites plot close to the junction of the four different source provenances (mafic-,

intermediate-, and felsic-igneous, and quartzose-sedimentary) and the samples of Setting Formation quartzites plot in the centre of the field for a quartzose-sedimentary provenance. Although the pelites and semi-pelites of the Pipe Formation appear to have had a greater contribution from a mafic igneous source than rocks of the same units further north, the trends are similar to those observed in the type section and the major element variations of the sedimentary rocks appear to be similar in the northern and central regions.

When the minor element compositions of the metasedimentary rocks collected from the central TNB are compared to those from the type section at the Pipe Pit, they appear to differ significantly. On a plot of Zr vs. Cr (**Fig. 8.42**), the Zr /Cr ratios of almost all of the semi-pelitic samples, including those from both the Manasan and Pipe Formations as well as the single quartzite sample from the Thompson Formation, are enriched in Cr relative to the same lithologies in the northern region and plot toward the range of Zr/Cr ratios in basaltic rocks. Because neither Cr nor Zr are expected to be mobile during diagenesis or metamorphism, the variations in Zr/Cr ratio are inferred to reflect primary variations in the compositions of the sediments. Thus, although the Zr/Cr ratio of the pelitic (or calc-silicate) sedimentary rocks may be used to discriminate between the upper and lower parts of the Oswagan Group in the northern region of the TNB (e.g., Pipe Pit, Thompson Pit, Oswagan Lake and Manasan Quarry), this ratio appears to work less well in the central TNB, possibly because of a different source within the neighbouring Superior margin or the earlier initiation of volcanic activity in this region.

### 8.6.3.2 Trace Elements

Trace element data for the suite of sedimentary and basement rocks are summarized on multi-element and element ratio plots in **Figure 8.43**. When plotted on a mantle-normalized multielement diagram similar to those conventionally used for mafic and ultramafic rocks, most of the samples exhibit the strong incompatible-element enrichment and Ta-Nb-Ti depletion that is characteristic of sediments derived from upper continental crustal rocks (**Fig. 8.43a**). Because the differences between the mantle-normalized patterns of the sedimentary samples are small relative to the overall variation in normalized elemental abundances and the various anomalies that are common to most sedimentary rocks, it is difficult to recognize inter-sample differences on mantle-normalized plots. In order to visualise the differences between sedimentary rocks better, their trace element compositions may be normalized to either an external sedimentary rock standard (e.g., North American Shale Composite: NASC) or an internal sedimentary rock standard (e.g., least carbonate-rich pelitic sample within the sample suite). In **Figures 8.43b to 8.43d**, the data for the TNB sedimentary and basement rocks are normalized to that of the typical Manasan Formation (Om2) semi-pelite shown in **Figure 8.43a**.

#### *Semi-pelites and Pelites*

In the semi-pelite normalized multielement diagrams (**Fig. 8.43b**), the majority of the pelitic and semi-pelitic rocks of the Oswagan Group have flat profiles with minor differences in the abundances of Zr-Nb-Ti-Th. These differences are clearly shown by the linear trends exhibited by the compositions of felsic gneisses in the Archean basement (and quartzites in the lowermost Manasan Formation) and metapelitic and arenaceous rocks in the Thompson, Pipe, and Setting Formations on a Th-Nb-Zr ternary diagram (**Fig. 8.44**). Whereas the  $[\text{Th}/\text{Nb}]_{\text{mn}}$  ratios of the felsic basement rocks are in the range 13-200, the  $[\text{Th}/\text{Nb}]_{\text{mn}}$  ratios of

metasedimentary rocks in the middle to upper Oswagan Group are in the range 8.4-11. Because HFSE should be relatively insoluble in both the water column originally overlying the sediments and in metasomatic fluids produced during metamorphism, the differences in the Zr-Nb-Ti-Th compositions of the metasedimentary rocks are interpreted to reflect the compositions of detrital minerals and to therefore represent variations in sediment sources. Whereas the lowermost rocks of the Oswagan Group may have been derived from the local felsic basement gneisses, the trace element compositions of the metapelites and quartzites of the mid- to upper Oswagan Group, particularly the Pipe Formation, suggest that the rocks higher in the sequence were derived from a different, less Th-enriched source.

Although the scatter of some of the samples toward the compositions of intermediate basement gneisses in **Figure 8.44** may suggest that a third detrital component was present during the deposition of the Oswagan Group sediments, more data will be required to confirm this trend.

### ***Iron-Formations***

On the pelite-normalized plots (**Fig. 8.45**), the sulfide and silicate facies iron-formations from all three sub-units of the Pipe Formation are strongly enriched in U, P, and Co and depleted in Zr, Hf, Ti, and LILE (e.g., K, Ba, Sr) relative to the typical Manasan pelite. Whereas the relative depletion of LILE in the iron-formations may have resulted from mobilization of these elements by metamorphic fluids after their formation, the low HFSE and high U, P, and Co contents of the iron-formations may reflect original compositional differences.

Comparison of the whole-rock elemental data for the Pipe iron-formations and the average compositions of iron-formations in several deposits within and around the Superior Province (**Fig. 8.46**) indicates that the enrichment of Co and P in the Pipe iron-formations is similar to that observed in many Algoma-type iron-formations, which are believed to have formed through volcanically-driven hydrothermal processes (e.g., James, 1954). Although this may be taken to suggest a hydrothermal origin for many of the Pipe iron-formations, other trace element signatures commonly observed in metal-rich ocean sediments and iron-formations considered to be of hydrothermal origin (e.g., pronounced negative Ce anomalies, positive Eu anomalies, and LREE depletion relative to the NASC) are not obvious in the data for the Pipe iron-formations. The absence of positive Eu anomalies, which are normally interpreted to reflect mobilization of  $\text{Eu}^{2+}$  from the source rocks, suggests a more oxidizing environment in the source than for most other iron-formations of this type, which would be consistent with proposed change from a less oxidizing atmosphere in the Archean to a more oxidized atmosphere during the late Proterozoic (e.g., Cloud, 1973; Holland, 1973). The absence of LREE depletion may reflect a more felsic (i.e., intermediate) source and/or greater leaching of LREE during alteration of the source rocks compared to Archean Algoma-type IF.

### ***Grass River Group Sedimentary and Tuffaceous Rocks***

On a mantle-normalized multielement plot, the Grass River Group arenites (Ga-c) appear to have profiles with elevated LILE (large-ion lithophile elements) and prominent negative Nb and Ti anomalies, similar to medium- to high-K basaltic andesites of the Missi Group on the south flank of the Kisseynew domain (**Fig. 8.47a**). These observations led Zwanzig (1999) to conclude that the metasedimentary rocks either represented intermediate tuffs derived from

the Reindeer Zone of the adjacent Kisseynew Domain of the THO or contained a significant component derived from such lithologies.

Felsic gneisses of the Grass River Group (Gb3) exposed between Five Mile and August Lakes exhibit multielement profiles that are similar to Missi Group metarhyolites (H. Zwanzig, unpublished data), with pronounced Th enrichments and large negative Nb, Eu, and Ti anomalies (**Fig. 8.47b**). These rocks are interpreted to be metamorphosed rhyolite tuffs. The geochemical compositions of the gneisses are consistent with the interpretation that the Grass River Group is correlative with the Missi Group (**Section 5.2.3**).

### 8.6.3.3 Nd Isotope Compositions

As part of the work to constrain the petrogenetic histories of the different elements of the magmatic system in the TNB and to investigate the processes of contamination and/or metasomatism that may have led to the incompatible element enrichment observed in many of the ultramafic bodies, 9 samples of Oswagan Group metasedimentary rocks from the type section at Pipe Pit were selected for Sm-Nd isotope analysis. These analyses supplement those presented by Ansdell & Bleeker (1997) for rocks from the northern region of the TNB, and fill gaps in the stratigraphic section. The results of the analyses are presented in **Table 8.8**.

Whereas the Sm-Nd isotope compositions of the Pipe Formation metasedimentary rocks are similar to those presented by Ansdell & Bleeker (1997) for other parts of the Oswagan Group stratigraphy and yield depleted-mantle model ages of 2.73-2.84 Ga (using the depletion model of Ben Othman et al., 1984), the Manasan quartzites are less radiogenic (i.e., lower  $^{143}\text{Nd}/^{144}\text{Nd}$ ) and yield model ages of ~2.87 and 3.05 Ga (**Fig. 8.48**). The results are remarkably coherent and indicate that the sediments were derived from Archean rocks with ages in the 2.7-3.0 Ga range. This spread falls well within the most common ages for units of the western Superior Province (Skulski & Villeneuve, 1999) and is in agreement with the distribution of ages of detrital zircons in the Oswagan Group (**Section 10**).

### 8.6.4 Summary

Although it was not possible to satisfy all of the original aims of the project with respect to the geochemistry of the Oswagan Group metasedimentary rocks, the major, minor, and trace element compositions of a suite of well-characterized samples from the type section of the Oswagan Group metasedimentary rocks at the Pipe and Thompson Pits in the northern region of the TNB and a suite of samples from the William Lake area in the central region of the TNB indicate the following:

**Table 8.8** Nd isotope compositions of metasedimentary rocks analyzed during CAMIRO Project 97E-02

Sample	Description	Nd (ppm)	Sm (ppm)	$^{147}\text{Sm}/^{144}\text{Nd}$	$^{143}\text{Nd}/^{144}\text{Nd}$	+/-	$\epsilon_{\text{Nd}}(1.9)$	$T_{\text{DM}}$
CHA-145	Sillimanite schist (Op3)	23.36	4.07	0.1053	0.511029	17	-9.1	2.83
CHA-130	Sulfide-bearing siliceous metasediment (OpP3)	16.59	2.97	0.1082	0.511100	8	-8.5	2.82
CHA-61	Sulfide-bearing silicate facies IF with chert (Op3)	21.29	4.14	0.1175	0.511272	33	-7.4	2.81
CHA-50	Siliceous metasediments layered with calc-silicates (Op3)	25.84	4.58	0.1071	0.511080	12	-8.6	2.81
CHA-34	Top of sulfide-facies IF (Op2)	15.55	2.76	0.1072	0.511068	8	-8.8	2.83
CHA-23	Pelite with dark bands, sulfide bearing (Op2)	20.60	3.58	0.1051	0.511072	5	-8.2	2.77
CHA-15	Sulfide-bearing silicate facies IF (Op1)	22.52	4.35	0.1167	0.511307	21	-6.5	2.73
CHA-03	Basal blue quartzite with pebbles (Om1)	3.32	0.51	0.0930	0.510770	10	-11.2	2.87
CHA-01	Basal quartzite (Om1)	3.05	0.53	0.1054	0.510890	12	-11.9	3.04

Analyses by Dr. K. Ansdell, University of Saskatchewan. For analytical methods, see **Appendix 1**.  $\epsilon_{\text{Nd}}(1.9) = 10^4 \times$  deviation in  $^{143}\text{Nd}/^{144}\text{Nd}$  ratio from the chondritic uniform reservoir (CHUR) at 1.9 Ga.  $^{143}\text{Nd}/^{144}\text{Nd}_{\text{CHUR}}$  at 1.9 Ga calculated from present day  $^{143}\text{Nd}/^{144}\text{Nd}_{\text{CHUR}} = 0.512638$ ,  $^{147}\text{Sm}/^{144}\text{Nd}_{\text{CHUR}} = 0.1967$ , and  $\lambda(^{147}\text{Sm}) = 6.54 \times 10^{-12} \text{ y}^{-1}$  (Jacobsen & Wasserburg, 1980).  $T_{\text{DM}}$  = depleted mantle model ages calculated using the mantle evolution curve of Ben Othman et al. (1984).

- 1) Similar lithologies in different stratigraphic units of the Oswagan Group metasedimentary rocks may be distinguished on the basis of their major and minor element compositions and reflect changes in either chemical maturity or sedimentary provenance.
- 2) Whereas the major element compositions of most of the pelitic and/or arenitic units of the Oswagan Group metasedimentary rocks are similar throughout the TNB, the minor element compositions of the lower parts of the Oswagan Group (e.g., Cr and Zr in units Om and Ot) appear to differ significantly between the two regions, suggesting that the two areas may have initially had slightly different sedimentary sources and/or formed in different sub-basins. This difference disappears in higher parts of the stratigraphic sequence (units Op and Os), indicating the possible formation of a larger, more interconnected basin.
- 3) There is a systematic increase in mafic component with stratigraphic height within the Manasan, Thompson, and lowermost Pipe Formations that may coincide with volcanism associated with rifting and the initiation of the hydrothermal activity responsible for the formation of the silicate and sulfide-facies iron-formations.
- 4) Although the different units of the Oswagan Group stratigraphy may be distinguished on the basis of their whole-rock compositions, the differences between the units are either relatively subtle (e.g., HFSE) or occur in elements that are generally compatible in mafic magmas (e.g., Cr and Co), hence cannot be used to distinguish between the assimilation of different units during the emplacement of the ultramafic bodies.

## 8.7 Granitoids and Gneisses

Preliminary geochemical data obtained on felsic igneous rocks (Archean gneisses, granites, and pegmatites) were reported in the 2000 Annual Report (CAMIRO Research Group, 2000). For this study 22 felsic gneiss and granitoid samples were analyzed for whole rock major and trace elements and 7 of the same samples were analyzed for Nd isotopic compositions. The results are reported in **Tables 8.9**, and **A9.1**. A detailed discussion of the geochemistry of the granitoids and gneisses is included in the 2000 Annual Report (CAMIRO Research Group, 2000). Although the number of samples is limited, several important points have emerged:

- 1) All the analyzed samples belong to a calc-alkaline series of trondhjemitic affinity and thus represent magmas generated along an active margin or volcanic arc.
- 2) The Archean gneisses that crop out in the TNB are not homogenous and fall in three groups: Sipiwesk gneisses, TNB gneisses, and Pipe pit gneisses. Their chemical characteristics indicate that they were derived from different sources and/or ages.
- 3) Some of the gneisses in the TNB do not appear to have undergone granulite facies metamorphism.
- 4) The chemistry of the Mystery Lake pluton is similar to that of classical Archean TTG series. This is in agreement with a U-Pb zircon age of 2.75 Ga and a Nd model age of 2.64 Ga (sample TB 99-15, **Table 8.9**) and would favour an Archean age for this pluton. In this case, the 1836 Ma monazite age (N. Machado, unpubl. data, 1999 TNB Project Annual Report) is a metamorphic age. If this result is confirmed it will indicate that Late Archean magmatism took place in the TNB. However, offshoots presumed to be derived from the Mystery Lake intrusion crosscut the Ospwagan Group (J. Macek, pers. comm., August 2001), suggesting that granitic magmatism post-dates Ospwagan sedimentation. Because this age of sedimentation is not well established, the true age of the intrusion cannot be specified. Further analysis of Mystery Lake samples are in progress to try resolve this issue.

**Table 8.9** Nd isotope data for Archean gneisses

Sample N°	Nature	Nd (ppm)	Sm (ppm)	$^{147}\text{Sm}/^{144}\text{Nd}$	$^{143}\text{Nd}/^{144}\text{Nd}$	$\epsilon_{\text{Nd}}(0)$	$T_{\text{DM}}$
TNB 99-2A	Sipiwesk gneiss	6.312	0.867	0.0830	$0.510524 \pm 9$	-41.2	2.96
TNB 99-27A	Archean gneiss	8.985	1.239	0.0833	$0.510354 \pm 9$	-44.5	3.18
TNB 99-6	Archean gneiss	70.62	12.06	0.1032	$0.510912 \pm 9$	-33.7	2.97
TNB 99-12A	Archean gneiss	18.99	3.128	0.0995	$0.510712 \pm 10$	-37.6	3.15
TNB 99-14	Archean gneiss	4.006	0.685	0.1033	$0.511059 \pm 9$	-30.8	2.76
TNB 99-15	Mystery Lake granodiorite	6.463	1.174	0.1098	$0.511256 \pm 13$	-27.0	2.64
TNB 99-42	N Jonas granite	12.24	1.597	0.0788	$0.510898 \pm 10$	-33.9	2.43

Errors at  $2\sigma$ .  $T_{\text{DM}}$  = model age in Ga.

Further constraints on the geodynamics of the TNB require information regarding the petrogenesis of the Proterozoic felsic magmatism, which has not been well characterized. Hence, during the 2000 summer field season sampling focussed mainly on the Proterozoic granites cropping out in the TNB and in the Kisseynew domain. A total of 32 samples were analyzed for whole-rock major elements, as reported in **Table A9.2**. These samples include 23 granites, 6 Archean gneisses, 2 pegmatites, and 1 aplite. Because the trace element analyses were not completed in time for their interpretation prior to the production of this



report and because this work was outside the scope of the original project, these data and their interpretation will be reported separately by A. Poutrel.

The compositional variations of the Archean and Proterozoic felsic rocks are shown in a normative Ab-Or-An classification diagram (**Fig. 8.49**: after O'Connor, 1965, as modified by Barker, 1979). The Archean gneisses mainly plot within the trondhjemite, tonalite, and granodiorite fields in this diagram and, hence, are typical of Archean TTG (e.g., Martin, 1994). Some gneisses show more potassic compositions and therefore plot in the granitic field. Granitoids, aplites, and pegmatites plot essentially within the granite and quartz monzonite fields. The less differentiated granitoids are more Na-rich and plot in the trondhjemite and granodiorite fields. In a A/NK versus A/CNK diagram (**Fig. 8.50**: after Maniard & Picoli, 1989), the majority of the samples plot in the peraluminous field, but close to the metaluminous field. Four samples (two granites and two Archean gneisses) are clearly metaluminous. These are the least-differentiated samples in the suite and have SiO<sub>2</sub> contents ranging between 56% and 64% (**Table A9.2**). In a A/CNK vs. SiO<sub>2</sub> diagram (**Fig. 8.51**), all samples plot close to the classical calc-alkaline trend.

Although the number of samples is small, the geochemical data confirm the results reported in the 2000 annual report, suggesting that the felsic magmatism in the TNB involved I-type magmatism (Chappell & White, 1974) followed by calc-alkaline magmatism. This result is confirmed by the large variation in SiO<sub>2</sub> contents of the analyzed samples (56-75 wt%: **Table A9.2**) without hyper-differentiation of any of the samples, a classical feature of I-type granitoids (e.g., Chappell & White, 1974, 1992). This result indicates that the majority of the Proterozoic granites in the TNB were derived by partial melting of igneous material (i.e., orthogneisses), and not formed by melting of aluminous sedimentary material (i.e., paragneisses). This is in agreement with the general presence of Archean inherited zircons in the Proterozoic granites (e.g. the Mystery Lake and Wintering Lake intrusions: Machado et al., unpubl. data, 1999 TNB Annual Report; **Section 10.2.4**) and the Nd model ages of the samples (**Table 8.9**). These compositions are typical of volcanic arcs and active margin environments.

## 8.8 Interpretations

### 8.8.1 Melting Processes and Sources of Mafic and Ultramafic Magmas

#### 8.8.1.1 Depth and Degree of Partial Melting

The low Cr contents in many of the komatiitic rocks in the Bah Lake assemblage and the dunitic portions of the TNB ultramafic bodies, as well as the highly forsteritic compositions of the olivines within the ultramafic bodies, indicate that the bodies must have formed from magnesium-rich komatiitic magmas (>20 - 22 wt% MgO) that separated from a highly refractory, olivine-rich mantle residue and were chromite under-saturated at the time of emplacement. Although the highly refractory nature indicated for the residues could reflect extraction of a larger volume of magma from a relatively fertile mantle source region or extraction of a smaller volume of magma from an already depleted source (the composition of the residue simply reflects the *total* integrated melt extracted through time), the moderately-depleted to slightly-enriched incompatible trace element compositions inferred for the parental liquids (**Section 8.4.4.2**) indicates that the source region for the magmas could not have been significantly depleted prior to the production of the TNB magmas and

that the magmas must have formed through high degree partial melting of a moderately-depleted source. By comparing the major element compositions of the TNB magmas to those produced during the experimental melting of a fertile spinel lherzolite under a range of pressures and temperatures (10 – 30 kbar and 1250 – 1525 °C: Hirose & Kushiro, 1993), it is possible to estimate the temperature and degree of melting necessary for the formation of the different parental magmas identified in the TNB, as well as the possible depth at which this melting occurred.

### ***Depth of Melting***

Melting experiments indicate that the SiO<sub>2</sub> contents of magmas produced from a fertile mantle source are relatively insensitive to the degree of melting, but decrease systematically with increasing pressure (Hirose & Kushiro, 1993). Given that one of the most significant differences between the compositions of the parental magmas to the ultramafic bodies and those of the Bah Lake assemblage volcanic rocks appears to be their initial SiO<sub>2</sub> contents, it is possible that the two groups of magmas were derived by melting at different depths. If the SiO<sub>2</sub> contents of the inferred parental magmas used with the MELTS program in **Section 8.4.4.1** are compared to the experimental results, the composition of the parental magma of the ultramafic bodies is consistent with having been produced at ca. 15-20 kb (45-60 km), whereas the composition of the parental magma of the Bah Lake assemblage rocks is consistent with having been produced at ca. 25-30 kb (75-90 km) (**Fig. 8.52**).

### ***Degree and Temperature of Melting***

Although the melting experiments of Hirose & Kushiro (1993) concentrated on the low to moderate degrees of melting required for the production of basaltic or picritic magmas, they indicate that the MgO content of a magma increases linearly with increasing degree of melting and melting temperature (**Figs. 8.53a and b**), which is consistent with melting of progressively more magnesian pyroxene and/or olivine in the source. If these trends are extrapolated to higher temperatures, then the parental magmas to the ultramafic bodies would have formed by ~50% melting and required a temperature in excess of 1600°C (vs. 1 atm liquidus temperature of ~1500°C calculated by the MELTS models: **Section 8.4.4.1**). Under such conditions, both orthopyroxene and clinopyroxene would be expected to have been completely melted in the source, leaving a residue that was composed primarily of olivine (see Herzberg and O'Hara, 1998). When the MgO contents of the ultramafic magmas that formed the TNB ultramafic bodies and the associated degrees of melting and melting temperatures required to produce them are compared to those of the parental magmas inferred for the contemporaneous ultramafic volcanism in other parts of the Circum-Superior Boundary Zone (CSBZ), e.g., Fox River Belt (~18 wt% MgO: D.C. Peck, pers. comm., 2003), Ottawa-Belcher Islands (~18 wt% MgO: Arndt et al., 1987), Cape Smith Belt (16-18 wt% MgO: Francis et al., 1983), and Labrador Trough (~12-15 wt% MgO: J. Mungall, pers. comm., 2003), the values for the TNB are the highest, suggesting that the mantle underlying the western CSBZ at this time may have been significantly hotter and experienced greater degrees of melting than that along other parts of the craton margin. On the other hand, several studies have recognized very magnesian xenocrystic olivines in similar rocks in the CSBZ (Arndt et al., 1987) and elsewhere (e.g., Larsen & Pedersen, 2000; Thompson & Gibson, 2000), suggesting that the most magnesian magmas are not always erupted, preserved, or sampled. Therefore, although it is possible that the mantle beneath the TNB was anomalously hotter than in other areas of the CSBZ, more detailed work will be required

to establish this. Similarly, it is not known whether the apparent general trend of decreasing MgO content from west to east around the northern margin of the CSBZ is real or just an artefact of selective exposure or incomplete sampling.

### ***Mantle Source Region***

The presence of parental ultramafic magmas that exhibit both moderately depleted (ultramafic bodies) and slightly enriched (Bah Lake Assemblage and mafic dikes) trace element signatures, combined with the high melting temperatures inferred for the ultramafic magmas, suggest that the magmas were derived from an anomalously hot but heterogeneous source. Comparisons with modern oceanic and continental flood basalts indicate that such characteristics are consistent with melting within different parts of a mantle plume (e.g., Campbell et al., 1989). However, owing to the large uncertainties that currently surround our understanding of ancient mantle dynamics, it is unclear whether the chemical signatures of plumes in the Paleo-Proterozoic were similar to present day examples. Consequently, although a plume origin for the TNB ultramafic magmas appears to be the most likely cause of the magmatism, its presence can only be inferred at the present time.

### ***Metallogenic Implications***

Because the degree of melting and eruption temperature of an ultramafic magma significantly influence both its chalcophile metal contents, S-saturation state (both within the source region and while *en route* to the surface), and its ability to incorporate external sulfur, the higher degrees of melting and higher temperatures inferred for the TNB ultramafic magmas would have been important factors influencing the metallogenesis of the associated sulfide ores.

Owing to their high degrees of melting, the magmas would have not only been able to dissolve all of the sulfide phase in the mantle source (leading to the enrichment of the magmas in both the moderately and highly chalcophile metals), but would also have been far from sulfide saturation during most of their transportation and emplacement in the crust, despite country rock assimilation and/or fractionation of olivine. Because they may have been significantly more sulfide-undersaturated than the magmas that erupted in other parts of the CSBZ, they would have been less susceptible to sulfide loss and would have been better able to retain their metals until they intersected an external source of sulfur.

As a consequence of their higher temperatures, the ultramafic magmas of the TNB would have also had higher heat capacities and lower viscosities than less magnesian liquids formed by lower degrees of melting. Because thermomechanical erosion of the country rocks is most effective when the magmas are flowing turbulently, either within lava channels (Huppert et al., 1984; Leshner et al., 1984; Williams et al., 1998), along magma conduits (Huppert & Sparks, 1985a, 1985b), or in channelized sills, and results in significant cooling of the magma (Huppert & Sparks, 1985a, 1985b), the higher heat capacities and lower viscosities of the TNB ultramafic magmas would have significantly enhanced their capacity for bulk assimilation of sedimentary rocks of the Ospwagan Group (in particular the S-rich iron-formations), leading to the production of greater quantities of immiscible sulfide liquid from which to form the ores. Whereas this would be an advantage in most environments (where the ability to form a deposit is limited by the supply of sulfide), in the TNB this may have actually lead to the production of larger-volume, but lower-grade deposits owing to the dilution of the metals in a greater mass of sulfide liquid.

## 8.8.2 Volcanic Architecture of Mafic and Ultramafic Rocks

Although mass balance dictates that the ultramafic bodies represent the cumulates formed from larger volumes<sup>7</sup> of ultramafic magmas that must have subsequently either erupted as picritic and/or basaltic volcanic rocks or been emplaced as sub-volcanic sills, the previous interpretation that the ultramafic sills in the Oswagan Group acted as feeders for the Bah Lake (previously Oswagan Formation) mafic rocks (Peredery, 1979; Bleeker, 1990) is not supported by the geochemical data generated in this study. Although there are a few crustally-contaminated and chalcophile element-depleted rocks in the Bah Lake assemblage and a few crustally uncontaminated and chalcophile-element unenriched rocks in the ultramafic sills (**Section 8.4.4.2**), the majority of the rocks in the Bah Lake assemblage are uncontaminated and undepleted in chalcophile elements (**Section 8.5.2.2**), indicating that they could not have been derived from the crustally-contaminated and locally mineralized residues represented by the ultramafic sills. Because the key elements on which these characteristics are defined (Th, Nb, Ni, and Ir) have been shown not to have been systematically mobilized in either the Bah Lake mafic rocks or the ultramafic sills during hydrothermal alteration or regional metamorphism, the differences between the two groups of rocks are inferred to represent primary variations that point to separate origins for the two groups of rocks.

In order to account for the “missing” mafic material, we have considered the possibility that the ultramafic sills may have originally contained greater abundances of mafic components. However, although some of the components of the Bah Lake assemblage are ultramafic and some of the components of the ultramafic sills are mafic, the amount of mafic (i.e., pyroxene and plagioclase-rich) material that is preserved in the ultramafic sills is insufficient for the sills to represent the feeders to the majority of the rocks in the Bah Lake assemblage. One response to this might be that the mafic and ultramafic portions of the sills became separated owing to different rheological responses during the prolonged and complex deformation in the TNB. However, this would also require the contaminated, chalcophile-element depleted products of the ultramafic sills to have been separated from the rest of the Bah Lake assemblage, which is considered unlikely. The only way that the ultramafic sills could have acted as feeders for the Bah Lake volcanic rocks appears to be if the Bah Lake magmas passed through them without forming a cumulate component and if the sills were

---

<sup>7</sup> The volume of this magma can be estimated from the volume of the ultramafic bodies and their average compositions using the equation below:

$$V_d / V_e = (C_e^i - C_o^i) / (C_o^i - C_d^i)$$

Where  $V_d$  = volume of evolved lava produced,

$V_e$  = volume of zone of enrichment (i.e., intrusion),

$C_o^i$  = concentration of element i in initial (unevolved) magma (~ Bah Lake assemblage komatiitic basalt),

$C_d^i$  = concentration of element i in evolved magma (missing),

$C_e^i$  = concentration of element i in cumulates.

If this is applied to the MgO contents of the ultramafic bodies, assuming an average olivine composition of Fo<sub>89</sub> ( $C_e^{MgO}$  = 48.6 wt%), ~21 wt% MgO in the initial magma and ~10wt% MgO in the evolved magma,  $V_d / V_e$  = 2.5. That is, the volume of the mafic material processed through the sills must have been 2 – 3 times that of the ultramafic bodies. If the evolved magmas were more evolved as they left the sills (e.g., 12 wt% MgO), or the initial magma less magnesian, this value would increase.

subsequently filled with cumulate rocks for which no volcanic product was preserved. If so, then the relationship between the two becomes irrelevant.

The observed geochemical inconsistencies between the ultramafic bodies and the Bah Lake assemblage and the observation that the ultramafic sills are rarely, if ever, emplaced at levels higher than the lower member (Os1) of the Setting Formation (**Section 5.4.4**) suggest that the relationship between the Bah Lake assemblage and the ultramafic bodies may originate through one of three different processes (**Fig. 8.54**):

- 1) The ultramafic bodies were emplaced after the deposition of the Os1 member of the Setting Formation, leading to the eruption of derivative magmas that were eroded before the deposition of the Os2 member of the Setting Formation and the eruption of the Bah Lake assemblage (Ob).
- 2) The ultramafic bodies were emplaced after the eruption of the Bah Lake assemblage and produced volcanic rocks and/or mafic sills that overlay the whole of the Ospwagan Group stratigraphy, including the Bah Lake assemblage, but which were tectonically removed or eroded off prior to deformation.
- 3) The ultramafic bodies were emplaced sometime after the deposition of the Os1 member of the Setting Formation, but the derivative magmas were erupted into a basin that was adjacent to the TNB and subsequently separated from it by faulting.

Although it was argued in **Section 5.2.2.5** that the Bah Lake assemblage was deposited autochthonously on top of the Setting Formation and is broadly in place (ruling out Scenario 1 above), for several reasons, a model in which the emplacement of the sills pre-dated the eruption of the basalts may be favoured. Firstly, because some ultramafic magmas were able to erupt through the Setting Formation to form the Bah Lake assemblage, it is unlikely that this level reflects the level of neutral buoyancy for an ultramafic magma; if the ultramafic bodies post-dated the Bah Lake assemblage, then the average density of the overlying crust would have actually been substantially greater than that experienced by the ultramafic magmas of the Bah Lake assemblage and the bodies would have been emplaced at higher levels in the stratigraphy. Secondly, the geochemical characteristics of the intrusive components of the Bah Lake assemblage are consistent with them being related to the volcanic components of the Bah Lake assemblage, but not with the ultramafic sills. The absence of contaminated and/or chalcophile element depleted mafic intrusions in the Bah Lake assemblages argues that the magmas derived from the ultramafic bodies did not pass through the rocks of the Os2 unit of the Setting Formation or the Bah Lake assemblage, making it unlikely that the ultramafic bodies postdate the eruption of the Bah Lake assemblage.

In the light of the stratigraphic arguments presented in **Chapter 5** and the geochemical variations described in **Sections 8.4** and **8.5** above, it is therefore proposed that the ultramafic bodies (and associated Ni-Cu-(PGE) mineralization) in the Ospwagan Group formed from an early pulse of voluminous komatiitic magmatism that was selectively intruded into the lower part of the sedimentary sequence and became contaminated via interaction with pelites and iron-formations, whereas the Bah Lake assemblage may represent a later pulse of less voluminous komatiitic and tholeiitic magmatism that was intruded and extruded at higher levels. However, because the absolute ages of the contaminated, mineralized ultramafic sills in the Ospwagan Group and the mafic-ultramafic lavas, sills, and dikes in the Bah Lake

assemblage are not well constrained, any interpretation of the relative timing of their emplacement remains speculative.

### 8.8.3 Assimilation Processes during Emplacement

During the emplacement of very hot, komatiitic magma into either consolidated or unconsolidated sedimentary rocks, the magma may be expected to cause devolatilization, partial, and/or complete melting of the wall-rocks with decreasing distance from the contact, leading to the production of a contaminated (ultramafic to mafic) silicate magma, crystalline solids (phenocrysts), a sulfide magma (if sulfide is present in the wall rocks), undissolved wall-rock xenoliths, and possibly a separate more silica-rich xenomelt phase (Leshner et al., 2001). Because the assimilation of the country rocks may not only produce the sulfide magmas required for the production of an ore body, but may also actually create space for the intrusion, an understanding of the assimilation processes during emplacement may be helpful in understanding the ore-forming processes.

As discussed in **Sections 8.4.4.2 and 8.4.4.3**, there is strong chemical evidence for the contamination of the magma by a crustally-derived component during emplacement and the production of immiscible sulfide magmas from which the ore formed, indicating that the magmas must have either assimilated the metasedimentary or basement wall-rocks during emplacement and that some of these rocks were sulfide-bearing. During the collection of samples for geochemical study, other (physical) evidence for the emplacement or assimilation processes that acted during the production of the ultramafic bodies (e.g., erosive contacts with the metasedimentary rocks, or syn-emplacement deformation around the bodies) was looked for in the drill cores and rare surface exposures of the ultramafic bodies. However, no clear evidence of either process was found owing to the combined effects of poor exposure, tectonization of the ultramafic bodies, and the limited amount of the contacts that were intersected by the drill holes. Rare enclaves of metasedimentary rock *were* found within a small number of ultramafic bodies, close to the contacts, but these appeared to be of tectonic rather than magmatic origin and were not studied in detail.

Although no physical evidence could be found for the emplacement and/or assimilation processes, several observations can be made from the geochemical data:

- 1) The olivine cumulate rocks in the majority of the intrusions must have formed from magmas that had incorporated either less than 25% by volume of a component formed by complete melting of the sedimentary wall rocks or a smaller volume of a component formed by incongruent (partial) melting of the sedimentary wall rocks. As demonstrated by the MELTS models, adding a contaminant rapidly drives the magma away from olivine saturation and toward orthopyroxene saturation, leading to the production of orthopyroxene cumulates. Although orthopyroxene cumulates have been identified in a few of the ultramafic bodies (e.g., Thompson, Oswagan Lake, and Otter Lake), such rocks appear to be quite rare in the TNB ultramafic bodies.
- 2) Melting of the wall-rocks would have been insufficient to create the space required for the ultramafic cumulate rocks, implying that some dilation was necessary. Unless the metasedimentary wall-rocks were already close to melting prior to the emplacement of the ultramafic magma, a large amount of energy would have been required to overcome the latent heat of fusion in order to produce even a partial melt. This energy must come

from either the cooling of the magma or the crystallization of olivine. Calculations using reasonable assumptions for the specific heat capacity ( $c_{wr}$ ), enthalpy of fusion ( $L_{wr}$ ), and liquidus temperatures of the wall-rocks ( $T_{fus}$ ), along with the temperature dependant latent heat of crystallization of olivine ( $L_{ol}$ )<sup>8</sup> indicate that for the heating and assimilation of 1g of wall rock, approximately 2.5g of olivine would have to crystallize (giving an  $r$  value of  $\sim 0.4$ ). Because heat loss by conduction would increase the amount of crystallization required, this represents an upper value for  $r$ . Although a higher value may be expected for a high-Mg komatiite magma owing to its higher initial temperature (possibly as high as  $r \approx 0.5$ : see Lesher & Arndt, 1995), the amount of assimilation is unlikely to exceed the amount of crystallization and the space produced by wall-rock melting would be less than that required by the cumulates.

- 3) There is no systematic correlation between the degrees of contamination (e.g., LREE/MREE or Th/Nb ratios) and either depletion in chalcophile elements or the presence of sulfide ores, indicating that a) the majority of the ultramafic bodies must have assimilated at least some of their wall rocks during emplacement, but that the presence of mineralization is dependent on there being sulfides in the assimilant, and b) contamination and felsification of the magma was insufficient to make an ore deposit. Although the solubility of sulfide in a magma is partially controlled by the fugacities and activities of S, O, SiO<sub>2</sub>, and Na<sub>2</sub>O (Haughton et al., 1974; Shima and Naldrett, 1975; Wallace and Carmichael, 1992), because sulfur dissolves in iron-rich magmas (FeO > 10 wt%) by replacing O bonded to Fe<sup>2+</sup>, the dominant control on sulfide solubility is the ferrous iron content of the magma. Contamination of the magma by pelitic sediment will therefore decrease sulfide solubility (owing to the dilution or oxidation of the iron by the silica- and/or more ferric iron-rich melt and the addition of SiO<sub>2</sub> and Na<sub>2</sub>O). Although this will eventually cause sulfide-saturation and the production of a sulfide liquid, the amount of sulfide produced by such a process will be small, leading to high R factors (R

---

<sup>8</sup> Heat required to melt wall rocks ( $H_{fus}$ ) = heat to bring rocks to melting temperature + enthalpy of fusion  
 $= (T_{fus} - T_{initial}) \times c_{wr} - L_{wr}$

Using the heat capacity constants of oxide components in silicate liquids (after Lange and Navrotsky (1992) and Navrotsky (1995)) and the compositions of the pelitic rock in **Table 8.2**,  $c_{wr} \sim 1436$  J/kg.

The temperature-dependant latent heat of fusion for sedimentary wall rocks may be approximated using that of albite, as estimated from curves fit to the enthalpy of fusion/crystallisation (Navrotsky, 1995; Williams, 1998) to give the expression:

$$L_{wr} = 161 \times T_{fus} + 56200 \text{ J/kg}$$

If the sediments are assumed to be at  $\sim 150^\circ\text{C}$  prior to emplacement of the magmas and to fuse at  $\sim 1130^\circ\text{C}$ , then the total heat required is:

$$H_{fus} = (1130 - 150) \times 1436 + (161 \times 1130) + 56200 = 1408 + 238 \text{ kJ/Kg} = 1646 \text{ kJ/kg}$$

Using the same source of enthalpies of fusion for different minerals, Williams (1998) determined that the latent heat fusion for olivine may be approximated by the expression:

$$L_{ol} = 456 \times T - 50260$$

At  $1550^\circ\text{C}$ ,  $L_{ol} = 656 \text{ kJ/kg}$ .

Assuming the sediments were not hot before emplacement, then the maximum amount of sediment that could be assimilated would be  $\sim 0.4$  times the amount of olivine that crystallises.

>1000) and primarily disseminated ores. Using the equations of Poulson and Ohmoto (1990), it may be shown that up to 1500 ppm sulfur may dissolve in a komatiitic magma containing ~11 – 11.4 wt% FeO<sup>t</sup> (**Table 8.2**, equivalent to 9.6 – 10 wt% FeO assuming a Fe<sup>3+</sup>/Fe<sup>2+</sup> ratio of 0.15; Middlemost, 1989). If it were possible to extract all this sulfur from the magma as sulfide, then the volume would only represent about 0.4 wt% of the total magma that passed through the chamber. As demonstrated by the relatively low PGE contents of the sulfide-bearing ultramafic cumulates (**Section 8.4.4.3** and **9.7**), the majority of the ultramafic bodies of the TNB formed under relatively low R factors and must have obtained a large amount of their sulfur from the sediments (Eckstrand et al., 1989; Bleeker, 1990).

#### 8.8.4 Environment of Deposition of Oswagan Group Metasediments

The results of the geochemical study of the Oswagan Group metasedimentary rocks support many of the observations made during the discussion of the stratigraphy of the TNB, in particular:

- 1) Volcanic rocks are absent, or at least not prominent, in the lower and middle parts of the sedimentary succession (**Section 5.3**). This is verified by the low Cr contents of the quartzites and semi-pelites of the Manasan and Thompson Formations, indicating negligible input of mafic or ultramafic detritus.
- 2) The majority of the sediments are relatively mature, suggesting that they were transported a considerable distance from their source (**Section 5.6.1**)
- 3) The initiation of mafic volcanism may have coincided with the deposition of the Pipe Formation (Op), in particular the banded oxide- and sulfide-ironstones and siliceous metasediments (**Section 5.6.1**). This is evident in the geochemistry of the metasedimentary rocks by the high Cr and Co contents of the semi-pelites of the Pipe formation, which would be consistent with the observed sporadic incorporation of aphyric dark glassy fragments (**Section 5.6.1**).
- 4) There was a significant change in sedimentary source region at the end of the deposition of the Pipe formation consistent with this representing the initiation of active rifting, as indicated by the transition toward turbiditic sedimentation during the deposition of the Setting Formation (**Section 5.3**). Although this is also documented in the geochemistry of the sediments as a decrease in Cr and increase in Zr content, no variation is observed in Th/Nb ratio (**Fig. 8.43**), suggesting that the HFSE compositions of the two potential source regions were similar.

#### 8.8.5 Exploration Implications

##### 8.8.5.1 Olivine Compositions

Although it might be expected that the olivines within mineralized bodies would be more forsteritic than those within non-mineralized bodies (owing to the increase in magmatic temperature and sulfide-undersaturation associated with the increase in MgO content: **Section 8.8.3**), there is no recognizable difference in the major element compositions of the olivines, indicating that the presence of mineralization is not critically dependant on the major element composition of the magma and that mineral deposits can form from magmas with a range of “average” MgO contents. Although it is difficult to gauge from the available



data, the initial magma composition (as recorded by the most magnesian olivines) may be more important than the average magma composition, as this is what would have originally been in contact with any sulfide-bearing wall rocks from which the ore may have formed.

Although Ni depletion in olivine appears to correlate with mineralized locations, the presence of Ni depletion in olivines from several supposedly non-mineralized bodies in the exposed part of the belt and the absence of Ni-depletion in olivines from parts of several bodies from mineralized locations (in particular Thompson and Pipe Pit) indicates that the presence of Ni-depletion is not an accurate indicator of mineralization. However, the fact that both Ni-depleted and Ni-undepleted olivines appear to be present in only the mineralized ultramafic bodies (e.g., Thompson and Pipe Pit) indicates that Ni-depletion must have occurred locally in these bodies and thus the variation in Ni contents may be represent a more reliable indicator of mineralization.

#### **8.8.5.2 Major and Minor Element Compositions of Ultramafic Bodies**

Many mineralized cumulate komatiites, including Kambalda, Perseverance, and Raglan are more magnesian, contain more forsteritic olivines, contain more cumulus olivine, and, if undersaturated in chromite, have lower Cr contents (Woolrich and Giorgetta, 1978; Lesher and Groves, 1984; Donaldson et al., 1986; Perseverance: Barnes et al., 1988; Lesher & Stone, 1996; Barnes & Brand, 1999; Lesher et al., 2001), which is consistent with them being derived from more magnesian magmas in areas of preferential lava/magma flow (e.g., Lesher and Groves, 1984; Lesher et al., 1984, 2001; Lesher, 1989; Hill et al., 1990, 1995).

The reason for this is believed to be that the lava/magma in dynamic lava channels and magma conduits is continuously replenished during crystallization, resulting in the accumulation of higher temperature, more primitive cumulus phases, compared to lava lobes, sheet flows, and sheet sills, which are less replenished and therefore fractionate more, resulting in the accumulation of lower temperature, more evolved cumulus phases. The compositions and relative proportions of the cumulus phases that have accumulated may be calculated using multicomponent least-squares minimization methods, but may be roughly estimated using the lever rule (see e.g., Lesher & Groves, 1984; Lesher, 1989) or by mass balance using elements that are abundant in only one of the cumulus phases (see above).

Woolrich and Giorgetta (1978), Donaldson et al. (1986), Lesher & Stone (1996), and Barnes & Brand (1999) have also shown that whole-rock Cr and Ni:Cr ratios may be effective discriminators between mineralized and non-mineralized komatiites. This is based on the observation that many *mineralized* cumulate komatiites plot along a trend of decreasing Cr with increasing Mg or Ni, corresponding to accumulation of olivine alone, whereas many *non-mineralized* cumulate komatiites have higher Cr contents, corresponding to accumulation of olivine + chromite. Barnes and Brand (1999) attributed this to differential settling of coarse olivine relative to fine chromite in lava channels relative to sheet flows, but systematic textural and mineralogical variations through the cumulate zones indicate that the cumulus phases probably crystallized *in situ* (see discussion by Lesher et al., 1984; Lesher, 1989) and that the differences are more reasonably attributed to changes in which phases are on the liquidus (Lesher & Stone, 1996). Experimental studies (e.g., Murck & Campbell, 1986) have shown that high-Mg (>20% MgO) komatiites are undersaturated in chromite and will therefore accumulate only olivine, whereas low-Mg (<20% MgO) komatiites are saturated in chromite and will therefore accumulate olivine + chromite in cotectic proportions

(~50:1, depending on  $fO_2$ ). Thus, cumulates formed from lavas that fractionated and became saturated in chromite *during* crystallization will contain a component of olivine derived from early high-Mg (chromite-undersaturated) liquids and a component of olivine-chromite derived from late low-Mg (chromite-saturated liquids), resulting in an intermediate Cr content (Donaldson et al., 1986; Leshner & Stone, 1996). The point at which the lavas become saturated in chromite varies from area to area (e.g., Alexo vs. Barberton vs. Belingwe vs. Cape Smith vs. Kambalda vs. Mt. Clifford vs. Shaw Dome) and from flow to flow within an area (e.g., Tripod Hill vs. Silver Lake members at Kambalda), consistent with differences in  $fO_2$  (Leshner & Stone, 1996). Importantly, Cr contents can be used to distinguish lava channels and magma conduits (olivine cumulates) from sheet flows and sills (olivine + chromite cumulates) in high-Mg komatiites (e.g., Abitibi, Western Australia, and Zimbabwe), but they cannot distinguish different facies in low-Mg komatiites (e.g., Cape Smith belt, probably Fox River belt).

However, the results of our study of mineralized and non-mineralized ultramafic bodies in the TNB are more complicated. There is considerable scatter in the MgO-FeO and MgO-Cr diagrams (**Fig. 8.12**) and although it appears that some mineralized ultramafic bodies are more magnesian, less Cr-rich, and derived from more magnesian magmas, there are significant overlaps and the loadings of Mg and Cr in the discriminant functions are relatively low, much lower for example than at Kambalda (Leshner, 1983). The reason for this is that most of the studies that have established correlations between mineralization and Mg (or Ni) or Cr contents are based on comparisons of different facies within *single* volcanic/magmatic systems. However, it is clear that Ni-Cu-(PGE) mineralization can form in a wide range of mafic-ultramafic magma types (Naldrett, 1989, 1999) and that the composition of the magma is not a critical control on the *formation* of Ni-Cu-(PGE) deposits (Leshner and Stone, 1996). Thus, by sampling such a wide range of intrusions in the TNB, we have, in effect, expanded the range of possible magma compositions from which mineralization may occur, which overlaps any differences that might occur in subvolcanic facies.

In fact, although the most magnesian *facies* of mineralized *units* are more likely to be mineralized, the most magnesian *units* in a sequence are not *always* the ones that are mineralized and the most magnesian *rocks* in a mineralized *facies* are not *always* the ones that contain the mineralization. For example, Muir (1979), Larson (1996), and Baird (1999) have shown that the cumulate komatiite sills in the lower part of the Tisdale assemblage (formerly upper part of the Deloro Group) in the Shaw Dome are systematically more magnesian than the cumulate komatiite flows in the overlying upper part of the Tisdale assemblage (formerly lower part of Tisdale Group). However, the flows are mineralized (Green and Naldrett, 1981), whereas mineralization has not been identified in the sills (Larson, 1996; Baird, 1999; Davis, 1997, 1999). The former are interpreted as lava channels that eroded footwall sulfide facies iron-formations, whereas the latter are interpreted as sheet sills that accumulated olivine, but did not extensively erode country rocks (Larson, 1996; Stone and Stone, 2000). Similarly, the mineralized *rocks* in many deposits have lower MgO contents than other parts in the same *unit* (e.g., Kambalda, Raglan).

Whether or not the most magnesian *units* in a *sequence*, the most magnesian *facies* in a *unit*, or the most magnesian *rocks* in a *unit* are more likely to be mineralized depends on the thermal and crystallization history of the unit/facies/rock:

- 1) If the *unit* or *facies* is too large and/or too dynamic and if the amount of S in the country rocks is too small, the magma will dissolve all of the S and not reach sulfide saturation until a late stage in the crystallization history of the unit, forming Type II (internal strata-bound disseminated) mineralization, which is often subeconomic. If the *rock* is an adcumulate, then the magma may never reach sulfide saturation.
- 2) If the *unit* or *facies* is not too large and/or too dynamic and if the amount of S in the country rocks is large enough, the magma will not be able to dissolve all of the S and will reach sulfide saturation at an early stage in the crystallization history of the unit, forming Type I (basal stratiform) mineralization, which is more likely to be economic.
- 3) Because Type I deposits form early in the crystallization history of the host *units*, the magma from which they form is more likely to have encountered cold floor/country rocks, to have been contaminated, and to have fractionated more than the magmas that flow through the channel/conduit at a later stage, after the floor/country rocks have been heated and after they have been insulated by underlying cumulate rocks. This means that the *rocks* that host or directly overlie the mineralization are often less magnesian than overlying rocks.
- 4) Although lava channels and magma conduits can be recognized on the basis of their high temperature cumulate mineralogy, the amount of accumulation depends on the rate and duration of flow, the rate of crystallization and/or assimilation (see below), and the timing of ponding. Channels/conduits that pond later in their crystallization history will contain a greater proportion of cumulate rocks (dunites and mesocumulate peridotites) and a smaller proportion of differentiated rocks (orthocumulate peridotites, pyroxenites, gabbros) than channels/conduits that pond earlier in their crystallization history (Leshner, 1989; Leshner & Stone, 1996). For this reason, it is critical to establish *maximum* magnesium contents of cumulate rocks and *maximum* Fo contents of olivines, rather than *averages*.
- 5) Although lava channels and magma conduits, by definition, remain areas of preferential lava/magma flow for extended period of time, there is no fundamental reason why a lava channel or magma conduit could not deposit sulfides and then pond immediately.

It is clear that it is critical to interpret geochemical data within the context of the physical volcanology.

#### **8.8.5.3 Trace Element Compositions of Ultramafic Bodies**

Mineralized ultramafic units in the TNB are enriched in HILE relative to MILE and are depleted in Nb-Ta-(Ti) relative to HILE of similar compatibility and therefore exhibit higher Th/Ti, higher Nb/Ti, and higher Th/Nb than non-mineralized ultramafic units. However, there is no systematic correlation between the degrees of mineralization and contamination (e.g., HILE enrichment, Nb-Ta-Ti depletion) in the TNB or in other deposits of this type (e.g., Barnes et al., 1995; Leshner & Arndt, 1995; Perring et al., 1996; Leshner et al., 2001). The reason for this is that the amounts of contamination produced during the mineralizing process depend on several factors (Leshner et al., 2001), including : 1) the stratigraphic architecture of the system (e.g., thickness and physical accessibility of the contaminant), 2) the fluid dynamics and thermodynamics of the lava/magma, 3) the physical, chemical, and thermal characteristics of the contaminant, 4) the amount of contaminant melted and

incorporated (e.g., amount of silicate partial melt: see Leshner & Burnham, 1999, 2001), 5) the S and metal content of the contaminant; 6) the initial sulfide saturation state of the magma, 7) the assimilation:crystallization ratio, 8) the amount of lava replenishment, and 9) the effective magma:sulfide ratio (R factor) of the system. Because these processes vary independently from deposit to deposit, from area to area within a deposit, and within a single area with time, there are many opportunities to decouple mineralization from contamination (Leshner and Arndt, 1995; Leshner and Stone, 1996; Leshner et al., 2001).

For example, with all else equal, the amount of contamination remains relatively constant if the S source is thick and/or continuously accessible (e.g., Perseverance, Raglan, Thompson), but decreases if it is thin and/or inaccessible (e.g., Kambalda). The melting rate and amount of contamination also vary with flow rate. Because the rate of thermal erosion is dependent primarily on the rate of heat conduction into the substrate or wall rock (Huppert & Sparks, 1985; Williams et al., 1998, 1999, 2002), it is low under laminar flow conditions, increases to a maximum as fully turbulent flow is reached and remains constant as the flow rate increases. However, because the volume of magma increases with increasing flow rate, the amount of contamination increases to a maximum as fully turbulent flow is reached but declines at higher flow rates because of dilution.

There are many other factors that may also result in decoupling of contamination and chalcophile element depletion (Leshner et al., 2001). For example, because komatiites are so strongly undersaturated in sulfide (Keays, 1982, 1995), a considerable amount of contamination may occur in komatiites before they reach sulfide saturation (Leshner & Groves, 1986; Leshner & Stone, 1996), which means that felsification (see Irvine, 1977; Naldrett, 1989) is not as viable a process for inducing sulfide saturation in komatiitic systems as it is in mafic systems (Leshner et al., 1999a). Another factor is that sulfide liquids (produced by either melting of the sulfide component of substrate or exsolution from the magma) are normally immiscible and rapidly deplete the lava in chalcophile elements owing to their very high sulfide-silicate liquid partition coefficients, whereas the silicate liquids produced by melting of the substrate, or crystalline silicate phases that fractionate from the magma, are normally miscible, but sometimes immiscible, and have less affect on the composition of the lava owing to their lower crystal-silicate liquid partition coefficients. The net result is that the amount of sulfides produced (the potential size of the ore deposit), the tenor of the sulfide ores (as a consequence of different R factors), and the geochemical characteristics of the lava (amount of apparent contamination) do not necessarily correlate with each other (Leshner et al., 2001). This explains why, for example, the non-cumulate portions of the sheet flow facies at Kambalda are significantly depleted in Ni and PGE (Leshner et al., 2001), indicating that these rocks (and only these rocks) equilibrated with sulfides, but why they are only weakly contaminated (Leshner & Arndt, 1995).

These factors appear to explain the different locations of contaminated rocks in different areas (Leshner and Arndt, 1995; Leshner and Stone, 1996; Leshner et al., 1999a, 2001): the thin (originally ~3m) interflow sediments at Kambalda would normally have been completely eroded upstream, exposing refractory basaltic or komatiitic substrates (depending on stratigraphic position), whereas the very thick ( $\geq 1$  km) felsic fragmental substrate at Perseverance, the very thick ( $\geq 1$  km) semi-pelitic sediments at Katinniq, and the thick (up to 10s of m) semi-pelitic sediments and thin (up to 10m), albeit very sulfide-rich (up to 100%), iron-formations at Thompson would have been continuously available for erosion. Of course,

because magmas may be transported considerable distances “downstream” (e.g., Leshner et al., 1984; Leshner and Campbell, 1993), the source of the contaminants may not always be evident.

The physical volcanological environment is the major control on whether or not contaminated and/or chalcophile element-depleted lavas are preserved. Contaminants drawn into rapidly- and turbulently-flowing channel-flow facies, regardless of whether extrusive or intrusive, are more likely to be assimilated, dispersed, and diluted. Furthermore, because the host units in stratiform deposits crystallize from lavas that were emplaced after the mineralizing event, they may be chemically and genetically unrelated to earlier lavas, which is clearly the case at Kambalda (Leshner et al., 1984; Leshner & Arndt, 1995), Perseverance (Barnes et al., 1988; Barnes et al., 1995), and Katinniq (Leshner et al., 2001). Contaminants drawn into less rapidly- and less turbulently-flowing sheet-flow facies, regardless of whether intrusive or extrusive, are more likely to be preserved, but they do not necessarily have to be preserved. Indeed, the compositions and textures of the sheet-flow facies at Kambalda (Leshner & Groves, 1984; Leshner, 1989) indicate that they are cumulate units and that they, too, probably crystallized from turbulently-flowing lavas. The point is that the presence of contaminated and/or chalcophile element-depleted rocks may be regarded as a positive indicator of favourable ore-forming processes. However, the absence of such rocks should not be regarded as a negative indicator (Leshner et al., 2001).

Importantly, contamination alone is normally not enough to induce sulfide saturation in *komatiitic* magmas (Leshner, 1989; Leshner and Stone, 1996; Leshner et al., 2001; Leshner and Keays, 2002). For example, the Paringa Basalt at Kambalda has been interpreted to have been contaminated by up to 30% upper continental crust (Leshner & Arndt, 1995), but is undepleted in PGE (Redman & Keays, 1985), some of the non-mineralized mafic-ultramafic sills in the Cape Smith belt have been interpreted to have been contaminated by up to 10% upper continental crust (or sediments derived by contamination of upper continental crust (Leshner et al., 2001), and some of the non-mineralized ultramafic sills in the TNB appear to have been contaminated by up to 40% Ospwagan Group sediments (this study).

#### **8.8.5.4 Highly Chalcophile Element Compositions of Ultramafic Bodies**

The amounts of PGE depletion or enrichment produced during the ore-forming process also depend on the factors noted above and because those factors vary independently from deposit to deposit, from area to area within a deposit, and within a single area with time, there are also many opportunities to decouple mineralization from chalcophile element depletion (**Table 8.10**; Leshner and Stone, 1996; Leshner et al., 2001).

For example, with all else equal, the amount of sulfide produced increases relatively linearly if the assimilant is thick and/or continuously accessible (e.g., Perseverance, Raglan, Thompson), but increases to a fixed plateau if it is thin (e.g., Kambalda). Importantly, because the amount of sulfides produced will vary with flow duration and accessibility of the assimilant, the magma:sulfide ratio may also vary with flow duration, resulting in some cases in dissolution of sulfide (Leshner & Campbell, 1993; Leshner & Stone, 1996; Leshner & Burnham, 1999, 2001; Leshner et al., 1999a, 2001). The best ore deposits (i.e., those with the highest grades, highest tenors, and largest masses) are probably produced at relatively high flow rates during long eruptions. Ironically, this is also the situation where geochemical

evidence (contamination, PGE-depletion) of the ore-forming process is most likely to be obscured (Leshner et al., 2001).

**Table 8.10.** Amount of sulfides produced, ore tenor, ore and magma geochemical characteristics in terms of flow duration and flow rate for a high-Mg komatiite system (Leshner et al., 2001).

	Higher Flow Rate	Intermediate Flow Rate	Lower Flow Rate
<b>Longer Flow Duration</b>	Larger amount of sulfides Higher ore tenor Mantle-like $\delta^{34}\text{S}$ , $^{206}\text{Pb}/^{204}\text{Pb}$ , $\gamma_{\text{Os}}$ Minor contamination Mantle-like $\epsilon_{\text{Nd}}$ and $\epsilon_{\text{Sr}}$ Minor PGE depletion	Larger amount of sulfides Intermediate ore tenor Mantle $\delta^{34}\text{S}$ , crustal $^{206}\text{Pb}/^{204}\text{Pb}$ , $\gamma_{\text{Os}}$ Intermediate contamination Crustal $\epsilon_{\text{Nd}}$ and $\epsilon_{\text{Sr}}$ Intermediate PGE depletion	Larger amount of sulfides Lower ore tenor Crustal $\delta^{34}\text{S}$ , $^{206}\text{Pb}/^{204}\text{Pb}$ , $\gamma_{\text{Os}}$ Strong contamination Crustal $\epsilon_{\text{Nd}}$ and $\epsilon_{\text{Sr}}$ Strong PGE depletion
<b>Inter-mediate Flow Duration</b>	Intermediate amt. sulfides Higher ore tenor Mantle-like $\delta^{34}\text{S}$ , $^{206}\text{Pb}/^{204}\text{Pb}$ , $\gamma_{\text{Os}}$ Minor contamination Mantle-like $\epsilon_{\text{Nd}}$ and $\epsilon_{\text{Sr}}$ Minor PGE depletion	Intermediate amt. sulfides Intermediate ore tenor Mantle $\delta^{34}\text{S}$ , crustal $^{206}\text{Pb}/^{204}\text{Pb}$ , $\gamma_{\text{Os}}$ Intermediate contamination Crustal $\epsilon_{\text{Nd}}$ and $\epsilon_{\text{Sr}}$ Intermediate PGE depletion	Intermediate amt. sulfides Lower ore tenor Crustal $\delta^{34}\text{S}$ , $^{206}\text{Pb}/^{204}\text{Pb}$ , $\gamma_{\text{Os}}$ Strong contamination Crustal $\epsilon_{\text{Nd}}$ and $\epsilon_{\text{Sr}}$ Strong PGE depletion
<b>Shorter Flow Duration</b>	Smaller amount of sulfides Higher ore tenor Mantle-like $\delta^{34}\text{S}$ , $^{206}\text{Pb}/^{204}\text{Pb}$ , $\gamma_{\text{Os}}$ Minor contamination Mantle-like $\epsilon_{\text{Nd}}$ and $\epsilon_{\text{Sr}}$ Minor PGE depletion	Smaller amount of sulfides Intermediate ore tenor Mantle $\delta^{34}\text{S}$ , crustal $^{206}\text{Pb}/^{204}\text{Pb}$ , $\gamma_{\text{Os}}$ Intermediate contamination Crustal $\epsilon_{\text{Nd}}$ and $\epsilon_{\text{Sr}}$ Intermediate PGE depletion	Smaller amount of sulfides Lower ore tenor Crustal $\delta^{34}\text{S}$ , $^{206}\text{Pb}/^{204}\text{Pb}$ , $\gamma_{\text{Os}}$ Strong contamination Crustal $\epsilon_{\text{Nd}}$ and $\epsilon_{\text{Sr}}$ Strong PGE depletion

Note: Geochemical and isotopic characteristics will differ in other areas depending on elemental abundances and isotopic ratios, and may be modified by alteration.

†  $^{207}\text{Pb}/^{204}\text{Pb}$  and  $^{208}\text{Pb}/^{204}\text{Pb}$  would be expected to behave similarly.

Thus, the application of chalcophile element depletion in mineral exploration depends on the scale and location of the depletion (Leshner & Stone, 1996; Leshner et al., 2001):

- 1) The identification of an entire volcanic *sequence* that is depleted in chalcophile elements indicates that sulfide segregation occurred prior to eruption, probably during ascent through the crust and/or during processing in a deep(er) crustal magma chamber. It is unlikely that an entire sequence of lavas would have been erupted through a single high-level magma chamber. The sulfides that segregated at this stage would have been most likely lost, owing to their very high density, very low viscosity, and very high surface tension and the low viscosity of the komatiitic magmas, which would facilitate coalescence and settling of sulfides (Leshner & Groves, 1986; cf. Bremond d'Ars et al., 2001). Indeed, the presence of the sulfides in the ultramafic sills in the TNB, which by nature of their very strong enrichment in olivine must have been dynamic, show that sulfides are very difficult to mobilize once segregated. In any case, any sulfides formed during later stages would be depleted in chalcophile elements (Campbell & Naldrett, 1979). Thus, this geological environment is probably less prospective than those below.

- 2) The identification of a specific volcanic stratigraphic **unit** (cooling unit) that is depleted in chalcophile elements within a **sequence** of otherwise undepleted lavas/sills indicates that sulfide segregation occurred at a specific stage of the eruptive event and/or within a specific part of the plumbing system. It is more likely that this process occurred at higher levels in the system. However, sulfide segregation could have occurred in a low-level magma chamber and/or kilometers “upstream” from the analyzed location. This situation is more favorable than the one above, but less favorable than the one below.
- 3) The identification of a **zone** or **facies** of a single cooling unit that is depleted in chalcophile elements within a unit of otherwise undepleted lavas/sills indicates that contamination and sulfide segregation occurred within that specific unit. This geological environment is more prospective than those above.

Most studies of this type, including this one, indicate that the majority of the magmas, especially those interpreted to represent parental magmas, are *not* depleted in chalcophile elements (Leshner and Stone, 1996; Leshner et al., 2001). This means that they did not equilibrate with a sulfide (or metal) phase in the mantle source region and did not exsolve a sulfide (or metal) phase during ascent or eruption (Keays, 1982, 1995; Leshner & Groves, 1986; Naldrett & Barnes, 1986; Leshner & Stone, 1996). The observation that chalcophile element depletion is observed only in parts of the host units, stratigraphically correlative with Ni-Cu-(PGE) mineralization, indicates unequivocally that sulfide saturation occurred *locally*, “upstream” from the present ore zones, not in a deeper subsurface magma chamber.

In the case of Kambalda where the most likely S source was a thin (originally ~3m) sulfidic interflow sediment overlying a refractory basaltic or komatiitic substrate, the identification of a **zone** of chalcophile element-depleted lavas within a **unit** of otherwise undepleted lavas indicates that contamination and sulfide segregation must have occurred locally. In the case of Perseverance, Raglan, and Thompson (and probably also Noril’sk and Voisey’s Bay), where the most likely S sources were thicker sequences of sediments or felsic volcanoclastic rocks, the identification of large **units** of chalcophile element-enriched lavas associated with **zones** of chalcophile element-undepleted lavas indicates that contamination and sulfide segregation occurred locally, although there is less certainty that the units are related. In all cases, the S incorporation and ore-forming processes may have occurred a significant distance “upstream” from the present ore zones.

Importantly, because Type I mineralization forms early in the crystallization history of the host units, the rocks above the ores may form from replenished magmas, the sulfide saturation state of which will depend on the thickness and accessibility of the S source (Leshner and Arndt, 1995; Leshner et al., 2001). This explains the different locations of chalcophile-element depleted rocks in different areas (Leshner and Arndt, 1995; Leshner and Stone, 1996; Leshner et al., 1999a, 2001): the thin (originally ~3m) interflow sediments at Kambalda would normally have been completely eroded upstream, exposing refractory basaltic or komatiitic substrates (depending on stratigraphic position), whereas the very thick ( $\geq 1$  km) felsic fragmental substrate at Perseverance, the very thick ( $\geq 1$  km) semi-pelitic sediments at Katinniq, and the thick (up to 10s of m) semi-pelitic sediments and thin (up to 10m), albeit very sulfide-rich (up to 100%), iron-formations at Thompson would have been continuously available for erosion. Of course, because molten immiscible sulfides may be transported considerable distances downstream (e.g., Leshner et al., 1984; Leshner and Campbell, 1993), the source of the S may not always be evident.

Note that the concept discussed above regarding Cr contents can also be applied to sulfides (Leshner, 1995). Magmas that are undersaturated in sulfide will accumulate only olivine, whereas magmas that are saturated in sulfide will accumulate olivine + sulfide in cotectic proportions (~60:1: Duke, 1986, depending on  $fO_2/fS_2$ ). Thus, cumulates formed from lavas that fractionated and became saturated in sulfide *during* crystallization will contain a component of olivine derived from early sulfide-undersaturated liquids and a component of olivine-sulfide derived from late sulfide-saturated liquids, resulting in an intermediate sulfide content. This explains the spread of S, Cu, Ni, and Co contents in rocks containing disseminated sulfides (e.g., **Fig. 8.12**). The point at which the lavas become saturated in sulfide varies significantly, depending on how much S had been added. It is possible that if enough olivine is accumulated and if the temperature of the magma remains high enough, it may never reach sulfide saturation.

#### **8.8.5.5 Discriminant Analyses**

The discriminant analyses indicate that although statistical methods may be used to identify compositional differences between ultramafic bodies with different mineralization states, multiple samples from individual bodies are required to ensure an accurate assessment of the mineralization potential of an unknown body. This, of course, makes this technique more useful for in the preliminary stages of exploration in areas where there is good outcrop and in the intermediate stages of exploration in areas where there is little outcrop (but multiple drill cores), but less useful in the preliminary stages of exploration in areas where there is little outcrop (or drill cores) or in the advanced stages of exploration where many drill cores are available that may have already established (physically or geophysically) whether an ore body is present at a mineable depth.

Non-mineralized samples in mineralized ultramafic bodies in the TNB are enriched in Al, Th, S, Ca, Mg, Ni, and Zn and depleted in Ti, Yb, Fe, and Nb relative to non-mineralized bodies, consistent with contamination and sulfide-saturation of a highly magnesian ultramafic magma. Although the nature of contamination and behaviour of chalcophile elements will vary with the nature and composition of the contaminant and the relative masses of magma, crystalline silicates, sulfide xenomelt, silicate xenomelt (if present), and residues (if present) in the system (Leshner and Burnham, 1999, 2001) and must therefore be established in each area, the contamination and metal depletion signatures are broadly applicable in most areas. However, it is essential to screen all of the samples alteration prior to use in the discriminant functions.

#### **8.8.5.6 Sedimentary Rock Compositions**

Although the different sedimentary rock units of the Ospwagan Group may be distinguished on the basis of their whole-rock geochemical compositions, the differences between units are subtle and/or involve elements that are abundant in mafic magmas, which means that although they might be helpful in aiding identification of stratigraphic units, they cannot be used to reliably distinguish between the assimilation of different units during emplacement of the ultramafic bodies.

Similarly, because all of the ultramafic, mafic, and metasedimentary rocks lie on essentially the same mixing lines in trace element geochemical and isotope geochemical space, it is not possible to distinguish between different levels of contamination of different sediment types.



#### 8.8.5.7 Volcanic Architecture

The results of this part of the study have important implications for the interpretation of the volcanic/subvolcanic architecture of the magmatic system that formed the TNB.

For example, mass balance calculations indicate that the large volumes of olivine cumulates in the mineralized sills in the TNB require that a volume of ultramafic magma of the order of 4-6 times that of the sills must have escaped from the sills. Lavas or other sills with contaminated and chalcophile element-depleted geochemical signatures that might correspond to these magmas have not been identified, which means that they were emplaced after deposition of the lower part of the Setting Formation and eroded before deposition of the upper part of the Setting Formation (**Fig. 8.54a**), that they were emplaced after the Bah Lake Formation and eroded (**Fig. 8.54b**), or that they were emplaced outside of the volume of preserved section and faulted in or out of the section (**Fig. 8.54c**), or that they were simply not sampled. In any case, this highlights one of the dangers in using the presence or absence of contamination or metal depletion signatures in lavas as a guide to identifying the potential for mineralization in subvolcanic systems of this type.

Of course, there are other reasons to be cautious when using this concept to identify potential exploration targets. For example, P.C. Lightfoot and C.J. Hawkesworth (pers. comm., 1998) and Arndt et al. (2003) have shown that the flood basalts at Noril'sk reported by Naldrett et al. (1992) and Brüggmann et al. (1993) to be depleted in PGEs and interpreted by them to be derived from the underlying mineralized sills do not have Sr isotopic compositions that are consistent with incorporation of evaporites. These data conflict with the very heavy S in the ores, which range up to  $+16\text{‰}$   $\delta^{34}\text{S}$ , similar to the evaporitic country rocks (Grinenko, 1985), and with geological data indicating that the intrusions transgress the country rocks (Naldrett et al., 1992). P.C. Lightfoot and C.J. Hawkesworth (pers. comm., 1998) and Arndt et al. (2003) have suggested that the PGE-depleted lavas could not represent the magmas that incorporated the very heavy S required to form the ore deposits in the sills. Leshner and Burnham (1999, 2001) have pointed out this is not necessarily correct, as the very extensive (up to 300m wide) contact metamorphic and metasomatic aureoles surrounding the sills, in which Ca sulfates have been converted to Ca-silicates, indicate that S was incorporated, at least in part, via a devolatilization and/or incongruent melting process, in which case Sr (which is geochemically similar to Ca) was likely retained in the skarns, changing the mass balance and causing the S and Sr isotopic systems to decouple. This problem will be addressed in a research proposal recently submitted to AMIRA by N.T. Arndt, C.M. Leshner, G. Czamanske, E.M. Ripley, C. Li, and others, but it is clear from the mass balance relationships discussed by Leshner and Burnham (1999, 2001) that PGE depletion and S isotopes are normally the best and most direct indicators of crustal contamination and sulfide segregation. Nevertheless, as is normally the case, ore-forming processes are commonly much more complicated than originally envisioned and considerable caution is warranted when applying techniques of this type.

#### 8.8.5.8 Melting Processes

As discussed above, the type and degree of partial melting during magma generation is not critical in generating Ni-Cu-(PGE) deposits, except in relatively low-degree partial melts where sulfides may be retained in the source.

The main effects of increasing degrees of melting are to 1) increase the abundances of Ni and IPGE in the magma and to decrease the abundances of Cu and PPGE in the magma (Barnes et al., 1985; Naldrett and Barnes, 1986; Keays, 1995), which influences the compositions of the ores that segregate from the magma, and 2) increase the temperature of the magma, which influences its ability to thermomechanically erode wall rocks and/or floor rocks. For example, the rocks in W56 in the William Lake area have the highest analyzed Fo contents and therefore crystallized from the most magnesian magmas sampled in the TNB. However, Ni-Cu-(PGE) deposits are associated with a wide range of magma compositions, including some that were emplaced at much lower temperatures than Thompson (e.g., Noril'sk-Talnakh, Voisey's Bay), so this is obviously not a very critical factor.

#### 8.8.5.9 Emplacement and Assimilation Processes

There is no clear evidence for the mode of emplacement (e.g., replacement vs. dilation) of the mineralized (or non-mineralized) ultramafic bodies in the TNB. Any transgressive contacts, syn-emplacement deformation of country rocks, or local contact metamorphic effects appear to have been destroyed by subsequent deformation and/or regional metamorphism. There is no *direct* physical record of any assimilation processes in the ultramafic bodies in the TNB, in the form of xenoliths, xenocrysts, silicate xenomelts, or restites of partial-melting. The Ni-Cu-(PGE) ores are interpreted to represent sulfide xenomelts, but they have not retained any textural or geochemical characteristics proving this.

However, there is *indirect* chemical evidence of contamination and the composition of the contaminant is consistent with it being Ospwagan Group sediments. Importantly, however, the trace element compositions of both mineralized and non-mineralized bodies may exhibit up to 40% contamination, indicating that contamination alone is insufficient to induce sulfide saturation and produce Ni-Cu-(PGE) mineralization.

Geochemical models suggest that many of the UM bodies exhibit up to ~18% AFC ( $r = 0.6$ ), at which point olivine would no longer be on the liquidus. It seems likely, therefore, that some of the enrichment occurred via an incongruent melting process (Leshner et al., 1999b, Leshner and Burnham, 1999, 2001), in which the magma preferentially incorporated lower temperature components and left behind higher temperature minerals, leading to greater trace element enrichment for the same degree of melting (Leshner et al., 1999a, 2001).

As discussed by Leshner and Burnham (1999, 2001), even if geochemical and isotopic equilibrium were attained during this process, retention of certain components in the residue would influence the mass balance and therefore the apparent degree of contamination. For example, an evaporitic rock containing very heavy S and very radiogenic Sr interacting with a picritic magma might volatilize/melt incongruently to form an immiscible sulphide melt, a miscible silicate melt, and a Ca-garnet- and Ca-pyroxene-rich residue (skarn). If S partitions preferentially into the sulphide and Sr into the residue, the sulphide ore will contain a relatively large proportion of heavy S relative to the total mass of sulphide, but the magma (host rock) will contain a relatively small proportion of radiogenic Sr relative to the total mass of silicate magma. This probably explains the discrepancies in the S and Sr isotopic data for Noril'sk noted by P.C. Lightfoot and C.J. Hawkesworth (pers. comm., 1998) and by Arndt et al. (in press). Similarly, a sulphidic sediment containing heavy S and very radiogenic Os interacting with a komatiitic magma might melt incongruently to form an

immiscible sulphide melt, a miscible silicate melt, and a refractory mafic residue. If S partitions preferentially into the sulphide phase and Os into the residue, the sulphide ore will contain a relatively large proportion of heavy S and a relatively small proportion of radiogenic Os. This probably explains the discrepancies in the S and Os isotopic data for Kambalda noted by Lambert et al. (1998a, b, 1999).

As indicated by the relatively low PGE contents of most sulfide-bearing ultramafic cumulates, the majority of the ultramafic bodies of the TNB formed under relatively low R factors and must have obtained a large amount of their sulfur from the sediments. Similar results have been reported for Dumont and Mt. Keith by Lesher and Keays (2002), suggesting that many Type II internal disseminated deposits also formed by incorporation of external S. However, it is important to note that the smaller the amount of S required, the lower the possibility and necessity of acquiring the S via a melting process (incongruent or wholesale). Instead, it becomes more possible to produce enough S via a devolatilization process, as envisioned for Duluth (e.g., Ripley, 1986).

## 8.9 Future Work

There were several tasks that could not be accomplished in this study for logistical reasons or lack of time, all of which could be done in the future to follow up on the results of this project:

- 1) Establish the contact relationships and age(s) of intrusion using enclaves and/or xenoliths within the ultramafic bodies and possible restite phases on their rinds. Use mass balance constraints to examine modal vs. non-modal (incongruent) melting processes. Requires 3D exposure of ultramafic bodies, which may restrict studies to Thompson Mine.
- 2) Examine whole-rock and mineral compositions of metasedimentary rocks adjacent to mineralization for metasomatic haloes (modal or cryptic). Elements of interest would include metals (e.g., Fe, Co, Ni, Cu, Zn, Pb, Au, Ag, PGE), semi-metals (e.g., As, Sb, Bi, Se, Te), and volatile metals (e.g., Hg, Cd).
- 3) Model selected ultramafic bodies in 3D to establish their internal structure and magma dynamics (e.g., number of magma pulses, variation in contamination as a function of depth, metal depletion).
- 4) Link magma chemistry to existing regional geochronological and geochemical database for mafic rocks to establish the time line for mafic-ultramafic magmatism/volcanism in the belt.